A *FLY*'S VIEW OF SALT INDUCIBLE KINASES: A SYNERGISTIC TUMORIGENESIS MODEL

by

Sercan Sayın

B.S., Molecular Biology and Genetics, Boğaziçi University, 2009

Submitted to the Institute for Graduate Studies in
Science and Engineering in partial fulfillment of
the requirements for the degree of
Master of Science

Graduate Program in Molecular Biology and Genetics
Boğaziçi University
2012

ACKNOWLEDGEMENTS

The first and foremost, I'd like to express my sincere gratitude to my supervisor Assoc. Prof. Arzu Çelik for her assistance and patience in during the all phases of this research. The environment created, insights shared, and opportunities raised by her were essential for this project.

I'd like to show my outmost thanks to Prof. Kuyaş Buğra. Without her, I would never find such an excellent chance to start my scientific career. The initial steps I've taken along the possibilities she created opened the way for this work.

I am very thankful Hatice Bahar Şahin for reigniting the vigor in this project. Her addition to our team as a member and joining to this work brought much needed, new level of criticism. She withstood steadfast against the questions and ideas I've raised. Without her support, this work would never have finished.

With Ece Terzioğlu Kara, Mustafa Talay and Arzu Öztürk, it was a wonderful experience to build our lab from scratch. Though it was a demanding experience, the excellent team work they put forward made research life almost effortless. I will never forget these days.

I would like to thank İbrahim Taştekin, Murat Atasoy, Xalid Bayramlı, Nuray Sönmez, Burak Tepe and Emir Tınaztepe for creating the best environment for the lab. Ideas we exchanged and afternoon tea times helped the transformation of the lab to an enjoyable place. I would also thank to Gamze Küser, Neslihan Zöhrap and he former members of the Retina lab, Cihan Erkut and Demet Candaş, for the priceless aid they provided. At last, I'd like to present my apologies for excluding the names of the remaining dear friends of mine from the MBG department. As I'm aware of dangers being an absent-minded friend, listing of all names properly would be impossible.

This project was funded by Boğaziçi University BAP Project 10B01P12 and EMBO Installation Grant 1656.

ABSTRACT

A *FLY*'S VIEW OF SALT INDUCIBLE KINASES: A SYNERGISTIC TUMORIGENESIS MODEL

The recent explosion of data generated by high-throughput assays on cancer necessitated reliable and fast *in vivo* models for evaluation new catalogue of candidate genes as tumor suppressors or proto-oncogenes and their subsequent trials in cancer therapeutics. *Drosophila melanogaster,* an acclaimed model organism for genetics studies, could now be proposed as the new pinnacle for modeling and screening those candidate genes. As an initiative study in Turkey, we tried to establish a multifaceted, synergistic cancer model based on the *Drosophila* compound eye, reinforced with fly glia and wing models, while using Salt Inducible Kinase (SIK) family as the choice of candidate genes. Metabolic deregulation in cancers is getting increased attention, thus SIKs were an excellent choice since they stand on the crossroad where metabolic and structural information in a cell meet. Using two backgrounds, low grade *sensitized* and high grade *eyeful*, we enquired the contributions on growth and metastasis by two existing *Drosophila* orthologs of human SIKs. Results showed that SIK2 could assume both suppressive and oncogenic roles; as optimal amounts of SIK2 could repress tumor growth while any fluctuations could enhance tumor and glial migration strength. SIK3, on the other hand, was found to act as oncogene when over-expressed in the studies. SIK3 gain could enforce several different outcomes; constitutive over-expression of SIK3 was highly lethal and could alter developmental fate choice of the respective context. Additionally, effects of SIKs on cancer tissues were investigated at cellular level via cell proliferation and death assays, which showed that SIKs could interact with major developmental pathways, such as Notch, TGF-β, FGF.

ÖZET

TUZ İNDUKLENEBILIR KINAZLAR HAKKINDA *SİNEK*BAKIŞI: BİR SİNERJİSTİK TÜMORİGENEZ MODELİ

Son dönemlerde yüksek verimli kanser taramalarında ortaya konan veri yoğunluğu, tümör baskılayıcı ve onkogen adayları içeren yeni gen kataloglarının ve bunların ileriki ilaç deneme aşamalarında değerlendirilmesinde güvenilir, hızlı *in vivo* deneysel modellerin varlığını zorunlu hale getirmiştir. Genetik çalışmalarda başarısı kabullenilmiş bir model olan *Drosophila melanogaster,* bu koşullarda kanser modelleme ve aday gen taramada yeni bir doruk noktası olarak sunulabilir. Bu yöndeki Türkiye'de ilk girişimi gerçekleştirmek adına, glia ve kanat doku modellerinden destek alarak, *Drosophila* bileşik göz dokusu temelli, çok yönlü, sinerjistik ve Tuz İndüklenebilir Kinaz (SIK) familyasına odaklanan bir kanser modeli kurulmaya çalışıldı. Bilimsel alanda kanser dokularındaki metabolik deregulasyon daha fazla dikkat çektiği günlerde, hücrelerdeki metabolik ve yapısal bilgi merkezlerinin kesişiminde bulunan SIKler ideal bir aday familya oluşturmuşturlardır. İnsan SIK'lerinin ortologu olan iki *Drosophila* SIK genini, düşük patolojik dereceli *sensitized* ve yüksek dereceli *eyeful* arka planlarında kullanarak, tümör gelişim ve metastaz seviyelerine katkısı araştırıldı. Sonuçlar göstermektedir ki, SIK2 hem baskılayıcı hem de onkogenik rolleri üstlenirken, fizyolojik olarak en uygun SIK2 seviyeleri dokularda tümör gelişimini baskılayabilmektedir. SIK2 seviyelerindeki dalgalanmalarsa tümör ve glia göçünü arttırır. Diğer taraftan, SIK3 yüksek anlatımları incelendiğinde, ilgili genin onkogenik etkisi gözlemlenmiştir. SIK3 seviyesindeki artış farklı sonuçlar doğurabilir. Yapısal olarak baskılanamayan aktif SIK3 dokular için hayli öldürücü etki gösterir ve dokuların gelişimsel kaderlerinin seçimlerinde kaymalara yol açabilmektedir. Ek çalışmalar olarak, hücre bölünme ve bölüm seviyelerindeki SIKlerin etkisi araştılırken, Notch, TGF-β, FGF benzeri gelişimsel açıdan önemli faktörlerle etkileşim içine olabileceği fark edilmiştir.

TABLE OF CONTENTS

LIST OF FIGURES

LIST OF TABLES

LIST OF ABBREVIATIONS

ACTH	Adenocorticotropic hormone
AMPK	5’ Adenosine mono phosphate dependent kinase
AMPK-RK	AMPK related kinase
AP	Anterior-posterior
bp	Base pairs
CC	Cone cell
cDNA	Complementary DNA
CNS	Central nervous system
Del	Deletion
DNA	Deoxyribonucleic acid
Dpp	Decapentaplegic
EGF-R	Epidermal growth factor receptor
ELAV	Embryonic lethal abnormal vision
ey	Eyeless
FGF-R	Fibroblast growth receptor
GFP	Green fluorescent protein
HDAC	Histone deacetylase
Hh	Hedgehog
IOC	Interommaditial cell
IRES	Internal ribosomes entry site
lGMR	Long glass multiple reporter
lola	Longitudinals lacking

MF	Morphogenetic Furrow
mRNA	Messenger
N	Notch
NVM	Number of visible metastases
PBS	Phosphate buffered saline
PC	Pigment cell
PCR	Polymerase chain reaction
PEF	Presence of eye folding
PFA	Paraformaldehyde
PR	Photoreceptor
psq	Pipsqueak
ptc	Patched
repo	Reversed polarity
RNA	Ribonucleic acid
RNAi	RNA interference
RT-PCR	Reverse transcriptaion PCR
TA	Thoracicoabdominal ganglion
TGF-β	Transforming growth factor β
UAS	Upstream activating sequence
UBA	Ubiquitin-associated
UV	Ultraviolet
Wg	Winglesss

1. INTRODUCTION

1.1. Cancer

In the postgenomics era, ever increasing building of databases fueled by high throughput data generating ushered a new hope in solving the puzzle, cancer. Yet despite concentrated efforts and other than localized cases of treatment success, ultimate victory over cancer is still a distant goal: immense data accumulation pinpoints heterogeneity of cancer and lack of dedicated, isolated causative pathways as well.

One of the most comprehensive reviews ever published available on cancer, by Hanahan and Weinberg in 2011, dissects cancers in several hallmarks and enabling capabilities, while tumor microenvironment provides the third dimension: The former are sustaining proliferative signaling, evading growth suppressors, resisting cell death, enabling replicative immortality, inducing angiogenesis, and activating invasion and metastasis, while the latter consists of genome instability and inflammation (Hanahan and Weinberg 2011).

Tumor cells sustain proliferation via aberrant receptor tyrosine signaling via either constitutive activation of receptors or loss of negative feedback. While, most are eliminated via resulting excessive oncogene signaling and activity, few can overcome crises such as telomerase bottleneck and, through genomic abnormalities occur in the process, abolish intrinsic and extrinsic tumor suppressors clustered around p53 and Retinoblastoma networks, thus cancelling programmed cell death. Major pathways then could alter their role: signal crosstalk, cofactors, epigenetics, non-coding RNA synergized with inflammation induced microenvironment could convert suppressive TGF-β signaling into the driving force of the pinnacle of cancer and most significant effector in bad prognosis, metastasis via induction of the epithelial-mesencyhmal transition. Meanwhile environmental stresses, a consequence of overcrowding, are surmounted by autophagy, increase in GLUT1 receptor expression, Warburg effect and angiogenesis (Thiery *et al.* 2009; Hanahan and Weinberg 2011; Ikushima and Miyazono 2012).

1.2. *Drosophila* and Cancer

Relative simplicity, reduced genetic redundancy, excellent genome annotation and complete online databases, longest history available in science as a model organism and as a result wide-ranging genetic tools provides *Drosophila melanogaster* as one of the emerging tools in cancer research, which has to resort more and more to relatively quick methods, without forsaking the chance of working in combinatorial genetic modifications and microenvironment studies (Brumby and Richardson 2005). Furthermore, the advantages stated above in addition to the ease of whole animal feeding and handling proves useful in the search for cancer therapeutics via drug screening (Gladstone and Su 2011). Differential telomerase maintenance, absence of angiogenesis, differential pharmacokinetics and pharmacodynamics between humans and flies stand as the only obstacles that prevent *Drosophila* to become the perfect model.

The genetic toolbox available for cancer research provides tissue specific over-expression, loss of expression, single nucleotide mutations via epithelial-mesenchymal transition, clonal expression analysis and single cell mutations for cell autonomous effects and microenvironment interaction, transplantation assays for migration. Differentiation, stemness, cell polarity, cell growth, proliferation, cell death, checkpoint control, metastasis can be explored within these techniques (Polesello *et al.* 2011). With morphogens that are conserved throughout evolution playing major patterning roles in their development, imaginal discs and larval brain stand as a useful model in studying S phase cells in addition to adult hematocytes; while wing discs can be utilized in modeling colon cancer (Brumby and Richardson 2005; Dichtel-Danjoy *et al.* 2009). Large numbers of fly lines, as in one case up to 3000, can be screened in single studies (Chi *et al.* 2010). On the opposite, accumulation of knowledge built on several publications could build elaborate genetic networks based on single gene aberrations, as active RasV12 models (Brumby and Richardson 2003; Uhlirova *et al.* 2005; Igaki *et al.* 2006; Vidal *et al.* 2007; Wu *et al.* 2010).

1.3. The *Eyeful* Cancer Model

The tools in the Eyeful model were generated by Maria Dominguez in 2005, and turned into a cancer model by three subsequent studies, performed by independent groups (Ferres-Marco *et al.* 2006; Palomero *et al.* 2007; Bossuyt *et al.* 2009; Zhai *et al.* 2012). The use of a synergistic approach powered by UAS-Gal4 system and the introduction of 2A tags, the Eyeful model utilized fly genetics to uncover hidden players in tumor formation and metastasis. With this aim, the model uses well established *Drosophila* larval eye development as a basis and, driven by an eye-specific driver ey-Gal4, introduces two backgrounds: *sensitized* and *eyeful* (Figure 1.2). The *Sensitized* background includes the over-expression of the Notch-ligand Delta, which causes overgrowth in the *Drosophila* eye, while *eyeful* backgrounds provides additional over-expression of two fly epigenetic memory control genes Longitudinals lacking and Pipsqueak. The activity of these genes amplifies Notch-induced phenotypes by increasing instability due to loss of histone H3 methylation followed likely by tumor suppressor silencing (Axelson 2006).

1.3.1. UAS-Gal4 Binary System

Derived from *Saccharomyces cerevisiae* Gal4 transcription binding protein and its target Upstream Activating Sequence (UAS), UAS-Gal4 binary system provides one of the hallmarks of *Drosophila* genetics, the ability to express and control several proteins individually in any spatio-temporal region with a single expression driver. This driver, first introduced in a publication by Fisher *et al.,* 1988, is constructed with a desired genomic location harboring a specific enhancer or promoter, which is then fused to the DNA binding domain of the Gal4 protein, inserted into *Drosophila* genome. In this way the Gal4 is produced in a manner faithful to the expression of the endogenous expression pattern of the region/gene of interest; while a secondary transgenic construct containing an UAS sequence in the 5’ of the target gene was introduced into flies with the aim of providing a binding partner of Gal4 and achieve transgenic protein over-expression initiation (Fischer *et al.* 1988).

1.3.2. Bicistronic Expression Using a 2A-Tag

The possibility of generating multicistronic constructs in order to express several proteins at the same time in the same place efficiently alleviates the need of repeated generation of transgenic fly lines. One way of achieving this is the use of Internal Ribosomes Entry Site (IRES). Although IRES sequences have been used frequently in the past in the meantime they proved to be inefficient in some cases in balancing expression of genes in equal amounts. Changes in the secondary structure of IRES mRNA can also lead to inhibition of secondary genes due to long nucleotide IRESs as well as large sequence of IRES itself can hinder gene expression (Attal *et al.* 2000). More recently a novel way to generate bicistronic messages has been introduced that alleviates some of the problems observed using IRES sequences. These are small, 20 amino acid long 2A peptides from the foot-and-mouth disease (FMDV) virus. These sequences code for self-cleaving proteases, where the amino acids are left attached to the protein, while the second sequence is released from the first one. The tag can be detected using an antibody. The use of these tags in *Drosophila* 2A remained unexplored so far (Furler *et al.* 2001; Szymczak and Vignali 2005; Szymczak-Workman *et al.* 2012).

1.3.3. Notch Signaling

The fundamental task of the Notch pathway is lateral inhibition, which selects a cell among a sea of undifferentiated neighbors and induces changes channeling the cell into differential fates. Lack of amplification via secondary messengers and cell autonomous transcriptional positive feedback confer a unique ability. As a result, the activity of Notch depends on external signal strength, and any imbalance between two neighboring cells will further enhance itself between these two cells, which would in time result in complete repression of Notch in one cell, while a strong Notch signal is retained in the other (Heitzler *et al.* 1996; Bray 1998; Krejci *et al.* 2009; Bray and Bernard 2010; Katanaev and Kryuchkov 2012).

The transcriptional control by Notch signaling occurs by ligand-induced metalloprotease cleavage of the intracellular domain of Notch (NICD), subsequent replacement of NICD of repressor of Su(H) transcription factor and histone

acetyltransferase recruitment. Ligands of Notch belong to single transmembrane proteins of the so-called DSL (Delta, Serrate, Lag2) family (Struhl and Adachi 1998; Zolkiewska 2008; Bray and Bernard 2010). *Drosophila* Notch receptor itself is composed of three lin12/Notch repeats (LNR) and 36 EGF-like repeats; the latter is target of Fringe, which has an important role in Notch regulation via glycosylation of Notch in the endoplasmic reticulum (Wharton *et al.* 1985; Stanley and Okajima 2010).

In cancer, aberrant Notch signaling is reported to be a node of attraction in many cancer types: T-cell acute lymphoblastic leukemia is diagnosed with ligand-independent constitutive activation of Notch signaling, for example (Ellisen *et al.* 1991). As expected, alterations in Notch have an effect on the neighboring tumor microenvironment, where induction of endothelial differentiation and angiogenesis are reported (Zeng *et al.* 2005).

1.3.4. Epigenetics Longitudinals lacking and Pipsqueak

Changing Notch levels is not enough to drive a cell towards tumorigenesis. The group of Maria Dominguez could show however that the alterations of additional factors in the background of these flies significantly enhanced the tumor formation potential. In particular, the over-expression of Longitudinals lacking (Lola) and Pipsqueak (Psq), two transcriptional repressors containing repression domains related to the BTB/POZ domain, which is found in proteins associated with development, chromatin remodeling, insulator activity, and carcinogenesis, presenting a background of high Notch expression drastically increases tumorigenesis. This seems to be accomplished by the reduction of trimethylation of Histone H3 on K4 (H3K4me3) levels in the manipulated cells, conferring systemic chromatin remodeling and consequent repression of gene expression to these cells (Ferres-Marco *et al.* 2006; Bonchuk *et al.* 2011). An interesting node seems to be that loss of H3K4me3 enables Class I but not Class II Histone Deacetylases to bind to Histone 3, thereby enhancing the closed chromatin phenotype (Huang *et al.* 2010).

Lola was shown to have roles in axon guidance, growth and dendrite maintenance. It is spliced to generate 20 isoforms that are expressed at differential levels to generate a neuronal code (Giniger *et al.* 1994; Spletter *et al.* 2007). Morphological effects of Lola are also present in other organs of *Drosophila*: central nervous system (CNS), adult salivary

glands, and male genitalia (Spokony and Restifo 2007). On the other hand, in egg chambers, Lola is proposed to be required for cell death through its role in chromatin condensation (Bass *et al.* 2007). In the wing disc, Lola has been shown to be a part of the cut gene network, in reinforcement of Wingless signaling (Krupp *et al.* 2005).

In parallel to the structural roles of Lola, Psq is involved in embryonic patterning due to receptor tyrosine kinase modulation, while also having a role in R3/R4 photoreceptor differentiation (Weber *et al.* 1995; Grillo *et al.* 2010).

Both genes are known to be targeting Polycomb group proteins, related to epigenetics memory maintenance (Huang *et al.* 2002; Ferres-Marco *et al.* 2006). Among various roles in development, acting as tumor suppressors, Polycomb genes are known to antagonize both JAK/STAT and Notch signaling in the developing eye (Martinez *et al.* 2009).

1.4. Development of the *Drosophila* Compound Eye

Organs composed of epithelial cells, precursors of adult structures in insects have been identified as early as the 19th century and first reports of *Drosophila melonagaster* counterparts of these organ precursors have been found in 1950. As for adult eyes of *Drosophila*, they also emerge through an imaginal disc, called eye-antennal disc, which has been an important model tissue for the dissection of many pathways since its introduction as a model in 1976 (Ready *et al.* 1976).

1.4.1. Major Cell Types and Events

Although, as its name implies, the eye-antennal disc gives rise to additional external organs: adult antenna, ocelli, maxillary palp and head cuticle, its development starts as early as embryonic stages with a total of 20 cells (Dominguez and Casares 2005). Along others, these cells will form 800 ommatidia, units of compound eye and interommaditial cells. Ommatidia itself are composed of more than 20 cells, including 8 light capturing photoreceptors (PRs), and 12 lens-secreting and supportive cone cells (CCs); 3 pigment cells (primary, secondary, tertiary PCs) form interommaditial cells (Cagan and Ready

1989). The other major type of cells present in the adult eye, glia, however, are generated outside the eye disc and migrate in later stages, totaling a number of 350 cells (Silies *et al.* 2010).

Immediately after the embryonic stage, *Drosophila* enters an active feeding stage and mobilizes during larval development, which marks initiation of potent proliferation in the eye-antennal disc. This remarkable increase is thought to start after mechanical contact with the so-called third dimension of the disc, the peripodial membrane, preceded by the release of morphogens to the eye disc proper (Cho *et al.* 2000; Gibson and Schubiger 2000). Cells of the peripodial membrane are different with their squamous epithelial morphology and regarded to have only a physical role in development: disc fusion and eversion (Atkins and Mardon 2009).

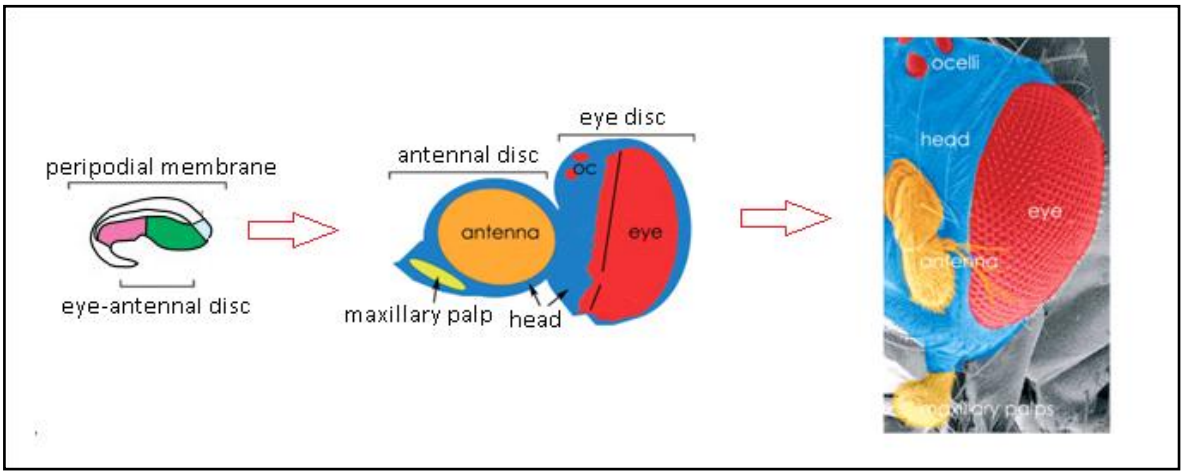

Figure 1.1.Major morphological changes occurring throughout Drosophila from L2 stage and adult structures generated (Dominguez and Casares 2005)

Proliferation in the eye disc starts with expression of the *Drosophila* homolog of Pax6, Eyeless, accompanied with others genes of the “Retinal Differentiation Complex” (Kumar 2001). Present evidence provides suppression of apoptosis during the first larval stage by eyeless. In the absence of eyeless, few cells survive to become pigment cells; and if, additionally, cell death is inhibited, the eye disc cells switch to antennal fate. The antennal fate is driven by cut gene expression, which starts subsequent to restriction of eyeless (Kenyon *et al.* 2003; Punzo *et al.* 2004; Lim and Tomlinson 2006).

The other crucial event occurring during these stages is the establishment of the dorsal-ventral axis, produced by major morphogens, which will pinpoint the position of differentiated cells and their later rotations towards the equator of the eye disc to form a chirality called Planar Cell Polarity (PCP) in the adult eye (Cho and Choi 1998; Dominguez and de Celis 1998; Papayannopoulos *et al.* 1998; Sato and Tomlinson 2007).

The third day in larval development, the third instar stage starts with a wave of differentiation, marked by the Morphogenetic Furrow (MF) in the posterior disc (Ready *et al.* 1976). As the MF expands towards the eye disc, cells enter the pro-neural state, marked with relevant gene expression, and G1 cell arrest. Once commitment is ensured, posterior to the MF, designated cells enter the "First Mitotic Wave" and produce the founding photoreceptor R8 and then the others R2, R5, R3 and R4. Subsequently, the "Second Wave" occurs and R1, R6 and R7 are recruited. PR identity, which will determine the type of rhodopsin to be expressed, occurs in the late pupal stage (Wolff and Ready 1991). The non-PRs, cone cells are formed pair wise in the second mitotic wave from the R7 equivalence group, with a two-row time gap between recruitments (Tomlinson and Ready 1987; Tomlinson 1988; Dickson *et al.* 1992).

1.4.2. Generation and Migration of Glia

Six types of morphologically different glia are reported in the literature within two major layers: PR axon wrapping glia, on top of the surface glia, which provides a tight epithelium, reminiscent of the blood-brain barrier (Hummel *et al.* 2002; Silies *et al.* 2007). These glia stem from the optic lobe, and migrate to the eye disc with an increasing rate during the third instar larval stage, which is induced at first by the PR axon innervating the optic lobe, and differentiate upon contact with PRs in the disc, although their migration can happen in the absence of neurons (Rangarajan *et al.* 1999; Hummel *et al.* 2002; Pielage *et al.* 2004).

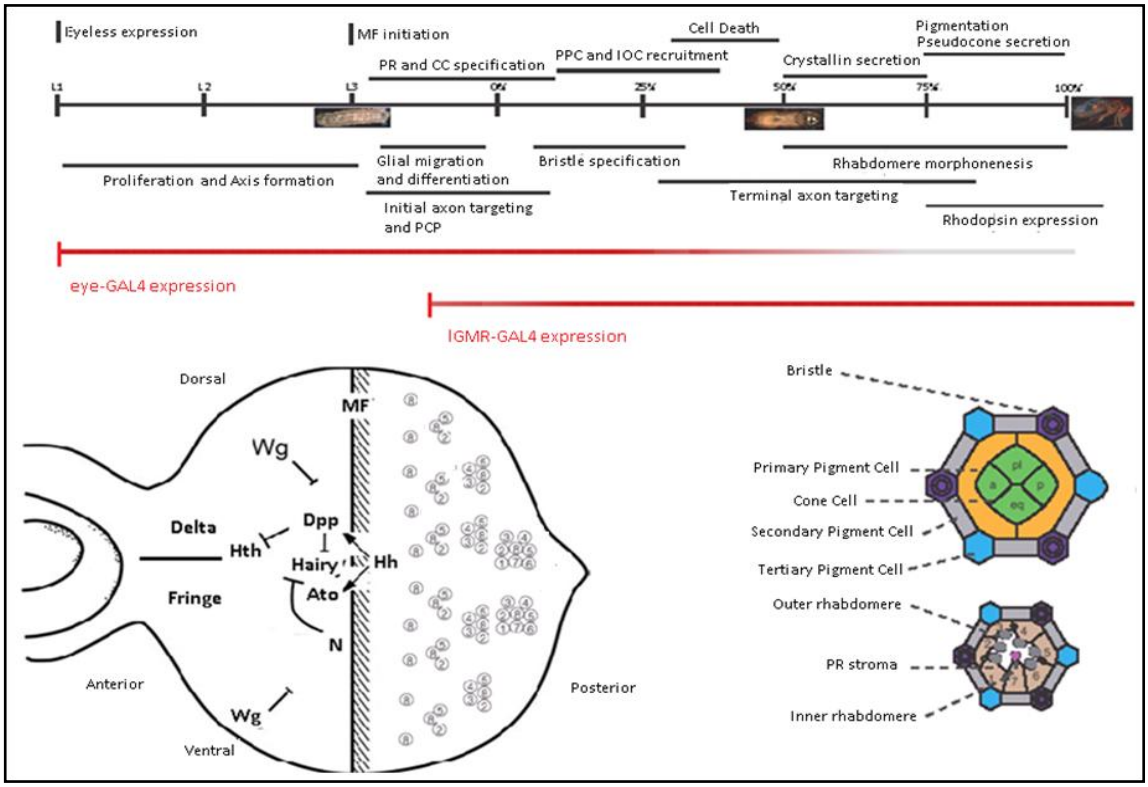

Figure 1.2. Timeline of developmental milestones of Drosophila eye, MF progression, PR recruitment and adult ommaditia (Dominguez and Casares 2005; Morante et al., 2007; Charlton-Perkins and Cook 2010; Katanaev and Kryuchkov 2012). Pigment cells are generated during the early pupal stages, where also bristle cells are specified, followed by highly active cell death during pattering of those cells, and fine-tuning of cell positions (Cagan and Ready 1989). Figure1.2 presents the timeline for cell the recruitment and following morphological changes.

1.4.3. Major Signaling Pathways

1.4.3.1. Notch Signaling. Notch signaling is a major tool in development of the eye: axis setup, cell fate, cell death, cell growth, and cell adhesion (Cagan and Reh 2010). In the early larval disc, axis via integration of Hedgehodge/Dpp signaling, Notch helps in formation of anterior-posterior axis. Axis is determined through expression patterns of its signaling partners Delta, Serrate, Fringe (Treisman and Rubin 1995; Chanut and Heberlein 1997; Roignant and Treisman 2009). Early contributions of Notch also include maintenance of eyeless expression (Kurata *et al.* 2000; Kumar and Moses 2001). Notch is essential at different levels of PR specification, reoccurring several times in antagonizing several partners. Notch is active during the recruitment of the first PR, R8, by inducing up-

regulation of proneural transcription factor Atonal in the cells modulated by Morphogenetic furrow. Moreover, suppression by Hairy of Notch anterior to morphogenetic furrow prevents ectopic PR induction (Baker and Yu 1997; Baonza and Freeman 2001). Differentiation of remaining PRs are too influenced by Notch, in particular in accordance with EGFR signaling, for controlling another Retinal Determination gene, Eyes absent, Eya (Hsiao *et al.* 2001). Notch/EGRF axis becomes essential again during recruitment of CCs from R7 Equivalence Group and later interommaditial cells, while differential induction of genes control neuronal fate adoption. In parallel, defects in Notch signaling causes chirality defects, while loss of Notch equals to loss of whole eye (Reinke and Zipursky 1988; Hart *et al.* 1990; Van Vactor *et al.* 1991; Freeman 1996; Panin *et al.* 1997; Spencer *et al.* 1998; Flores *et al.* 2000; Voas and Rebay 2004; Wech and Nagel 2005; Nagaraj and Banerjee 2007).

Though no direct evidence is available, there are pathways parallel to Notch signaling in control of eye disc growth: the Homothorax (Hth), Hippo signaling, Insulin/mTOR axis. While Hth induces cell proliferation and survival by forming transcriptional complexes and might have role in expression of cell cycle genes as cyclinE myc, the Insulin/IGF/mTOR axis controls FOXO transcription targets, and the Hippo pathway inhibits apoptosis by leading to the expression of the target microRNA bantam (Bessa *et al.* 2002; Oldham and Hafen 2003; Peng *et al.* 2009).

1.4.3.2. Hedgehog, Decapentaplegic and Wingless. Hedgehog (Hh, Sonic Hedgedog homolog), Decapentaplegic (Dpp, major TGF-β homolog), and Wingless (Wg, Wnt homolog) are the three major morphogens controlling the Morphogenetic Furrow. They are directly related to proper eye disc formation as deregulation of these pathways causes multiple compound eye formation. Moreover, Dpp and Wg expression is required for ectopic eye formation in the whole Drosophila; these transdetermination weak points are marked with their expression (Maves and Schubiger 1998; Maves and Schubiger 2003).

The expression pattern of Hh and Dpp changes from the peripodial membrane to the eye disc proper at the onset of third instar larvae. This is accomplished by the JAK/STAT ligand Unpaired that releases Dpp from Wg inhibition at the posterior tip of the eye disc. This results in proneural fate alignment of cells in the MF and sensitization for

effects of Hh. Moreover, Hh receiving cells direct this information to the cell anterior via Hh release, contributing to MF progression (Heberlein *et al.* 1993; Heberlein *et al.* 1995; Strutt *et al.* 1995; Dominguez and Hafen 1997; Tsai *et al.* 2007).

1.4.3.3. The FGF Pathway. Although reports stating the existence of Integrin-dependent differentiation of glia, the major pathway governing both differentiation and prior migration are FGF signaling (Murakami *et al.* 2007). One of the two *Drosophila* FGF molecules, Hearthless, is expressed in glia cells from the optic lobe to the eye disc; yet the differential expression of FGF receptors, Pyramus and Thisbe, determines the process. While the former is expressed in glia and plays a dual role as a mitotic autocrine signal and driving force in homophilic migration, the latter causes glia to differentiate and wrap PR axons in PRs (Franzdottir 2000). Moreover, a recent paper reported a role for the other *Drosophila* FGF receptor, Branchless (bnl), which inhibits anomalous glial migration (Mukherjee *et al.* 2012).

1.5. Wing Cell Migration Model and Wing Disc

A recent study by the Cagan group proposes the wing disc as a model for metastasis through its stratified epithelial layer. In this system patched-Gal4 is used as a driver to express genes in a stripe in the wing disc, thus enabling genetic manipulation of cells in the anterior-posterior (AP) axis. GFP expression is used as a marker for manipulated cells, thus, invasion of cells can be monitored *in vivo.* Upon depletion of Src inhibitor Csk via RNA interference, cells migrate beyond their regular developmental position, to be eliminated by apoptosis. When cell death is inhibited synergistically, modulating the JNK pathway, the results are enhanced significantly and thereby open a way for testing additional genes modulating this phenotype (Vidal *et al.* 2006).

Like the eye-antennal imaginal disc, the *Drosophila* wing disc also can be recognized early in embryonic development at a stage where it is composed of approximately 20 cells. Furthermore, wing discs develop into a single cell epithelial layer in the third instar larval stage, similar to the eye disc proper. Major players in development of the wing disc are also shared with the eye disc: Notch, Dpp, Wg, Hh and EGF-R

signaling, combined with wing disc specific factors like Engrailed (en), Apterous (ap), Vestigial (vg) interspaced within the organizing centers (Klein 2001).

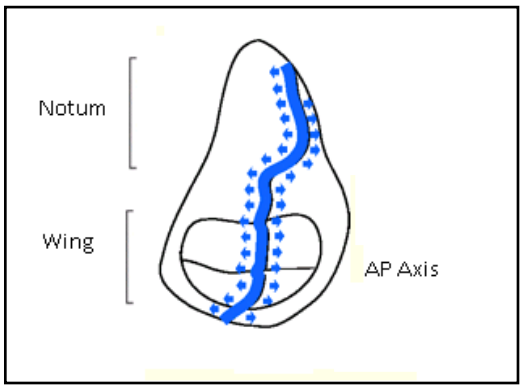

Figure 1.3. Drosophila wing disc, AP axis and adult organ boundaries (Lin 2004)

In one of the earliest events, wing development is resolving the division between adult wing and notum structures, a task accomplished via formation of AP axis based gene expression patterns. The AP axis, even though suggestions of embryonic origin exist, is established in the second instar larval stage with ventral Wg along with Hh expression (Basler and Struhl 1994; Goto and Hayashi 1997; Baonza *et al.* 2000; Wang *et al.* 2000).

1.6. Salt Inducible Kinases

Salt Inducible Kinases, belonging to 13 AMPK-related family kinases (AMPK-RK) primarily are associated with cellular and systemic metabolism. They are serine/threonine kinases identified by a common sucrose non-fermenting-1 (SNF-1) homology domain (SNH) and PKA inhibition motif (Horike *et al.* 2002; Takemori *et al.* 2003; Katoh *et al.* 2004; Bright *et al.* 2009). While first evidence of existence of these proteins comes from the myocardium, where SIK1 marks myocardial cell precursor and plays a role in their development and survival through interacting with cell cycle control, the actual nomenclature arises from salt-fed adrenal glands where biogenesis-related genes were in search, SIK1 was cloned consequent to exhibiting highest induction (Ruiz *et al.* 1994; Wang *et al.* 1999; Berdeaux *et al.* 2007; Romito *et al.* 2010). The remaining members of SIKs, SIK2 & SIK3, were later identified via sequence-based homology and found to be conserved throughout the animal kingdom (for *Drosophila* CG4290 as SIK2; CG15072/42856 as SIK3, no SIK1 homolog is reported so far), where also initial data

emerged regarding relevant expression patterns: SIK1 and SIK2 in an overlapping pattern covering adrenal cortex and adipose tissue, in contrast to ubiquitous SIK3 expression (Katoh *et al.* 2004).

In addition to a SNH domain, which contributes to SIK folding and a C-terminal PKA motif adjacent to a nuclear localization signal, the remaining protein motifs of SIKs are the AMPK homology domain and the Ubiquitin-associated (UBA) domain (Horike 2003, Okamato 2004). The UBA domain interestingly does not interact with ubiquitin; yet two independent groups report different roles for this domain: SIK2 UBA is required in Lkb1-dependent activation of SIK1 via UBA-kinase domain interaction; SIK1 UBA domain binds to Smad7 causing eventual repression of TGF-β signaling (Jaleel *et al.* 2006; Kowanetz *et al.* 2008) .

The most significant upstream effector of SIKs is the master tumor suppressor Lkb1 which also activates all AMPK-RKs: Threonine residues in the T-loop of SIKs are phosphorylated by the Lkb1 : STRAD : MO25 complex, which in return catalyzes 14-3-3 scaffold binding to the T-loop, thereby increasing affinity towards SIK target to be translocated to the cytoplasm. Moreover, loss of Lkb1 could lead to SIK activity in total (Lizcano *et al.* 2004; Al-Hakim *et al.* 2005; Jaleel *et al.* 2006; Shaw 2009). Moreover, at least SIK1 and SIK2 are shown to stabilize their activity by autophosphorylation, which is subsequent to SIK1 phosphorylation by GSK3β (Hashimoto *et al.* 2008). Another upstream major effector in activation of SIKs is calcium calmodulin-dependent protein kinases (CaMK) (Sjostrom *et al.* 2007; van der Linden *et al.* 2007). Downstream targets of SIKs show a variety of functions, mainly related to energy metabolism, including a function as transcriptional cofactors. Interestingly, SIKs share some of these targets between the group, as well as other AMPK-RKs, or directly Lkb1, suggesting probable compensation in relevant signaling pathways; yet few studies considered this prospect in detail (Shaw 2009).

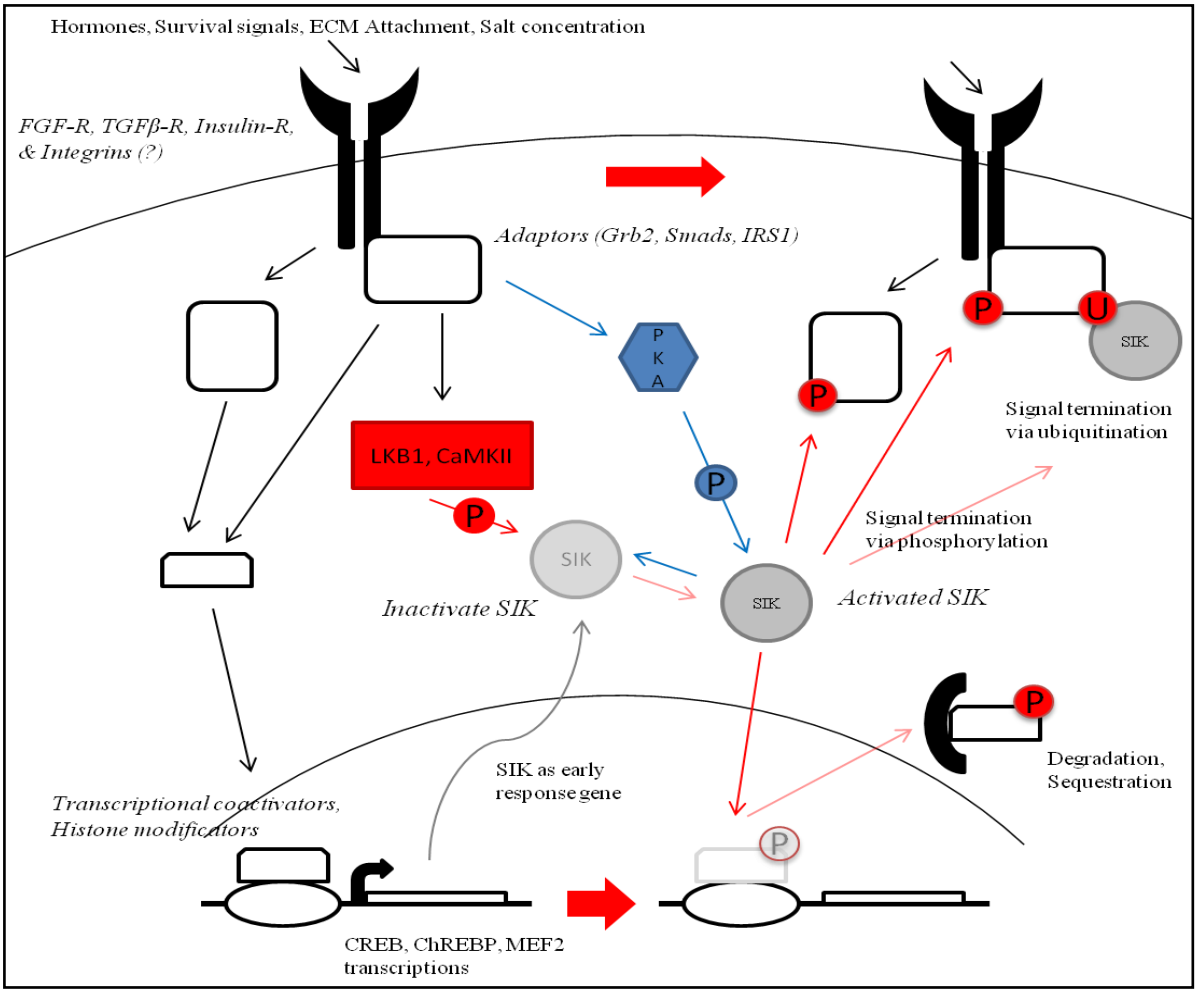

Figure 1.4. A Simplified View of Salt Inducible Kinases and Relevant Signaling Members.

1.6.1. SIKs in Metabolic Control, Proliferation, Survival

Role of Salt Inducible Kinases in metabolism seems to be fine-tuning systematic information brought by hormones such as adenocorticotropic hormone (ACTH) and internal energy monitoring, acting in temporal control of cellular reactions via early response gene, by mostly controlling gene transcription switches.

SIK2 phosphorylates insulin receptor IRS-1 in adipocytes, causing silencing of insulin derived responses, and hinting to a possible, contributing role in development of Type II Diabetes (Takemori *et al.* 2003). In parallel, pancreatic islet cells repress SIK2 through cyclic AMP, releasing CRTC2; which is also reported to be active cofactor of CREB transcription after relocation to the nucleus subsequent emancipation from SIK2, which is activated by Insulin/Akt (Screaton *et al.* 2004; Dentin *et al.* 2007). During re-

feeding both neuronal *Drosophila* SIKs, shows a similar pattern, repressing CRTC, and FOXO via HDAC4 sequestration, as mutants of SIKs show higher lipid and glucagon, longer survival (Wang *et al.* 2008; Choi *et al.* 2011; Wang *et al.* 2011). This control on the insulin pathway has a drastic effect on the tissue size also: repression on SIK2 increases liver size, when p300 becomes active and bind to Class II HDACs (Bricambert *et al.* 2010).

SIKs play also a role in lipogenesis as hinted above. SIK1 represses Srebp1-c and StAR expression in hepatocytes, resulting in program switches, while nutrient crises activates SIK2 in adipocytes, also in association with thermogenesis (Du *et al.* 2008; Muraoka *et al.* 2009; Yoon *et al.* 2009; Jefcoate *et al.* 2011).

Another dimension in metabolic effects of SIKs is control of cellular salt concentrations, which seems to be restricted responsibility of SIK1. Physiological effects of Na^+,K^+/ATPase modulation varies: in neurons, SIK activity is thought to increase membrane depolarization; while in cardiac cells, SIK1 is associated with growth; in lungs, it has a role in edema clearance. Salt control by SIK1 requires CaMK activation (Feldman *et al.* 2000; Sjostrom *et al.* 2007; Eneling *et al.* 2011; Popov *et al.* 2012).

Neuronal effects of SIKs are not limited to membrane depolarization. Another process where SIK1 is implicated is plasticity. Cocaine-induced SIK1 activation results MEF2 transcription termination when HDAC5 is transported to nucleus after it is phosphorylated by SIK1 (Dietrich *et al.* 2012). Gene expression in neuronal cells includes chemoreceptor transcription control, which depends again on HDAC/MEF2 axis by *C. elegans* SIK homolog kin-29 and SIK3, while kin-29 mutants exhibit several effects: insulin dependent increased lifespan, decreased body size, and dysregulation of stress-induced hibernation stage dauer. Mouse SIK3 mutants show chondrocyte hypertrophy and age dependent dwarfism. These phenotypes are also dependent on neuronal inhibition of TGF-β, which is shown to interact with SIK1 in several negative feedback loop contexts (Lanjuin and Sengupta 2002; Maduzia *et al.* 2005; van der Linden *et al.* 2007; Brown *et al.* 2008; Kowanetz *et al.* 2008; van der Linden *et al.* 2008; Lonn *et al.* 2012; Sasagawa *et al.* 2012). Cerebral ischemia models also produced interesting, yet opposite role for SIK1 and SIK2. The earliest reports describe the induction of SIK1 expression in concussive brain

injuries and later, SIK1 is found to be promoting survival against ischemia (Giza *et al.* 2002; Cheng *et al.* 2011). On the other hand, loss of SIK2 function, rather than gain, promotes survival via release of SIK2 hold on MEF2 transcription, which might be parallel to inhibition on melanogenesis by SIK2, an important survival factor (Horike *et al.* 2010; Sasaki *et al.* 2011)

1.6.2. SIKs in Cell Structure

Cell morphological changes brought about modulation of SIKs are scantly documented. In an attempt to elucidate the role of Lkb1 in *Drosophila* eye polarity and identify the contribution of its downstream its targets contribution, fly SIK3 has been shown to partially phenocopy the loss of Lkb1 in stainings of apical-basal polarity markers and was marked as a possible player in development or maintenance of adherens junctions, similar to other AMPK-RKs evaluated in the work (Amin *et al.* 2009). Within a more detailed account in epithelial and renal cells, E-cadherin expression is linked to Lkb1 driven SIK1 expression, which is also shown to repress epithelial-mesenchymal transition drivers (Eneling *et al.* 2012). In addition, SIK1 was proposed to have a role in Alzheimer's disease subsequent to the discovery of SIK1-dependent tau 12E8 phosphorylation, which brings stability to tau, in expense of toxicity in neurons (Drewes *et al.* 1995; Augustinack *et al.* 2002; Yoshida and Goedert 2012).

1.6.3. SIKs in Cancer

Human mammary epithelial cells, transfected with constitutively active Akt, provided the first direct evidence of the involvement of SIK in cancer. A special case of apoptosis based on correct cell attachment mediated mainly by Integrins and Focal Adhesion Kinase, anoikis, is suppressed in this cell culture-based screen when specific sh-RNAs induced loss of SIK1. Eventually SIK1 was found to be the mediatory link between Lkb1 and p53. However, *in vivo* effects of SIK1 are limited; loss of SIK1 can only generate micrometastasis when tumor cells are injected into NOD/SCID mice (Gilmore 2005; Cheng *et al.* 2009).

Although bioinformatic analyses exist implying SIK2 to be tumor suppressor exist, a number of indirect contradictory evidences accumulated in the literature (Katoh 2004). In Karpas42 cell lines, the SIK genomic locus 11q23 is amplified and this over-expression of SIK2 was shown to downregulate the CREB target BIM a pro-apoptotic; yet no significant correlation is evident in primary cell cultures (Nagel *et al.* 2010; Poretti *et al.* 2011). Stronger data come from studies with ovarian cancer cell lines where SIK2 is required for cell cycle progression by phosphorylating cNAP in the centrosome and activating Akt. Blocking SIK2 drops the rate of mitosis among SK-OV3 cell lines, in addition to increasing anti-tubulin drug paclitaxel response (Ahmed *et al.* 2010). Similarly, depletion of fly SIK3 causes aberrant spindle formation within mitotic cells, thereby hindering the process (Bettencourt-Dias *et al.* 2004).

Marker screening in prediction of ovarian cancers remains an important factor in early diagnosis and prognosis. In a screen to expand catalogue of available markers for ovarian cancers, SIK3 has been found to be over-expressed via phage display screen. The antibodies derived from ascetic fluid of an ovarian cancer patient have been found to be associated with a certain 150kDa band. Subsequently, these antibodies were presented to a phage display system, in which phages found to be selective specifically for those antibodies were presented to *Escherichia coli* hosts and propagated. The sequencing of propagated clones revealed SIK3 is the target of ascetic antibodies. In later experiments, SIK3 modulation was found to be in positive correlation with cancer potency. Inducing SIK3 resulted in increased cell mitosis and consequent transformation of low grade ovarian tumor cells (OVCAR3) to high grade cells as reversal in potency occurred in SK-OV3 line upon loss of SIK3 in NOD/SCID mice. Histochemical analysis showed high coexpression between SIK3 and the well-known oncogene c-Src (Charoenfuprasert *et al.* 2011)

1.6.4. SIKs and FGF

In our department, the result of two yeast two-hybrid screen using FGFR2 as bait and follow-up studies identified SIK2 as an interactor of the FGF pathway of Müller glial MIO-M1 cells, which increase their proliferation rate in response to reduction of SIK2 inhibition of FGFs (Özcan 2003; Küser 2012). While PKA inhibition of SIK in glia was established, FGF pathway members Gab1 and A-raf were proposed as interaction nodes

due to the presence of SIK2 phosphorylation motifs; *in vitro* phosphorylation of Gab1 was confirmed. In addition, in hyperglycemic conditions, glia were as shown to increase Insulin/Akt signaling, which are inhibited by SIK2, thereby preventing over-proliferation (Küser 2006; Küser 2012).

While SIK1 was found to be absent in Müller Glia, SIK3 expression levels showed an increase between days P10-P20, indicating a possible role in the maintenance of differentiated glia (Candaş 2007; Vural 2008).

2. PURPOSE

The aim of this work is to elucidate the possible involvement of Salt Inducible Kinases in cancer using a cooperative tumorigenesis model in *Drosophila* based on two backgrounds, eyeful and sensitized. The effects of loss-of-function and gain-of-function effects of SIKs were investigated, and the consequences of manipulation of SIK levels on cell viability, proliferation and differentiation were assessed. Furthermore, this work represents one step towards modeling human diseases in our lab within a compact model, *Drosophila melanogaster*, thereby helping to understand the evolutionary link between SIKs of Human and Fly origin and preparing an economical model for drug screens. As a technological improvement the functionality of T2A tags in *Drosophila* were tested. The successful demonstration of its functionality would contribute a new tool to the Fly community.

3. MATERIALS AND METHODS

3.1. Biological Material

All flies present in the study were raised in fly incubators at constant temperature of 25°C, 60% humidity, along with a 12:12 day: night cycle unless otherwise noted for virgin fly collection and those transgenic lines unstable at these conditions, with a temperature for incubation of 18˚C. Fly food was prepared freshly using the mixture and protocol provided by Applied Scientific, USA.

Table 3.1. *Drosophila melanogaster* lines used in the study.

Fly Lines				
UAS constructs	**Chr. #**	**Description**		
UAS-SIK2 Fly	3	(5X) UAS fusion of *SIK2* fly cDNA		
UAS-SIK2 Fly CA	3	(5X) UAS fusion of *SIK2* fly cDNA, harbors S1032A modification		
UAS-SIK2 Fly KD	2	(5X) UAS fusion of *SIK2* fly cDNA, harbors K170M modification		
UAS-SIK3 Fly	3	(5X) UAS fusion of shorter 20soforms of *SIK3* Fly cDNA		
UAS-SIK3 Fly CA	2	(5X) UAS fusion of *SIK3* fly cDNA, harbors S563A modification		
UAS-SIK2 Human	3	(5X) UAS fusion of *SIK2* human cDNA		
UAS-SIK3 Human	3	(5X) UAS fusion of *SIK3* human cDNA		
UAS-GFP	2	(5X) UAS fusion of *GFP* cDNA		
GAL4 constructs				
ey-GAL4	2	Expresses GAL4 in pattern of eyeless gene		
lGMR-GAL4	2	Glass enhancer driving GAL4 in post-morphogenetic eye disc		
repo-GAL4	3	Expresses GAL4 in glia		
ELAV-GAL4	3	Expresses GAL4 in the nervous system		
ptc-GAL4	2	Expresses in a column of cells along A-P border in wing disc		
Mz97-GAL4	2	Expresses GAL4 in wrapping glial cells		
Deficiency Lines				
$SIK2^{\Delta 41}$	1	X1953962~1955112 deletion covering SIK2 fly genomic locus		
VDRC RNAi lines		**Transformant ID**	**Construct ID**	**RNAi Library**
SIK2	3	26496	11275	GD
	3	26497	11275	GD
	2	103739	102292	KK
CG42856	3	39864	8535	GD
	3	39866	8535	GD
	2	107458	109965	KK

Table 3.1. *Drosophila melanogaster* lines used in the study (continued).

Fly Lines (continued)		
Other Transgenes		
Sensitized	2	Provides Delta over-expression under ey-GAL4
Eyeful	2	Provides Delta, lola and psq over-expression under ey-GAL4
w1118	1	Loss of function allele of white gene
yw122; QB	1,2,3	Quadruple balancer line harboring CyO / Sp ; TM2 ; / TM6B

3.2. Chemicals and Supplies

Chemicals, supplies and equipments are provided in the following Appendix C in alphabetical order.

3.2.1. Buffers

Buffers prepared manually are given below; commercial buffers can be found in the appendix section.

Table 3.2. Contents of buffers and solutions.

Buffers & Solutions	
Name	**Content**
BNT Solution	PBS BSA 0.1% Tween20 0.1% NaCl 250mM
Laemli's buffer 3X	Tris-Cl pH6.8 150mM SDS 6% Glycerol 30% Bromophenol blue 0.3% Dithiothreitol (DTT) 300mM
Orange G 10X	Orange G 0.2% Glycerol 30%
PBS	NaCl 137mM
	KCl 2.7mM
	Na_2HPO_4 10mM

Table 3.2. Contents of buffers and solutions (continued).

Buffers & Solutions (continued)	
Name	**Content**
PBS (continued)	KH_2PO_4 1.8mM
PBX3	PBS Triton X-100 0.3%
Resolving gel 8%	Tris-HCl pH 8.8
	Acrylamide 29 1%
	SDS 20%
	APS 10%
	TEMED
Running buffer 10X	Tris base 250 mM Glycine 1.9M SDS 1% pH 8.3
Stacking gel 4%	Tris HCl pH 6.8 Acrylamide 29 1% SDS 20% APS 10% TEMED
TAE Buffer 1X	Tris-HCl 40mM Ethylenediaminetetraacetic acid (EDTA) 1mM Acetic acid 0.1%
TBS 10X	Tris base 200mM NaCl 1.5M pH 7.6
TBS-T 1X	TBS Tween 0.1%
Transfer buffer, 1X	Tris base 25mM Glycine 190M EtOH 20%

3.2.2. Oligonucleotide Primers

Primers designed were ordered from Iontek (Turkey) and used in the final concentration of 10pmol/µl subsequent to dH_2O dilution.

Table 3.3. Primers and their relevant templates, optimal melting temperatures and predicted product lengths.

Primer List					
Product	**Primer Name**	**Primer Sequence 5'-3'**	**Tm (^oC)**	**Template ID**	**Product Length (bp)**
SIK2 human	sik2_human_f_bglII	AGATCTATGGTCATGGCG	53,8	NM_015191	2781
	sik2_human_r_xhoI	CTCGAGCTAATTCACCAGG	57,5		
SIK3Fly	sik3_cds_f_notI	GCGGCCGCATGGCCACCACA	68,7	FBcl0162999	2109
Primer List *(continued)*					
Product	**Primer Name**	**Primer Sequence 5'-3'**	**Tm (^oC)**	**Template ID**	**Product Length (bp)**
SIK3Fly *(c)*	sik3_cds_r_xhoI	GGGGCTCGAGTAATATTTTAGTTAGC	64,6	FBcl0162999	2109
SIK3Human	sik2_human_f_ecorI	TAGAATTCATGCCCGCCCGTAT	62.1	NM_025164.3	3795
	sik2_human_r_xhoI	AACTCGAGCACGCCTGCCTG	64.6		
SIK2 EST	sik2_rt_f	CAGATGAACCTCAAGACTTCC	59,5	Total fly cDNA	203
	sik2_rt_r	GGCGTCGATGTATGATAGTC	58,4		
SIK3 EST	sik3_rt_f	ATCAAGGATCAGCATTTGCTC	57,5		301
	sik3_rt_r	TTTGCATATAGCTTTGCAGCTC	58,4		
Actin79b EST	actin79b_rtpcr_cont_f	ATGTATCCAGGTATCGCTGAC	59,5		167
	actin79b_rtpcr_cont_r	TGCTTGGAGATCCACATCTG	58,4		

Table 3.4. List of primers used for sequencing cloned DNA products.

Sequencing Primer List			
Gene	**Primer Name**	**Primer Sequence 5'-3'**	**Tm (^oC)**
SIK3Fly	sik3_cds_seq1	CGATGGACCCAAGTCGGATA	60,5
SIK3-human	sik3_h_seq1	CAGGAAAGCCAGGTAGGAG	59,5
	sik3_h_seq2	TTGGTGCGCTATTTGTCAAT	54,3
	sik3_h_seq3	AGTGGAGGGACTTTCAGG	56,3
	sik3_h_seq4	CCCATCTGTTTTCGGACCA	57,5
SIK2-human	hki_f2	ATCATGTTGCTGGGCAGTGAC	61,2
	hki_f3	TCCTGGTGCGGAAGGGATG	61,6
	M13_f	CGCCAGGGTTTTCCCA	53,5
	M13_r	CAGGAAACAGCTATGACC	53,8

3.2.3. Antibodies

While primary antibodies used in the study are kept at 4°C, secondary antibodies were stored at -20°C, in dark.

Table 3.5. List of antibodies, relevant species where antibodies were raised, dilution rates, and suppliers.

Antibodies				
Name	**Antigen**	**Species**	**Dilution**	**Supplier**
Primary Antibodies				
Caspase 3	Activated Caspase 3	Rabbit	1:500	BD Pharmigen
ElaV	ElaV	Rat	1:50	Hybridoma Bank
ElaV	ElaV	Mouse	1:50	Hybridoma Bank
GFP	GFP	Rabbit	1:500	Invitrogen
mCherry	dsRed	Rabbit	1:1000	Clontech
pH3	Phosho-Histone 3	Mouse	1:250	Millipore
repo	Repo	Mouse	1:20	Hybridoma Bank
SIK2	human SIK2	Mouse		Biolegend
SIK3	human SIK3	Mouse	1:50	Abcam
Secondary Antibodies				
Alexa 488	Rabbit	Goat	1:800	Invitrogen
Alexa 555	Mouse	Goat	1:800	Invitrogen
Alexa 647	Rabbit	Donkey	1:800	Invitrogen
Alexa 647	Rat	Donkey	1:800	Invitrogen
Cy3	Mouse	Donkey	1:800	Jackson Laboratory
Cy3	Rat	Donkey	1:800	Jackson Laboratory

3.3. Molecular Techniques

3.3.1. Polymerase Chain Reaction

In order to produce PCR fragments with a high proof-reading capability, Advantage® 2 Polymerase Mix (Clontech) was used in the primary amplification of obtained CDS listed in the Table 3.2. Primers List with the designed primers with their relevant Tm's. With a total reaction volume of 50µl including 5µl of Advantage 2 PCR buffer 10X, primers 0.5µM, 50ng DNA and 0.5µl of Advantage 2 Polymerase 50X, the PCR reactions were performed with 12 cycles of elongation with the rule of 1' elongation per 1kb of fragment. The remaining conditions were 95°C for 5' for initial denaturation, accompanied with elongation cycles of 95°C for 30'', annealing temperature, -4°C lower of

the Tm, for 30’’, and elongation at 72°C. Subsequent to final elongation at 72°C for 10’, the DNA products were kept at 4°C until further use.

For the common needs of DNA amplification, during PCRs, GoTaq Flexi DNA polymerase 50X (Promega) with addition of GoTaq Colorless Flexi Buffer 5X and Magnesium Chloride 25mM (Promega) was used as explained in the product manual.

3.3.2. Agarose Gel Electrophoresis

The visualization of DNA was achieved through running it after mixing with a 1/10 volume of OrangeG 10X in an agarose gel, prepared by TAE buffer 1X and 30ng/ml ethidium bromide. Along the desired DNA, 1kb DNA Ladder (New England Biolabs) was loaded onto gel to accurately determine length of DNA fragments. Electrophoresis was applied at constant 90-120V using Bio-Rad Labs equipment and followed by visualization under UV with a transilluminator (Bio-Rad, California, USA).

3.3.3. Gel Extraction of DNA

The desired bands visualized under UV were cut from the gel with a sterile scalpel. Following the instructions in the manual of QIAquick Gel Extraction Kit, the cut gels were dissolved, applied to QIAquick columns, washed andeluted with 30µl of elution buffer. The quality and the concentration of elutes were determined by Nanodrop spectrophotometer.

3.3.4. Ligation and Transformation

Ligations were carried out at room temperature for 1 hour within a total volume of 10µl, harboring at most 100ng DNA. The ratios of vector: insert were calculated in each case according to respective length of the fragments and concentrations available with final ratios of 1:1, 1:3, 3:1 and 1:0. The common enzyme used in ligations was 1U T4 DNA ligase (New England Biolabs) along with 1x T4 DNA Ligase Reaction Buffer. Ligations into pGEM-T Easy vector were performed using its own buffer and ligase (Promega).

For transformation purposes, competent bacteria of the *Escherichia coli* Top10 strain were used. 50µl frozen cells were thawed on ice, and in each run, half of the ligation mixture, 5µl, was added, gently mixed and incubated for 10'. The following heat shock at 42°C was applied for 90' and cells were quickly returned to ice. Bacteria transformed with vectors containing ampicillin resistance were then spread onto agar plates containing 100mg/ml ampicillin and grown for overnight at 37°C.

3.3.5. Isolation of Colonies

Colonies were picked with a sterile tip and dipped into dH_2O. Meanwhile, same tips were streaked to a back-up agar plate, where each colony was labeled and grown at 37°C. Bacteria were denatured at 95°C in Thermocycler (Biorad) and, after the reaction was stopped, the remaining PCR mix containing primers and GoTaq polymerase and dNTPs was added. PCR was performed for 35 cycles and PCR products on an 1% agarose gel. Bacterial colonies that were identified as positive in the PCR were inoculated overnight in 1.5ml of LB broth including the relevant antibiotic. Approximately 14 hours later, 200µl of bacterial culture was reserved for longer preservation at -80°C and the remaining bacteria culture was used for isolation of the plasmid according to QIAprep Spin Miniprep Kit (Qiagen). The DNA plasmids were eluted with 50µl elution buffer.

3.3.5. Restriction Digestion of DNA

Unless stated otherwise, restriction reactions were carried out as recommended by the manufacturers (New England Labs & Fermentas). Analytical digestions were performed with 1µg DNA for 2 hours, while digestions of DNA fragments to be used in cloning were run overnight in order to achieve higher efficiency.

3.3.6. Sequencing Analysis

DNA was sent in purified plasmid form with a concentration of 100ng/µl for sequencing by Macrogen, Inc Korea.

3.3.7. Preparation of SIK3 Fly for Over-expression

With the purpose of over-expressing fly proteins SIK3 in the study and introducing 2A cleavable tag a novel tool for *Drosophila* community, pUAST-attb based vector was modified to include T2A: mCherry fusion, which was cloned beforehand in our lab to the multiple cloning sites (XhoI and KpnI) of pUAST-attB. The cDNA template FBcl0162999, corresponding to SIK3, was purchased from Bloomington Drosophila Genomics Resource Center. SIK3 fly cDNA was amplified by high fidelity DNA polymerase Advantage 2 Polymerase (Clontech), which prohibited mutations with its high proof reading capabilities, with sik3_cds_f_notI & sik3_cds_r_xhoI primers in 13 cycles. The choice primer sites were carried out the natural stop codon was omitted from PCR product .Visually confirmed and gel purified PCR product was TA cloned to pGEMT-Easy. Candidate colonies then were evaluated with colony PCR using sik3_cds_seq1 & sik3_cds_r_xhoI. One of the mutation-free colonies was retrieved from pGEMT-Easy via double restriction digestion with NotI and XhoI enzymes, which were also used to cut the backbone vector. After confirming ligation of the insert and vector via EcoRV digestion successfully, the Midi product of the prepared construct was sent to Genetivision, Inc. to be injected in a landing site (For relevant figures, see Appendix B).

3.3.8. Preparation of Human SIK3 Clone for Fly Over-expression

Two parallel methods were use to clone human SIK3 into fly over-expression vectors. The first method was involved restriction digestion of SIK3 from pCMV6 vector via restriction digestion with EcoRI and XhoI enzymes. Subsequently, the insert was ligated to EcoRI and XhoI digested pUAST vector. The selected positive colonies were selected via diagnostic digestion, sequenced. The product was sent for injection to Genetivision, Inc. USA (Company), with the aim of creating the transgenic fly to the one of the landing points in the *Drosophila* genome among the selection of the company, namely P1(2R)55C2. However, injections performed by them turned to be unsuccessful. As a solution, a new method was employed. The cloning of SIK3 human, instead of pUAST, to the pUAST-mCherry as EcoRI and XhoI restriction sites were selected for cloning. NM_025164, TA cloned to pGEMT Easy, was successfully amplified and prepared for sequencing (For relevant figures, see Appendix B).

3.3.9. Preparation of Human SIK2 Clone for Fly Over-expression

SIK2 human template NM_015191 from pcDNA4 vector was amplified by Advantage 2 Polymerase (Clontech) in the first step and it was followed by TA cloning to pGEMT-EASY vector. Verification of SIK2 human pGEMT-Easy clonings was performed with EcoRI diagnostic digest. Upon sequencing of the positive colonies, a positive colony picked, cut with NotI and XhoI, and verified by EcoRI digestion. NotI and XhoI digested SIK2 human insert retrieved through gel purification was ligated to pUAST- T2A: mCherry. Validation was performed with BglII-XhoI restriction digestion and the construct was sent to be injected to a landing site (For relevant figures, see Appendix B).

3.3.10. Semi-Quantitative Reverse Transcription Polymerase Chain Reaction

Reverse transcription coupled PCR is a frequent method utilized in order to compare levels of mRNA in a given tissue by amplification of appropriate cDNAs. In this study, RT-PCR was used to analyze changes in mRNA levels in wild-type flies and expression levels altered by RNAi.

3.3.10.1. Tissue Preparation and Total RNA Extraction. Third instar larvae were collected. Eye disc dissections were performed in ice-cold PBS on dissection pads. Tissue samples were collected immediately in ice-cold Trizol (Roche). Samples were kept in 1ml Trizol at -80°C until further used. In order to resume extraction, 500µl isopropanol was added at room temprerature. Subsequent to 10’ incubation and centrifugation at maximum speed at 4°C for 15’, the supernatants were removed. The wash step was performed via addition of 70% EtOH, which would be left to air-dry after centrifugation at 4°C. The isolated RNA was dissolved in 20µl DEPC-treated dH_2O.

3.3.10.2. cDNA Synthesis. Freshly made total RNAs was used to generate cDNA used with SuperScript First-Strand Synthesis System for RT-PCR (Invitrogen) and oligo(DT) primers. While final concentrations of samples were kept equal, up to 8µl of RNA, corresponding to 5µg total RNA at maximum, were mixed with 1µl of 10mM dNTP and 1µl oligo(DT). Subsequent to incubation at 65°C for 5’ and then on ice for 1’, RNAs were added to reaction mixture, which was composed of 10X RT buffer, 25mM $MgCl_2$, 0.1M

DTT, RNaseOUT inhibitor, and Superscript II reverse transcriptase in a total of 20µl. The reactions took place at 42°C for 1 hour. The products were stored at -20°C.

3.3.10.3. PCR and Analysis. RT-PCR primers were designed using Perl Primer software. Total cDNA was used to determine relative mRNA levels between control and experimental groups. Initially, the critical PCR cycle conditions for experimental and the control actin79b primers were determined. For each group, PCRs results were reinforced with a second PCR with an additional two cycles of amplification. The relative difference between successive PCR products would provide confidence on amplification quality and absence of over-saturation as expected ratio 1:4 was maintained. The levels of PCR products in different backgrounds were compared and normalized to the control actin79b PCR product and quantified using ImageJ.

3.3.11. Protein Expression Analysis

3.3.11.1. Total Protein Preparation. Embryo Lysis Buffer was freshly prepared and 20 females from F1 flies of the genotype of interest, as in scheme X.X, were collected. Their heads were dissected in ice-cold PBS on dissection pads, and transferred to the lysis buffer. Heads were homogenized properly by using sterile pipette tips. Following a brief vortex and spin down, the mixture was incubated on ice for 15'. The remaining insoluble debris was removed after centrifugation at 10.000 rpm for 10' at 4°C, while the lipid layer was avoided during supernatant collection. The supernatant was incubated at 99°C for 5' subsequent to addition of 120µl 3X Laemli's buffer and a 2M DTT mixture. The final product was stored at -20°C for Western blot analysis.

3.3.11.2. Western Blot. Protein extracts of 25µl were loaded to an 8% resolving gel and run under constant current of 30 mA. Subsequently, proteins were transferred to nitrocellulose membranes for 2 hours under 200 mA. While ensuring the quality of protein integrity and quantity with Ponceau's Red staining, membranes were washed with TBST for 3 times for 10'. In order to reduce non-specific binding, membranes were blocked with 5% milk powder for 1 hour at room temperature. Membranes were incubated with primary antibody in 2% milk at 4ºC overnight and after several washes with TBST the secondary antibody was applied in 1% milk for 30 minutes at room temperature. Following three successive

washes with TBST for 10 minutes each, membranes were incubated in LumiGlo for 3 minutes for detection and exposed in the image acquisition apparatus Stella (company) for 10 minutes.

3.4. Histological Techniques

3.4.1. Immunohistochemistry for Larval Eye and Wing Discs

Drosophila larvae were collected in ice-cold 1X PBS on a dissection pad, and the larval CNSs attached to larval mouth were quickly dissected. Immediate to dissection of each larval CNS, the specimen was put into a 1.5ml microfuge tube containing PBS. PBX3 was removed and replaced by 4% paraformaldehyde in which tissues was fixed for 20'. Three 10' washes with PBX3 at constant low-speed shaking were followed by a blocking step in BNT solution that was applied for 1 hour. Subsequently, primary antibodies were added in BNT and the tissues were incubated overnight at 4°C. Removal of the primary antibody mix was performed by three PBX3 washes. Secondary antibodies were added and incubated at room temperature for 2 hours in the dark. After several PBX3 washes to remove the secondary antibody, larval imaginal discs and brains were transferred onto a dissecting pad where tissues were prepared and mounted individually in Vectashield (Vector Laboratories) on Fisherbrand Plus Microscope Slides (Fisher Scientific). Microscopic analyses were performed via visualization under a fluorescent microscope (Zeiss) or a confocal microscope (Leica).

3.4.2. Immunohistochemistry for Sections of Adult Head and Whole Flies

The flies were anesthetized by CO_2 and bathed in PBX3 for 5 minutes either as a whole or only the head after dissection on CO_2 pad with a fine dissecting forceps. Later, the specimens were embedded in Tissue-Tek O.C.T. Compound (Sakura Finetek) and quickly frozen at -80°C. Samples were sectioned on a cryostat into 12μm sections and placed onto Fisherbrand Superfrost Slides. After tissue sectioning was completed, the slides were air dried at room temperature. The fixation was carried out with 4% PFA for 15 minutes. The staining procedure was performed as outlined in 3.4.1.

3.4.3. Image Analysis

Analysis of the images was performed with ImageJ software, which was utilized for color channel merging, color adjustments, and cell counting.

3.5. Fly Genetics

3.5.1. Generation of Transgenic Fly Lines

Generated fly transformation vectors were sent to the company Genetivision Inc, USA for injection. Selections of stable transgenic lines were either performed by Genetivision, Inc or in our lab by crossing flies to balancer lines.

3.5.2. Fly crosses:

Virgin female flies were collected in abundance from the driver lines and balanced with a GFP carrying chromosome (to avoid homozygous lethality of most GAL4 lines); 6-7 virgin females were then crossed with males of the relevant genotype in a ratio of 3:2 females versus males. According to successive experiment, by-products in F1 progeny without GAL4 were selected, either in larval or adult stage, under fluorescence microscope for in vivo GFP expression. Remaining flies were then dissected, or phenotypically evaluated further. A list of the crosses performed in this study is given in Table 3.5.

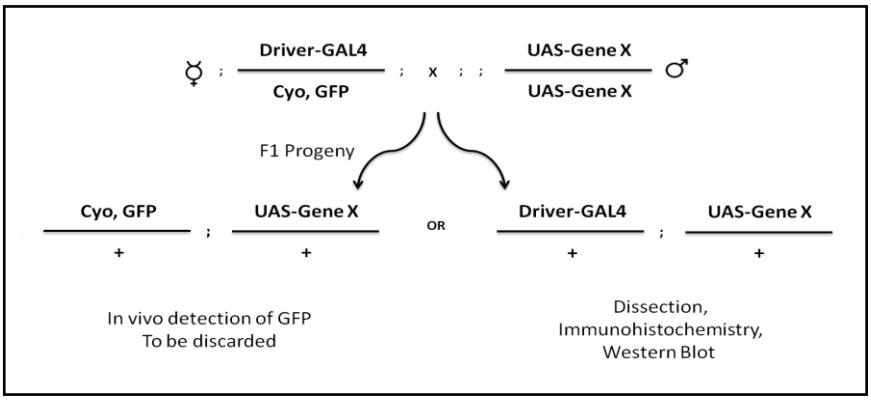

Figure 3.1. Representative cross between a virgin female carrying a Gal4 line in her second chromosome and a male carrying a UAS line in his third chromosome.

Table 3.6. List of Fly Crosses Performed with Following Experiments.

Fly Crosses						
	Tumorigenesis			**Migration**		**Western, RT-PCR**
Transgene	***sensitized***	***eyeful***	**ey-GAL4, lGMR-GAL4**	**repo-GAl4**	**ptc-GAL4**	**ELAV-GAL4**
UAS-SIK2	✔	✔	✔	✔	✔	✔
UAS-SIK2 CA	✔	✔	✔	✔	✔	✔
UAS-SIK2 KD	✔	✔	✔			
$SIK2^{\Delta 41}$	✔	✔	✔			
UAS-SIK3	✔	✔	✔	✔	✔	✔
UAS-SIK3 CA	✔	✔	✔	✔	✔	✔
UAS-SIK2 Human	-	-	-	-	-	-
UAS-SIK3 Human	-	-	-	-	-	-
w1118	✔	✔	✔	✔	✔	✔

3.5.3. Tumorigenesis Analyses

Evaluation of SIKs as tumor suppressors or oncogenes was performed by evaluation of two distinct score sets, *presence of eye folding* (PEF) and *number of visible macrometastases* (NVM), and subsequent determination of statistical significance by χ^2 test against background values. After each cross set as illustrated in Table 3.5.1 and control crosses of combining background and w118 flies, flies were raised in standard conditions of 25°C. For PEF score estimation, due to their independent emergence, each eye of the progeny was surveyed individually for the appearance of folding. While the severity of folding was not included, which otherwise can be estimated by counting the number of foldings per individual eye, the presence of at least one folding was recorded as positive. NWM scoring is performed by counting number of visible macrometastases, which can be easily observed due to the accumulation of eye pigments in these tumors, outside the enlarged eye field of sensitized flies. Each individual macrometastases per fly was taken into account.

Statistical analyses were carried by use of 2x2 contingency tables and further by standard χ^2 tests where test crosses were compared to the background score. In each test group, at least a number of 120 specimens were analyzed.

3.5.4. Migration Assays

3.5.4.1 Glia Migration Assay. Third instar larval eye disc of flies carrying UAS lines driven with the glia-specific driver repo-GAL4 were dissected as previously described in 3.4.1. The rates of retinal basal glia migration onto the eye disc was evaluated by the number of repo-positive glia in the disc divided by the number of differentiated photoreceptor rows posterior to the MF and compared to the control group, which is the progeny of the cross between repo-GAL4 and w118 line.

3.5.4.2 Wing Migration Assay. Wing discs of third instar larvae carrying UAS-SIK lines under the control of the driver ptc-GAL4 were dissected and the A-P boundary of the wing discs were analyzed for invasion by ptc positive cells, which were visualized by GFP expression in the invaded tissue.

3.6. Bioinformatic Analyses & Data Mining

3.6.1. Protein Structure Analysis

The protein sequences corresponding to SIK2 & SIK3 Fly mRNAs were retrieved from Flybase and loaded onto Simple Modular Architecture Research Tool SMART (Schultz *et al.*, 1998) to visualize the domain structure. The same study was performed with PFAM. Later short protein motifs in these proteins were searched in Scansite 2.0 (Obenauer *et al.* 2003). NCBI curated reference sequences of Human SIKs were analyzed in the same manner.

3.6.2. Alignment and Phylogenetic Analysis

Considering the evolutionary distance between SIK homologs, starting from *Saccharomyces cerevisiae* as stated in Unigene, NCBI Protein Blast was chosen to be the primary method for finding the homologs of SIK Fly proteins. All homologs were chosen form ref.seq. database, except NCBI and Ensembl predicted proteins. Alignment of the respective mRNA sequences of the respective proteins was performed, using default settings at the ClustalW server of EMBL-EBI. Mega5b7 Build: #5101201 was utilized for

phylogenetic analysis, after files were converted to meg format: Using the Kimura2 algorithm parameter adjusted for coding DNA sequences in Neighbor-Joining method or Maximum Likelihood method based on the Tamura-Nei algorithm, along with pair-wise deletion and Bootstrap test of phylogeny with repeats of 1000, the initial phylogeny was constructed (Kimura 1980; Tamura and Nei 1993). Due to convergence of several Lkb1-AMPK members onto similar proteins at their conserved serine-threonine kinase domains in the early invertebrates and lack of curated evidence, these mRNA sequences were omitted from later alignments.

3.6.3. PAML Analysis

Subsequent to loading files from ClustalW, the selected sequences were modified by removal of gapped columns manually in Genedoc 2.6.002 software. Extraction of phylip, text files from Genedoc and phylogenic tree data from Mega as newick standard files, the respective ctl files edited and three ω models were run using codeml.exe of PAML, which calculates evolution rates within a given cladogram and statistically asses its significance to a maximum likelihood method (Yang 1997).

3.6.4. Expression Pattern Analysis

EST Profiles of ref. seq. human SIKs from NCBI, combined with micro-array data retrived from Oncomine and Affymetrix based FlyAtlas Organ/Tissue Expression pattern of are collected, and compared (Shyamsundar *et al.* 2005).

3.6.5. Cancer Database Analyses

Using three publicly available databases, Cancer Genome Project by NIH, cBIO by Memorial Sloan-Kettering Cancer Center and Mutome by Roche, all reported somatic mutations in the literature were collected, except silent mutations which have no effect in end-product protein. The predicted impacts of these mutations were analyzed independently by two methods, Mutation Assessor and PolyPhen2, using different algorithms. Moreover, via cBIO, the effects of SIK mutations on molecular signatures and patient survival were inquired. Using Mutome by Roche and Oncomine, SIK levels among

several cancer types were evaluated. As Mutome database were used to gather information on genome-wide statistically significant data on loss or gain in the copy number of SIK genomic region, while Oncomine to evaluate gene expression. (MacDonald and Ghosh 2006).

4. RESULTS

4.1. Bioinformatic Analyses of Salt Inducible Kinases

4.1.1. SIK2 Fly Shows Homology for Both Human SIK1 and SIK2

Every study covering proteins diverged hundred million years ago should reconstruct homology carefully and faithfully; however both qualities are a scarcity in the automatically generated pipeline data of public resources. The problem manifests itself when SIK orthologs were enquired, several public databases presented different proteins as homologs of human SIKs (data not shown).

With the purpose of carrying out phylogenetic analysis of SIKs, Mega5 software was used to build up homology trees from the ClustalW aligned protein sequences which were derived from public databases. Among different algorithms to calculate distance between protein sequences, the calculation methods which represented best approximations of the consensus in the literature were selected. The fidelity of the constructed trees was evaluated by the bootstrap method; any tree containing several unreliable branches, which were marked by a score lower than 50 at the root of relevant branch depicted in the tree, was discarded.

Constructing the SIK family homologs exhibits a frequent problem. As most of the conservation lied in the domain providing kinase activity for SIKs, which is well conserved among the super-family, several different proteins gave hits for the same gene. This is especially valid for the fly homolog of SIK2 and reflected itself in the following phylogenetic trees. Figure 4.1 shows an initial reconstruction of all SIK family members and their homologs. The first striking feature was the clustering of SIK1&2 in vertebrates; Fly SIK2 resided in the most distant branch, indicating the possibility of a gene duplication event. Meanwhile, the SIK3 cluster formed another root, departing for the other SIK lineage before divergence of the fly SIK2. Although bootstrap values instilled confidence, the tree was not without problems: *Gallus gallus* and *Danio rerio* species in the SIK1 branch were misplaced.

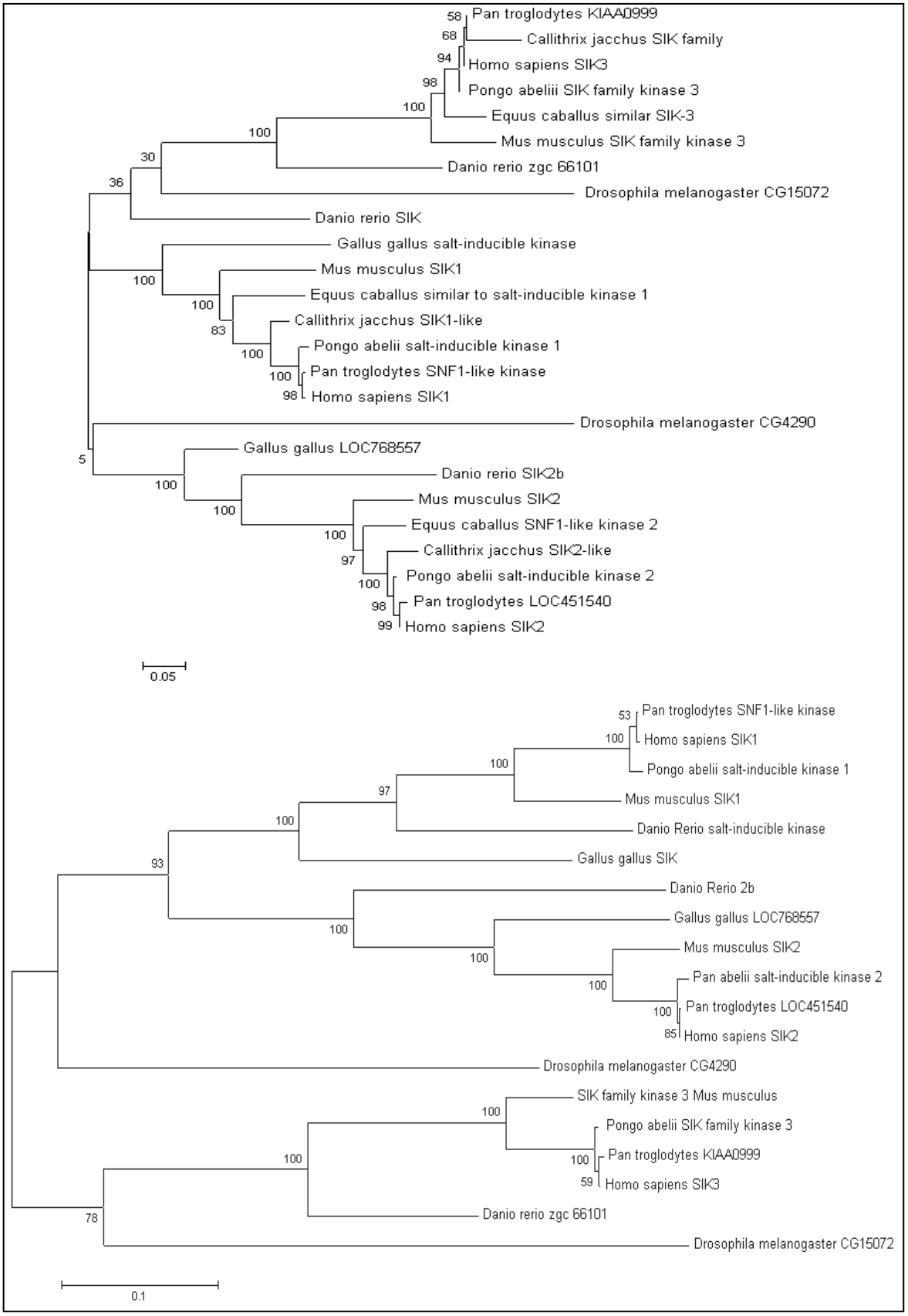

Figure 4.1. Kimura2 and Tamura-Nei algorithms based homology trees for SIK proteins across species.

The second and expanded phylogenetic tree with addition of *Equus Caballus* and *Callithrix jacchus*, presented other problems. In the phylogeny, putting more information in the higher groups seemed to destabilize the early branches. This time, fly SIK2 clusters with the SIK2 group, while causing a low bootstrap score as low as 5. Additionally, the SIK1 homolog of zebrafish was located in the SIK3 homology group, as the distance between SIK3 and other branches diminished. Yet, these results opened the possibility of a closer relation between human SIK1 and fly SIK2.

A possible relation between fly SIK2 and human SIKs can be easily visualized in Figure 4.2 with a straightforward protein blast. When both human SIK1 and SIK2 were aligned against fly SIK2, excluding the kinase domain, the respective homology domains of human SIKs do not overlap with the fly SIK2 protein. Rather, they aligned at other regions, which in total cover almost the whole fly SIK2 sequence.

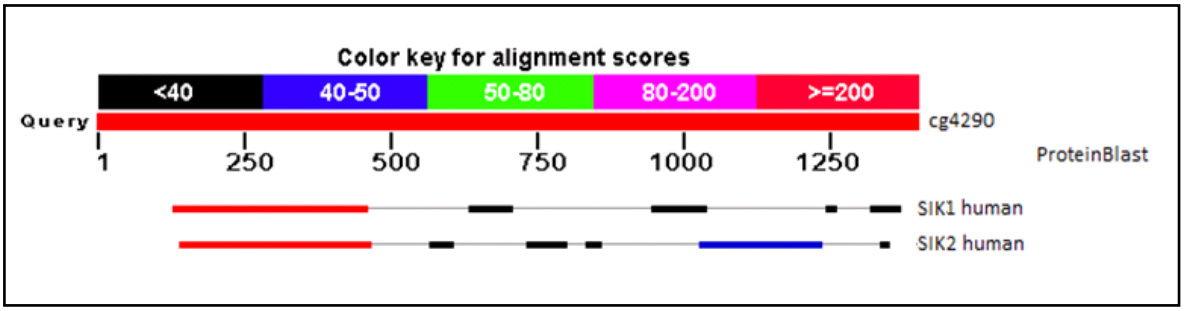

Figure 4.2. Combined protein blast for fly SIK2 versus human SIK1 and SIK2.

Another way to elucidate the relationship between fly SIK2 and SIK1&2 was to investigate similarities in the protein level from a functional perspective. The construction of functional domains in the SMART database search revealed that, other than the well-known serine-threonine kinase domain, which plays a role in controlling activity of a substrate protein via phosphorylation and can cause changes in stability and cellular localization, it was not possible to find a shared domain (Figure 4.3). Interestingly, the only exclusive domain was harbored by SIK1 is the ubiquitin-associated-domain (UBA), which is known to be primarily associated with protein degradation.

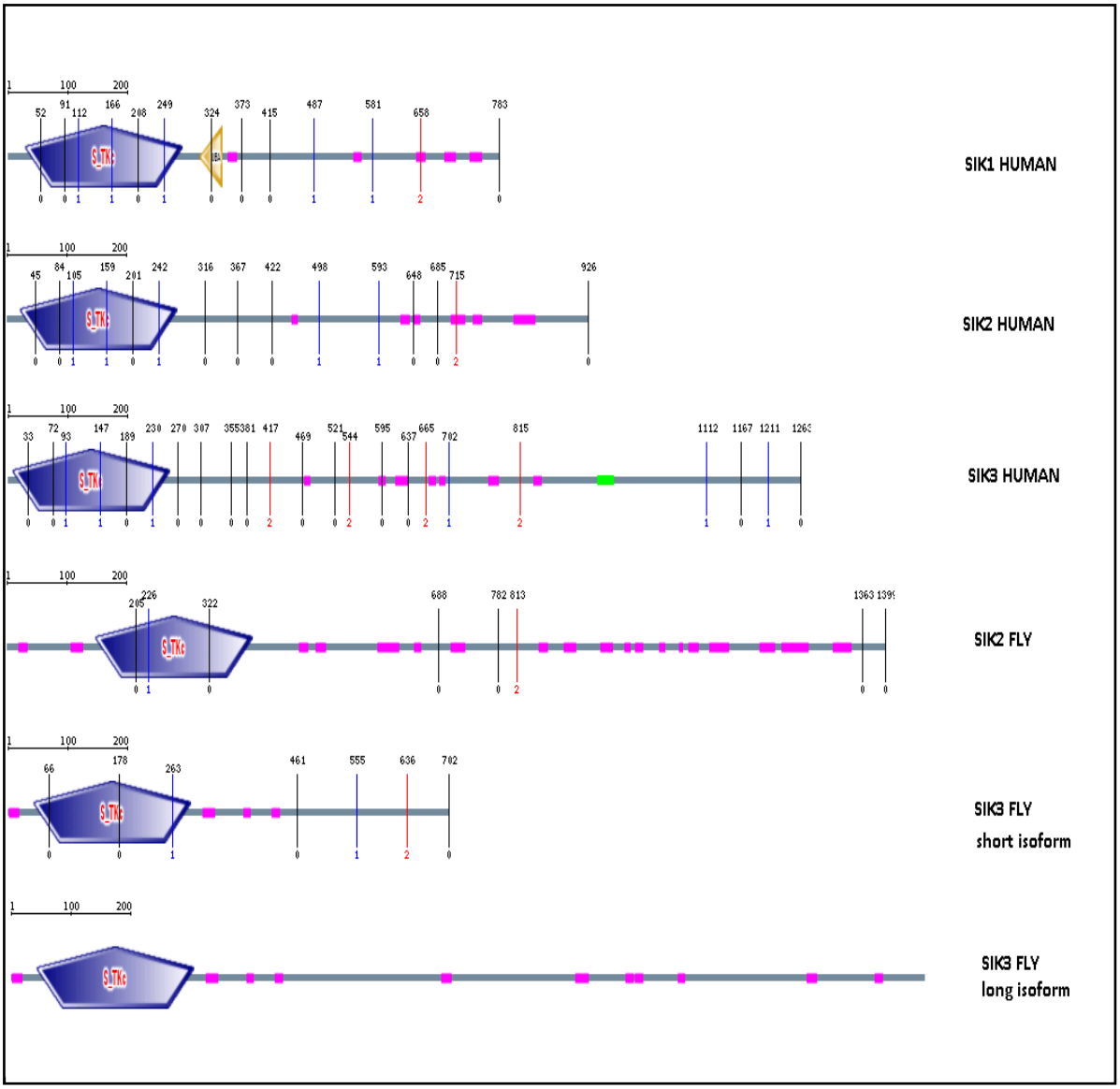

Figure 4.3. SMART protein domain prediction for human and fly SIK proteins.

Similar motifs in SIK proteins were analyzed with Scansite, which is program that provides motif search for several groups of protein interactions (Table 4.1). Results with medium stringency search criteria were discarded due to high number of motif predictions and presence of possible false positives (data not shown). High stringency results showed that SIKs interact with many proteins related to significant biological roles, including survival, cell cycle control, DNA damage, and the cytoskeleton; yet it was not possible to identify respective motif homologies of human and fly proteins within these clusters.

Table 4.1. Protein motifs predicted by Scansite for human and fly SIK proteins.

Scansite2.0 High Stringency Protein Motifs								
	Tyrosine kinase group	**Src hom. 2**	**Src hom. 3**	**Basophilic S/T kinase group**	**Acidophilic S/T kinase group**	**DNA damage kinase group**	**Proline-dependent S/T kinase group**	**Kinase binding site group**
SIK1 human			Intersectin	PKA		DNA PK		PDK1
			Amphiphysin			ATM		Erk D
SIK2 human		Fyn	Abl	PKA	GSK3			Erk
			Nck 2nd					Erk D
			Intersectin					
			Src					
			Amphiphysin					
			PLCg					
			Itk					
			c-Cbl					
SIK3 human				PKA	Casein Kinase 2	ATM	Cdk5	Erk D
				PKC zeta			Cdc2	
				PKC mu			Erk1	
SIK2 fly		Itk	Itk	PKC	Casein Kinase 1	DNA PK	Cdk5	Erk D
			Abl	PKA	GSK3		Cdc2	
				PKC delta			Erk1	
				CaMKII				
				AMP_Kinase				
SIK3 fly	Src	Crk		PKA				PDK1
				PKC epsilon				Erk D
				PKC delta				
				Akt Kinase				
				CaMKII				
SIK3 fly_l	Src	Crk		PKA			Cdk5	Erk D
				PKC epsilon			Cdc2	PDK1
				PKC delta			Erk1	
				Akt				
				CaMKII				

Comparison between the expression levels of human and fly SIKs revealed a pattern containing both overlaps and exclusive regions. Fly SIK2 expression was found to be highly increased in the brain, eye, thoracico-abdominal ganglion, heart, fat body, male reproductive tract according to the FlyAtlas, which suggests a correlation in expression for human SIK1. Fly SIK3 data showed expression in the brain, thoracico-abdominal ganglion, salivary gland, hindgut, larval fat body and only significant increase in ovary; yet in all cases fly SIK3 expression remained much lower (>1:10) compared to fly SIK2 (Table 4.2). We identified the respective tissues of enriched human SIK expression using public micro array data (Figure 4.4). Strikingly, both SIK2 and SIK3 showed very broad expression

patterns where SIK3 levels were elevated in brain, testis, muscle and breast, while increased SIK2 expression was observed in colon and stomach. In contrast to the other SIKs, SIK1 showed clear restricted and high-level expression primarily in adrenal glands, kidneys, pancreas, thymus, the female reproductive tract, and prostate.

Table 4.2.Expression patterns of fly SIKs.

Fly SIK Expression						
Tissue	**mRNA Signal**	**Enrichment**	**Affy Call**	**mRNA Signal**	**Enrichment**	**Affy Call**
	SIK2			**SIK3**		
Brain	143 ± 5	17.30	Up	10 ± 1	1.00	None
Head	48 ± 3	5.80	Up	2 ± 0	0.30	None
Eye	103 ± 9	12.41	Up	4 ± 1	0.42	None
TA Ganglion	117 ± 1	14.10	Up	10 ± 2	1.10	None
Salivary gland	22 ± 6	2.66	None	13 ± 5	1.42	None
Crop	12 ± 2	1.50	None	9 ± 2	1.00	None
Midgut	5 ± 1	0.70	None	3 ± 0	0.30	None
Tubule	4 ± 0	0.60	Down	6 ± 1	0.70	Down
Hindgut	9 ± 0	1.10	None	13 ± 1	1.40	None
Heart	26 ± 1	3.16	Up	3 ± 1	0.31	None
Fat body	28 ± 10	3.39	Up	4 ± 3	0.48	None
Ovary	1 ± 0	0.20	None	20 ± 1	2.10	Up
Testis	6 ± 0	0.80	None	9 ± 1	1.00	None
Male accessory glands	18 ± 1	2.20	Up	2 ± 0	0.20	Down
Virgin spermatheca	7 ± 1	0.91	None	1 ± 0	0.18	Down
Mated spermatheca	9 ± 1	1.10	None	1 ± 0	0.14	Down
Adult carcass	41 ± 5	5.00	Up	7 ± 2	0.70	None
Larval CNS	91 ± 5	10.98	Up	3 ± 2	0.38	None
Larval Salivary gland	4 ± 0	0.48	None	3 ± 1	0.38	None
Larval midgut	9 ± 0	1.18	None	3 ± 0	0.33	None
Larval tubule	4 ± 1	0.50	None	8 ± 2	0.90	None
Larval hindgut	5 ± 2	0.65	None	2 ± 1	0.28	Down
Larval fat body	7 ± 2	0.90	None	13 ± 2	1.40	None
Larval trachea	3 ± 1	0.36	None	1 ± 0	0.15	Down
Larval carcass	6 ± 1	0.78	None	3 ± 0	0.37	None
S2 cells (growing)	16 ± 1	2.02	Up	17 ± 1	1.80	Up
Whole fly	**8 ± 2**			**9 ± 2**		

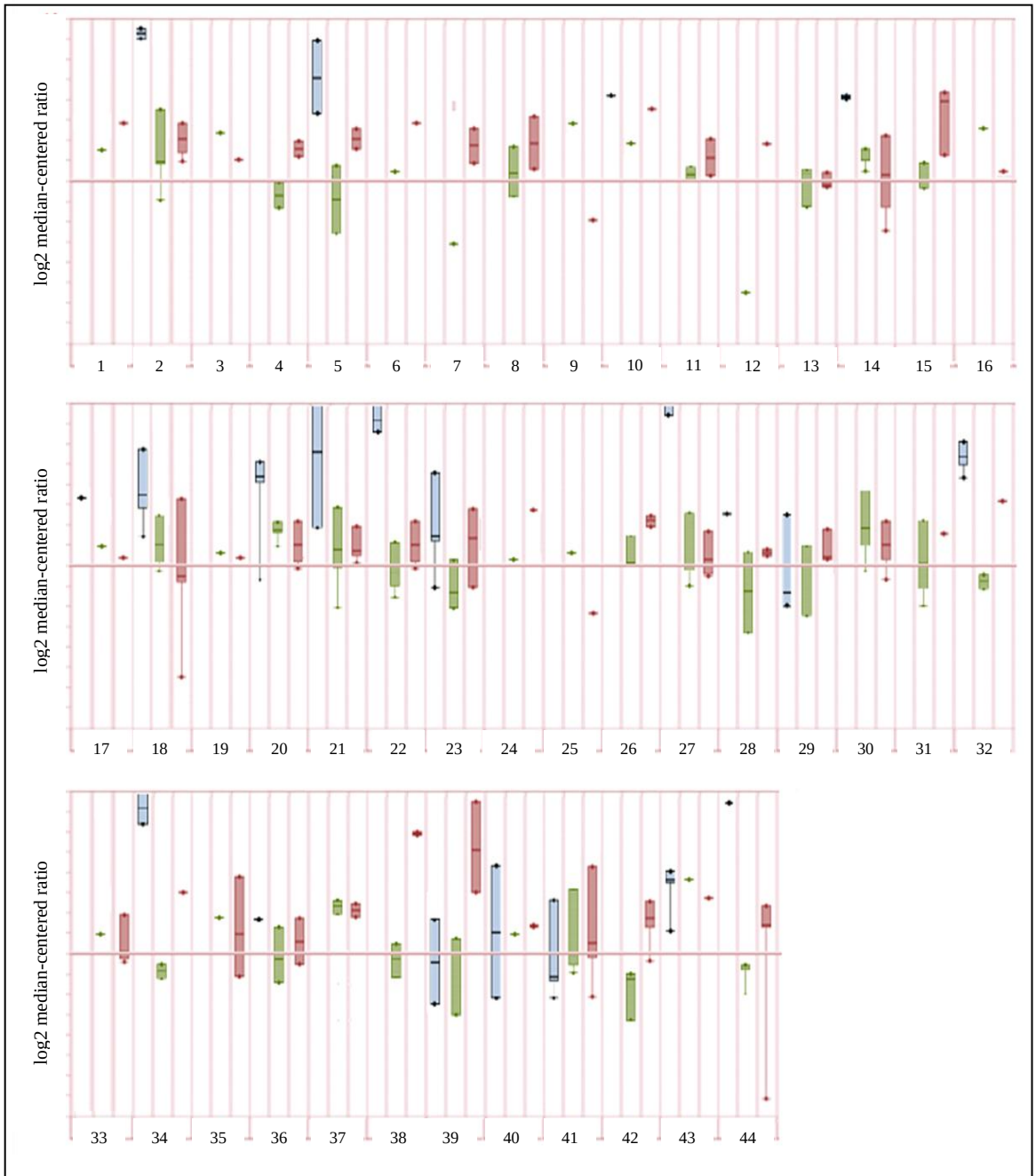

Legend

1. Abdominal Muscle	9. Colon	17. Gallbladder	25. Myometrium	33. Pylorus	41. Thyroid Gland
2. Adrenal Gland	10. Diaphragm	18. Heart	26. Occipital Lobe	34. Seminal Vesicle	42. Tonsil
3.Ascending Colon	11. Duodenum	19. Ileum	27. Ovary	35. Sigmoid Colon	43. Vagina
4. Axilary Lymph Node	12. Endocervix	20. Kidney	28. Pancreas	36. Spleen	44. Wall of Uterus Body
5. Bladder	13. Esophagus	21. Liver	29. Parathyroid Gland	37. Stomach	
6. Breast	14. Fallopian Tube	22. Lung	30. Parotid Gland	38. Temporal Lobe	
7. Buffycoat	15. Frontal Lobe	23. Lymph Node	31. Pericardium	39. Testis	
8. Cervix Uteri	16. Fundus of Stomach	24. Muscle	32. Prostate Gland	40. Thymus Gland	

Figure 4.4. Expression patterns of human SIKs. Blue represents SIK1, while SIK2 is shown in green, and SIK3 in red.

4.1.2. SIKs are Under Strong Natural Selection

A probable duplication event in the history of Salt Inducible Kinases enabled us to test the notion of SIKs as a part of a physiologically crucial metabolic network. Therefore, PAML analysis was applied. By calculating the ratio of a non-synonymous substitution rate over synonymous substitutions, the free ratio model, where ratio calculated without any restrictions, showed a general tendency of strong natural selection in all branches of SIK evolution. Highest score emerged subsequent to speciation events after divergence of SIK1&2 branches. Zero and two ratio models, applied for the verification of the free ration model, clearly showed that, indeed, in this cladogram scheme the resulting rate of evolution is very low. Either forcing an equal rate of dn/dS ratio (zero model) or fix one of the branches to positive evolution (two ratio model, ω_2=2) to an otherwise negative rate, was highly different in statistical terms of p-value<0.001 (Figure 4.5).

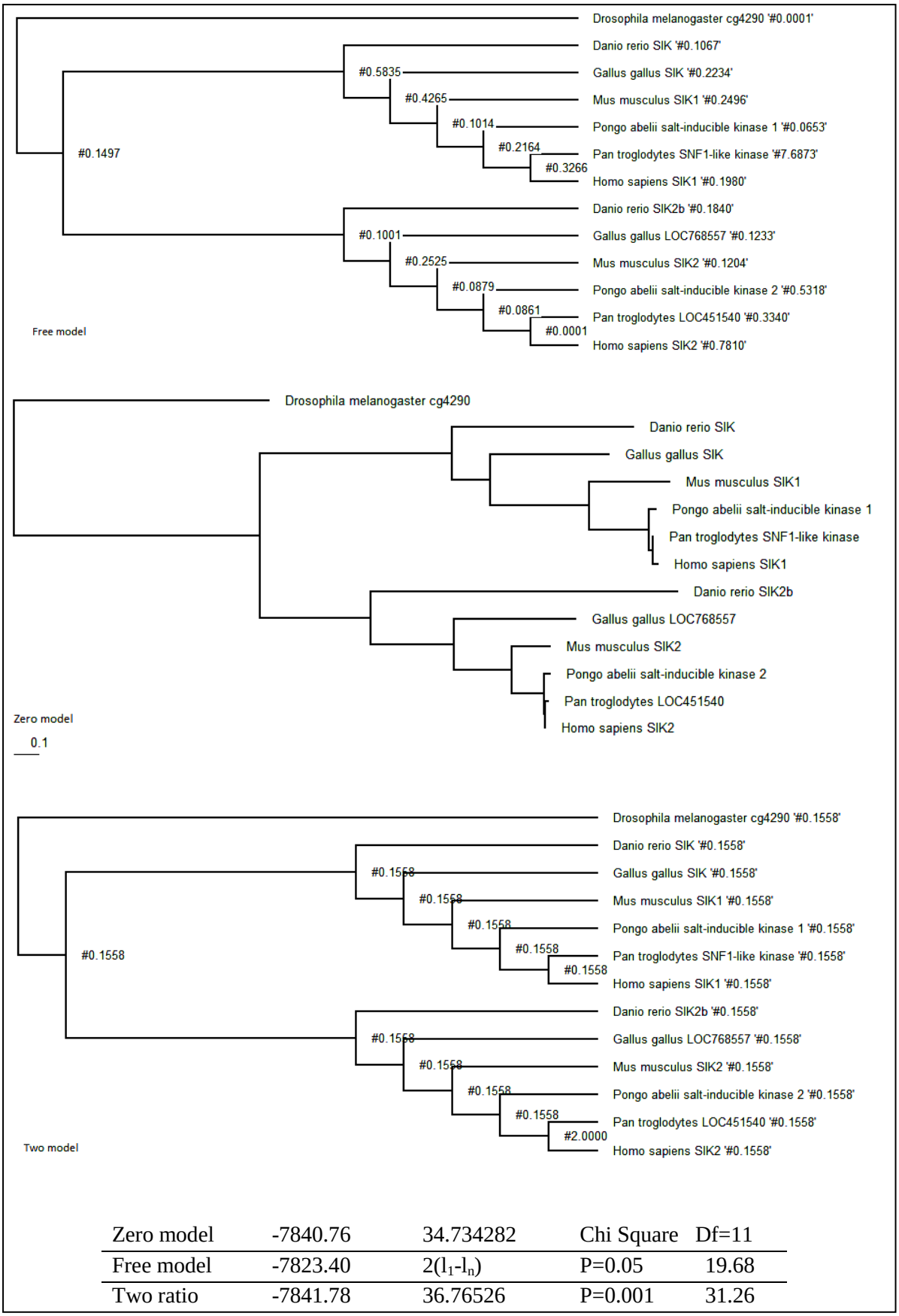

Zero model	-7840.76	34.734282	Chi Square	Df=11
Free model	-7823.40	$2(l_1-l_n)$	P=0.05	19.68
Two ratio	-7841.78	36.76526	P=0.001	31.26

Figure 4.5. SIK PAML cladograms and statistical difference between models.

4.2. Salt Inducible Kinases in Cancer Databases

The availability of faster, cheaper sequencing techniques, now possible with RNA itself, and higher computational power set a trend in cancer research. Via public databases, it is possible to analyze the role of a given protein from various angles, although some aspects, like whole genome sequencing of all cancer types for example, of these databases are still in their infancy. As a result, we decided to compare and reinforce our data of the possible roles of SIKs in tumorigenesis generated *in vivo* with *in silico* data.

4.2.1. Cancer Mutations of SIKs Hit Functionally Significant Domains

Table 4.3. Available SIK mutations in cancer databases.

Mutations			
Protein	**Mutations**	**Cancer Type**	**Source**
SIK1	E153K	Colorectal Carcinoma	TCGA-AA-A01R
	G211S	Glioma	cBio Provisional/Sanger COSMIC
SIK2	E103X	Colorectal Carcinoma	TCGA-AG-A002
	T608P	Colorectal Carcinoma	TCGA-AA-3715
	R356Q	Colorectal Carcinoma	TCGA-AA-A00J
	F166L	Colorectal Carcinoma	TCGA-AG-A002
	G497E	Glioma; astrocytoma Grade IV	cBio Provisional/Sanger COSMIC
	A635V	Glioma; astrocytoma Grade IV	cBio Provisional/Sanger COSMIC
	V95E	Malignant melanoma	cBio Provisional/Sanger COSMIC
	K137N	Esophageal carcinoma	cBio Provisional/Sanger COSMIC
	T458I	Germline	Roche Mutome
	R809Q	Germline	Roche Mutome
	P825L	Germline	Roche Mutome
SIK3	S1056X	Colorectal Carcinoma	TCGA-AG-A002
	Q458X	Colorectal Carcinoma	TCGA-AA-3525
	Q159K	Colorectal Carcinoma	TCGA-AA-3549
	E85K	Colorectal Carcinoma	TCGA-AA-3710
	L372P	Colorectal Carcinoma	TCGA-AA-3947
	F120C	Colorectal Carcinoma	TCGA-AA-A00N
	L667F	Serous Ovarian Cancer	TCGA-13-0890
	R560C	Serous Ovarian Cancer	TCGA-24-1551
	R666C	Serous Ovarian Cancer	cBio Provisional/Sanger COSMIC
	L773F	Serous Ovarian Cancer	cBio Provisional/Sanger COSMIC
	H389L	Breast, Ductal Carcinoma	cBio Provisional/Sanger COSMIC
	A1209V	Breast, Ductal Carcinoma	cBio Provisional/Sanger COSMIC
	E702Q	Breast, HER-positive carcinoma	cBio Provisional/Sanger COSMIC
	H686Y	Stomach carcinoma	cBio Provisional/Sanger COSMIC
	P836S	Non Small Cell Lung Carcinoma	cBio Provisional/Sanger COSMIC
	S882C	Kidney Carcinoma	cBio Provisional/Sanger COSMIC
	H331L	Somatic	Roche Mutome
	A1103V	Somatic	Roche Mutome

Using three publicly available databases, Cancer Genome Project by NIH, cBIO by Memorial Sloan-Kettering Cancer Center and Mutome by Roche, we collected all reported somatic mutations in the literature, except silent mutations, which have no effect on the final protein product (Table 4.3). So far, only very a few mutations have been identified and published for SIK1 and no germline mutations of SIK3. Except for germline SIK2 mutations and mutations in carcinomas only for SIK3, no clear pattern in the distribution of mutations according to tissue types exists. Overall, mutation frequencies remain low, fluctuating around 1% in the respective cancer type (data not shown). When we analyzed the predicted impacts of these mutations by two independent prediction methods (Mutation Assessor and PolyPhen2) using different algorithms, most of these would hinder SIK kinase function in a high probability (Table 4.4). These mutations reside either in the kinase domain directly associated with its activity or, in case of SIK3, the glycine-rich domain which affects its affinity to its binding partners.

Table 4.4. Domains of SIKs targeted in cancers and putative effects.

Mutations											
Cancer Type	**Mutations**			**Hit Domains**		**Mutation Assessor**			**PolyPhen-2**		
	All	**Missense**	**Nonsense**	**Kinase**	**Glycine Rich**	**High**	**Medium**	**Neutral**	**Probable Damage**	**Possible Damage**	**Benign**
SIK1											
Colorectal	1	1		1		1			1		
Breast											
CNS	1	1		1		1			1		
Blood											
Kidney											
Cervical / Ovarian											
Lung											
Pancreas											
Skin	1	1						1			1
Stomach											
Urinary tract											
Sarcoma											
Germ line											
Other Carcinoma											
Other											
SIK2											
Colorectal	3	2	1	1			2	1	3		
Breast											
CNS	2	2					2		2		
Blood											
Kidney											
Cervical / Ovarian											
Lung											
Pancreas											
Skin	1	1		1		1					

Table 4.4. Domains of SIKs targeted in cancers and putative effects (continued).

Mutations (*continued*)											
Cancer Type	**Mutations**			**Hit Domains**		**Mutation Assessor**			**PolyPhen-2**		
	All	**Missense**	**Nonsense**	**Kinase**	**Glycine Rich**	**High**	**Medium**	**Neutral**	**Probable Damage**	**Possible Damage**	**Benign**
SIK2 (continued)											
Stomach											
Urinary tract/bladder											
Sarcoma											
Germ line	3	3					1	2	1	1	1
Other Carcinoma	1	1						1			
Other											
SIK3											
Colorectal	6	4	2	3	1	1	2	1	3	1	0
Breast	3	3			1	1			3		
CNS											
Blood											
Kidney	1	1			1						1
Cervical / Ovarian	4	4					3		4		
Lung	1	1			1				1		
Pancreas											
Skin											
Stomach	1	1			1						
Urinary tract											
Sarcoma											
Germ line											
Other Carcinoma											
Other	2	2		1			2			1	1

4.2.2. Loss of SIKs could be observed in several cancers

The Roche Company screened approximately 3000 genomes, and the only significant changes were observed for the deletion of SIK1 and in case of SIK3 a widespread significant genomic loss was evident (Table 4.5). Only amplification in haematopoietic tissue remained non-significant in the context of gain of SIK3. The Roche database does not provide information for SIK2.

Oncomine revealed significant loss of SIK2 and SIK3 in different cancers belonging to several tissue types, some overlapping the Roche data (Table 4.5; thresholds chosen, lenient: p-value 0.001, fold change 1.5, gene rank all and strict: p-value 0.001, fold change 1.5, gene rank 1%). Though lower in frequency, both SIK2 and SIK3 showed also gains; yet these were lost when the selection criteria were narrowed to be include only highest ranking genes (<1%), whereas SIK2 loss in breast and blood cancers, SIK3 loss in colorectal and germ line cancers remained pivotal.

Since tumors show heterogeneity within themselves, Oncomine also offered the analysis in a subset of a population of cancers where a major driver event, such as a decisive genomic alteration is absent outside the subset (Cancer Outlier Profile Analysis, COPA, p-value: 0.001, fold change: 1.5, gene rank: 1%). In this outer analysis, expression of SIK3 was found to be down-regulated at higher frequencies, while ovary cancer showed the highest loss rate. SIK2 levels fluctuated in a wider range in outer analysis; in some cases, both high levels of gain and loss were observed. Interestingly, SIK1 turned out be highly important for pancreas cancers and loss in every one of two pancreas cancers were observed in outer cases. However, globally for outer, cases of SIK1 loss were reported in less than 1% of cancers.

Table 4.5. Cases of change in level of expression of SIKs through several cancers.

Bioinformatic Analysis of SIKs in Cancer								
	Roche Genomewide Chromosome (Q value <=0.25)		**Oncomine**					
			Lenient		**Strict**		**Outer Strict**	
	Amplification	**Deletion**	**Gain**	**Loss**	**Gain**	**Loss**	**Gain**	**Loss**
SIK1								
Colorectal								
Breast		0.0112	5%	29%			6%	
CNS		0.0281						
Blood		4.05E-4		10%				
Kidney								
Cervical / Ovarian							20%	
Lung		0.0832						
Pancreas								50%
Skin		1.91E-6						
Stomach								
Urinary tract								
Sarcoma								
Germ line								
Other Carcinoma		3.59E-9	20%					
Other								
Total		**5.15E-15**	**2%**	**7%**			**0%**	**0%**
SIK2								
Colorectal	n/a	n/a	6%				3%	6%
Breast				24%		6%		2%
CNS								
Blood			23%	13%		3%		5%
Kidney								
Cervical / Ovarian							20%	20%
Lung				32%				
Pancreas								
Skin								
Stomach				14%				
Urinary tract								
Sarcoma								
Germ line			10%					3%
Other Carcinoma			11%	4%				12%
Other								
Total			**3%**	**9%**		**1%**	**0%**	**1%**

Table 4.5. Cases of change in level of expression of SIKs through in cancers (continued).

Bioinformatic Analysis of SIKs in Cancer (*continued*)								
	Roche Genowide Chromosome (Q value <=0.25)		**Oncomine**					
			Lenient		**Strict**		**Outer Strict**	
	Amplification	**Deletion**	**Gain**	**Loss**	**Gain**	**Loss**	**Gain**	**Loss**
SIK3								
Colorectal			9%	27%		1%		10%
Breast		0.0112	3%	12%				2%
CNS		0.0281		25%				4%
Blood	0.749	4.05E-4	16%	12%				3%
Kidney				25%				13%
Cervical / Ovarian								29%
Lung		0.0832		15%				4%
Pancreas				17%				
Skin		1.91E-6						
Stomach			14%					
Urinary tract				30%				
Sarcoma				14%				14%
Germ line				22%		1%		
Other Carcinoma								
Other								
Total			**3%**	**15%**		**1%**		**3%**

4.2.3. SIKs in Colorectal Carcinoma

The most inclusive data available of SIK mutations on a particular type of cancer is colorectal cancer. Using cBIO, we inquired the effects of these mutations on molecular signatures and patient survival (Table 4.6). For the subset of patients with mutations in SIK3 a better prognosis was possible, which is statistically significant. On the contrary, SIK2 mutations shortened the patient survival rates. Due to the low frequency of SIK1 mutations (1 missense mutation, <1%), it was not possible to assess the real impact of SIK1. Still, in the patients with SIK1 mutations, a shorter prognosis was observable.

Loss of SIK3 causes a possible compensatory increase in SIK2. The common view is that compensatory relationships exist among members of the AMPK-RK. e analyzed whether the loss of SIK3 in tumors coincides with changes in other AMPK-RKs in the same samples (Figure 4.6). cBIO also provides probability of co-occurrence. Unsuprisingly, among sixteen genes of AMPK-RKs, nine showed mid to high levels of correlation with changes in SIK3, among them five were statistically significant.

Table 4.6. SIK Mutations in Colorectal Carcinoma.

Effects of SIK Mutations in Colorectal Carcinoma											
Gene	**Survival in Mutation Group**										
	Net Effect	**Logrank p(<=0.5)**	**Protein**	**Epitope**	**p value***	**Net Change**	**Net Effect**	**Protein**	**p value***	**Net Change**	**Net Effect**
SIK1	Shorter	0.7	RB1	pS807/811	0.34	higher	oncogenic	CASP7	0.84	higher	suppressive
			AKT1/AKT2/AKT3	pS473	0.18	lower	oncogenic	MSH6	0.40	higher	suppressive
			MAPK1/MAPK3	pT202/Y204	0.14	lower	oncogenic	AR	0.31	lower	oncogenic
			RAF	pS338	0.13	higher	oncogenic	BCL2	0.30	lower	suppressive
			ACACA/ACACB	pS79	0.12	higher	oncogenic	CCNB1	0.28	lower	oncogenic
SIK2	Shorter	0.5	ERBB2	pY1248	0.00	lower	oncogenic	NOTCH3	0.032	higher	oncogenic
			AKT1/AKT2/AKT3	pT308	0.01	higher	oncogenic	BCL2L1	0.050	lower	suppressive
			CHEK2	pT68	0.09	lower	suppressive	MAPK14	0.054	lower	suppressive
			ACACA/ACACB	pS79	0.09	lower	oncogenic	RAD50	0.057	lower	suppressive
			EIF4EBP1	pS65	0.09	higher	oncogenic	GSK3A/GSK3B	0.063	higher	oncogenic
SIK3	Longer	0.35	WWTR1	pS89	0.01	higher	oncogenic	ERRFI1	0.01	higher	suppressive
			EGFR	pY1068	0.02	lower	suppressive	SMAD3	0.01	higher	suppressive
			ACACA/ACACB	pS79	0.03	lower	oncogenic	NCOA3	0.01	lower	suppressive
			ERBB2	pY1248	0.04	lower	suppressive	PTGS2	0.02	higher	oncogenic
			RELA	pS536	0.04	lower	suppressive	MYC	0.02	lower	suppressive

	MARK1	BRSK1	PRKAA2	PRKAA1	NUAK1	PRKAG3	MARK2	NUAK2	SIK2	PRKAB2	PRKAG2	BRSK2	STK11	PRKAB1	PRKAG1	SIK1
SIK3	0.032528	0.252038	0.015842	0.17472	0.007761	0.007761	0.119562	0.880438	0.119562	0.909148	0.090852	0.938633	0.938633	0.031088	0.968912	0.968912

Figure 4.6. Evaluation of exclusivity of AMPK-RKs in colorectal cancer. Yellow (weaker)/Orange (stronger) color indicate co-occurrence, blue indicates exclusivity. Values are P values.

4.3. Salt Inducible Kinases in Tumorigenesis Analyses

With the purpose of modeling Salt Inducible Kinases while using an *in vivo* model we selected two canonical human SIK homologs in *Drosophila*, fly SIK2 and SIK3 as the initial target in the study. SIK contributions in tumor backgrounds were performed via the expression of several different fly SIK transgenic lines in these backgrounds, either resulted in gain or loss-of-function phenotypes of SIKs. Over-expression lines included wild type protein expressions, UAS-SIK2 and UAS-SIK3, constitutive over-expressions which were accomplished by nucleotide substitution in SIK proteins and thereby inhibiting of PKA phosphorylation, UAS-SIK2-CA and UAS-SIK3-CA. Loss-of-functions were performed with RNA interference lines, UAS-SIK2 KK RNAi and UAS-SIK3 KK RNAi; if available null mutants and kinase dead lines were used, as for SIK2, SIK2$^{\Delta 41}$ and UAS-SIK2-KD.

4.3.1. Validation of Genetic Tools Used in Tumorigenesis Assays

The quality of over-expressions was assessed by western blot analyses which were performed with samples collected from flies with neuronal expression driver ELAV-Gal4 (Figure 4.7). Short and major SIK3 fly isoforms were not detected to be over-expressed with SIK3 around the predicted 75kD size, while slight induction of the longer isoform could be seen around 150kD with fly SIK3 WT and fly SIK3-CA lines. The SIK2 human antibody was able to detect the 75kD band in both control and with higher amounts in fly SIK3 WT and fly SIK3-CA; thus the human SIK2 antibody seems to cross-react with the fly SIK3 protein and confirming SIK3 over-expression fidelity. In the null mutant line of SIK2, SIK2$^{\Delta 41}$, SIK2 could be detected, which reinforced the idea that the SIK2 human antibody was not specific to fly SIK2. Note that, stronger SIK3 signals were achieved when SIK2 levels were experimentally manipulated. Due to cross-reactivity of human anti-

SIK2, SIK2 levels could not be calculated and over-expression fidelities were assumed faithful according to contributor publication (Choi *et al.*, 2011). These antibodies were also used in the detection of SIKs in the imaginal discs (For relevant figures, see Appendix A).

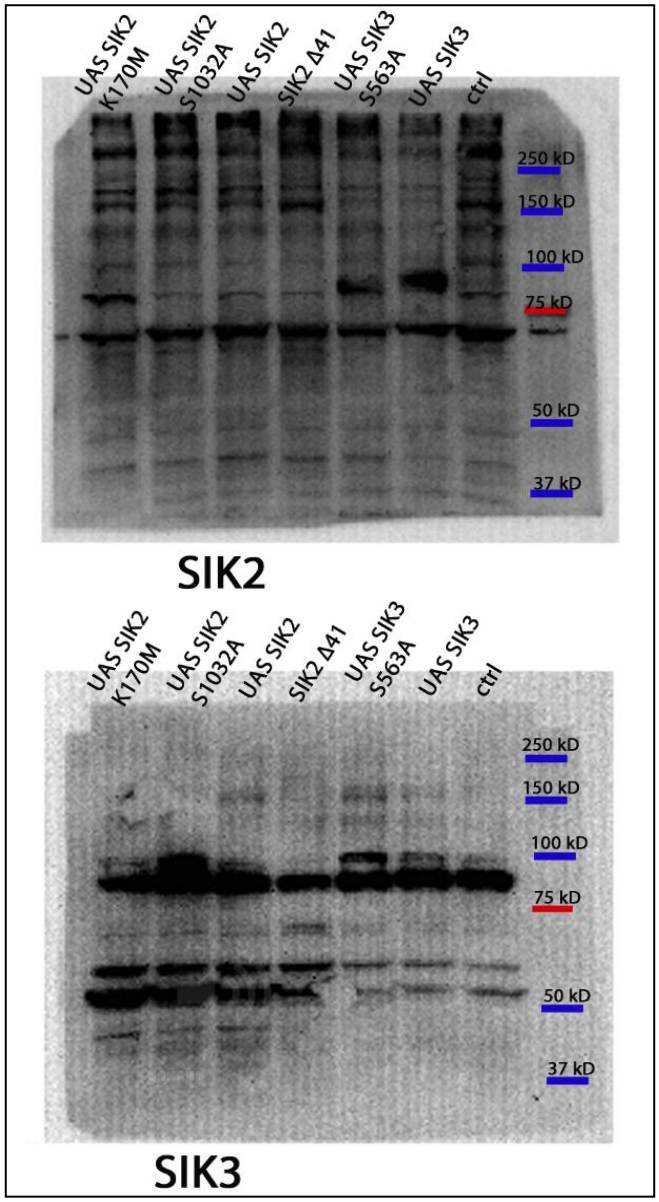

Figure 4.7. Western blotting for SIKs (upper: anti-SIK2 human, lower: anti-SIK3 human)

Western analyses in Figure 4.7 also shows that T2A, the self-cleavable tag we introduced to the *Drosophila* community, worked efficiently in flies. The tag itself was derived from the foot-and-mouth disease (FMDV) virus. It has the ability to self cleave itself during protein translation; as a result, the primary message in a bicistronic mRNA could be free of hindrance of the secondary product, mCherry in our case. The T2A in our

study was introduced to the UAS SIK3 construct, which was found to be expressed at its native protein weight and without the addition of mCherry protein weight (28kD). In other words, the mCherry was cleaved from the over-expressed SIK3. mCherry over-expression itself was confirmed by *in vivo* visualization of the relevant fluorescence signal from intact live animals (Figure 4.8). SIK3 over-expression was also confirmed *in vivo* with immunohistochemisrty (Figure 4.9).

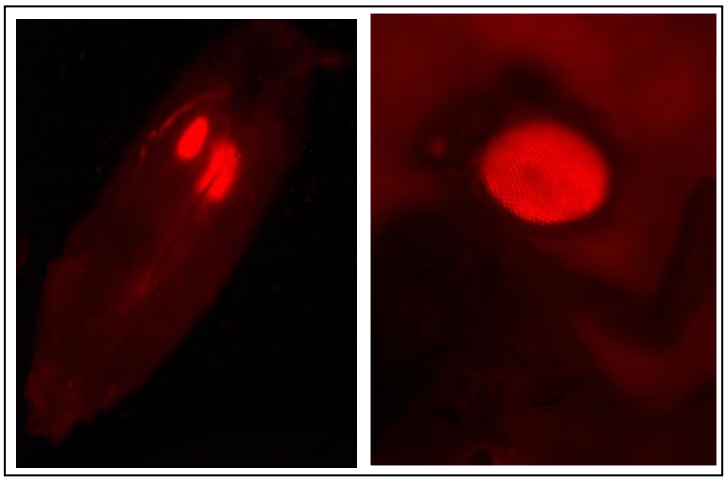

Figure 4.8. mCherry signal generated by lGMR-Gal4 driven fly SIK3::T2A::mCherry expression in pupal eye discs and adult fly eye.

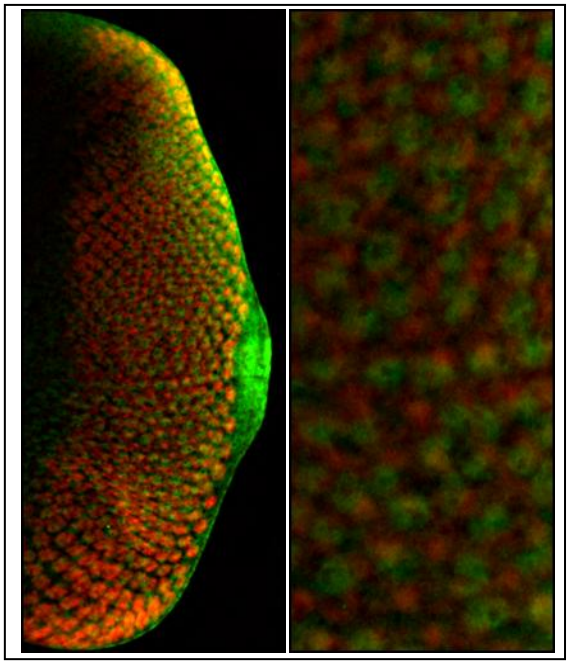

Figure 4.9. ELAV-Gal4 driven fly SIK3::T2A::mCherry, stained with anti-human SIK3 antibody (Green; ELAV red).

Although RNA interference is a quick, cheap and efficient method to study loss-of-function phenotypes an important consideration is to figure out how efficiently the down-regulation of the gene of interest is achieved. Additionally, the presence of off-target effects especially when studying genes with close relatives remains a problem and necessitates control experiments even when using SIK-RNAi lines reported previously in the literature. Using primers specific to SIK3 and spanning intron-exon boundaries to enable cDNA-specific amplification even in the presence of fly genomic contamination, SIK3 expression was found to be in the exponential phase at 29 cycles. SIK3 just emerged in the 1% agarose gel at this cycle. Actin specific primers were used to normalize expression. Although, *eyeful* control bands shows some level of saturation, thus making normalization partially unreliable, SIK3 knockdown is obvious, and SIK3 levels after knockdown equals to 40% of those in the control (Figure 4.10). Interestingly, PCRs with the total SIK2 RNA interference in the eyeful background with specific SIK3 primers showed that, there is a 250% induction in SIK3 mRNA levels, which strongly suggests the presence of compensation between members of the SIK family.

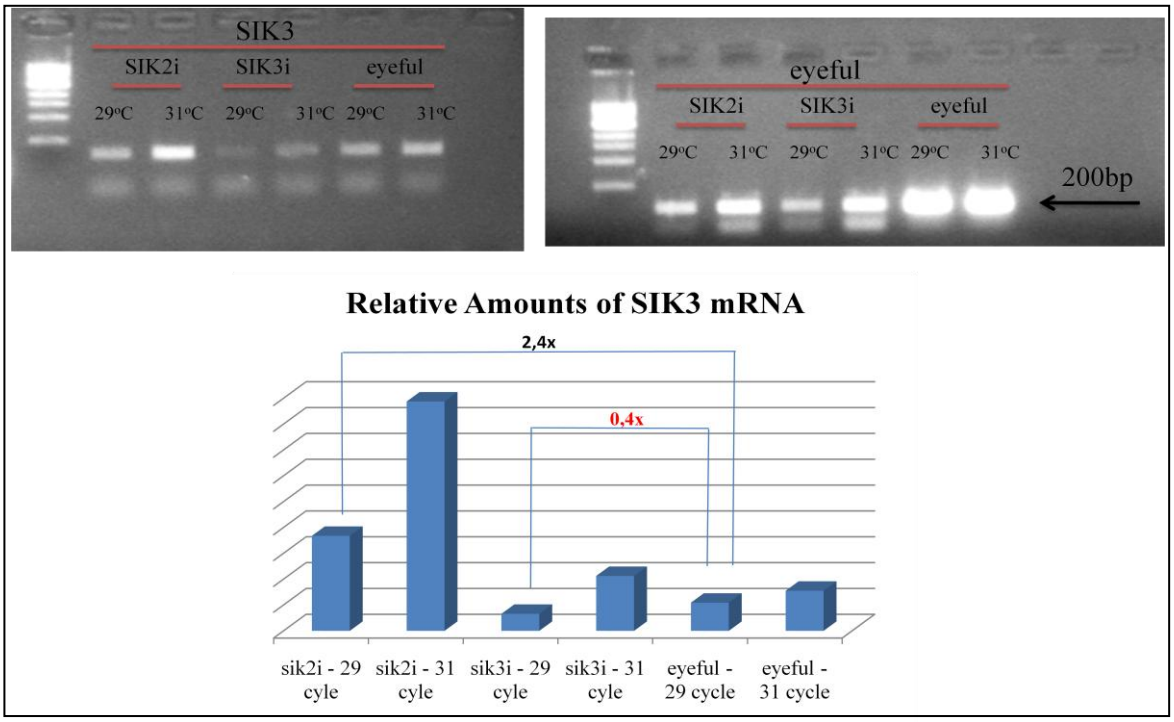

Figure 4.10. PCR results of SIK3 in three total cDNA samples, SIK2 knockdown, SIK3 knockdown and *eyeful* background and actin controls. Normalization to actin levels obtained at 29°C.

4.3.2. SIK Response in Tumors Depends on the Context

Fly SIK2 and SIK3 were combined with two cancer backgrounds, low grade cancer model *sensitized* and high grade cancer model *eyeful*. *Sensitized* and *eyeful* backgrounds provided the necessary medium to evaluate behavior of SIKs in cancer. *Sensitized* harbored an over-expression of Notch, a well known protein in developmental context and a candidate oncogene. Over activation of Notch signaling results in a benign growth in the eye tissue. On the other hand, *eyeful* included additional over-expressions of epigenetic controllers lola and psq, which brought silencing of tumor suppressors and consequently more aggressive tissue growth and occasional metastases. Tumor growth and metastasis, as well as other morphological changes that could be observed in an adult fly, were exemplified in Figure 4.11. The presence of at least one excessive folding and eye tissue outside of the wild type eye field was counted as a positive score for tumor growth (% presence of eye folding, PEF) and metastasis (%number of visible metastases, NVM) respectively. The loss of differentiated eye tissue in the adult flies were counted as eye loss phenotype and smaller, yet fully differentiated eyes due to tissue growth decrease were discarded. If uniformity of the adult eye color was lost in the experimental progeny, these were counted among eye color change phenotype. All phenotypes were evaluated with χ^2 analyses against the control group, w118 line which only harbors a single mutation causing white colored flies and is the background of all transgenic lines used in the study.

During the tumorigenesis experiments, as the consensus temperature in *Drosophila* experiments, 25°C were used for both *sensitized* and *eyeful*. Reflecting chromosomal instability and epigenetic variations in cancer, one of the tumorigenesis backgrounds used in the study, *eyeful* showed great fluctuations in phenotypes described above. Therefore, due to fact that the *eyeful* background itself generated high scores and thus increased the signal-to-noise ratio to a level where additional SIK manipulations could not be screened properly subsequent to background subtraction, a second temperature was also used: 18°C.

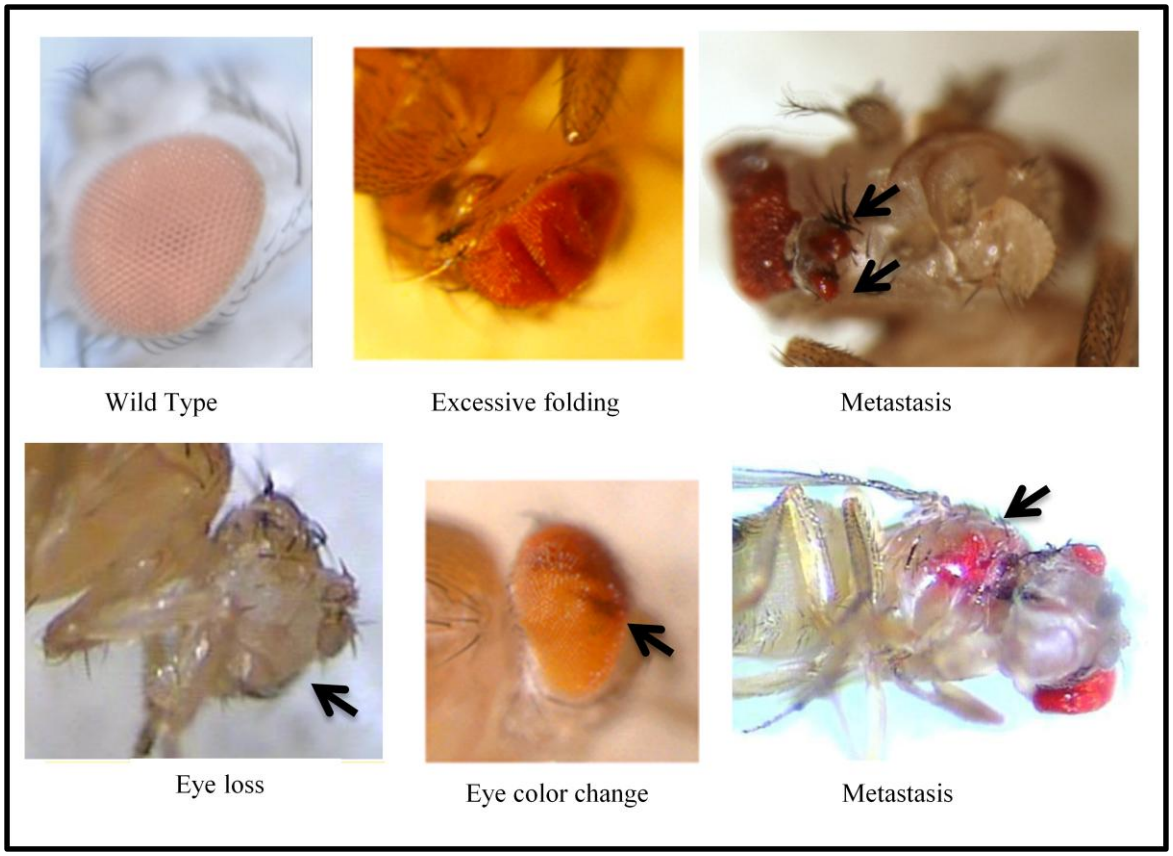

Figure 4.11. Comparison between wild type fly eyes (in the uppermost right) to fly SIK phenotypes. Excessive folding occurs due to tissue enlargement and contributes to tumorous eye phenotype (%PEF). Metastases to the head (upper) and to the body (lower) constitute the total metastasis score (%NVM).

The control line w118 produced 1, 21, 47 %PEF scores and 0, 9, 33 %NVM during modeling overgrowth and metastasis for three experimental setups, *sensitized* at 25°C, *eyeful* at 18°C and *eyeful* at 25°C respectively (Figure 4.12). In comparison to these scores, for growth, UAS-SIK2 over-expression decreased %PEF scores 12 and 30 for *sensitized* at 25°C and *eyeful* at 25°C. However, only statistically significant result produced came from the low amounts of over-expression achieved at 18°C in eyeful lowered %PEF to 1 ($p<0.001$). In *sensitized* at 25°C, high amounts of SIK2 increased metastasis to 1% (1 from a batch of 123 counted flies), which was absent in the background. The stronger induction of SIK2 via CA, under low amounts of expression, decreased %PEF scores from 21 to 6 (*eyeful* at 18°C, $p<0.001$). On the contrary, growth and metastasis were highly induced with SIK2-CA in *sensitized* at 25°C, 12 and 38 percent wise ($p<0.001$). In a stronger tumorigenesis background, SIK2-CA was proved to be less effective statistically,

increasing %NVM to 76 ($p<0.1$). Gain of SIK2 didn't have any statistically significantly effect on dedifferentiation of tumors; even SIK2-CA did increase loss of differentiation to 19% from its control levels at 9%. As a result, one could argue that outcome of SIK2 amplification in a tumor cell depends on levels of SIK2 available to it; while both suppression and enhancement of tumors are possible.

The first fly line used for SIK2 loss-of-function assays was UAS-SIK2 KK, which did not produced significant results; even in the case of *eyeful* at 25°C, %PEF score was lowered to 28 due to SIK2 interference and induction of metastasis in *sensitized* at 25°C (1 metastasis from 86 flies). On the other hand, null mutant and dominant negative kinase dead versions of SIK2 turned out be more potent. SIK2$^{\Delta 41}$ decreased %PEF scores to 6 in *eyeful* at 18°C and to 27 in *eyeful* at 25°C, while only the former was statistically significant ($p<0.001$). The kinase dead version statistically decreased excessive growth (10%, $p<0.01$) while increased metastases rate to 32 in *eyeful* at 18°C. Higher amounts of dominant negative form of SIK2 expression did not affect tumorous growth of the eye tissue in *sensitized* at 25°C and *eyeful* at 25°C; metastasis rate was increased for the former (22%, $p<0.001$), while decreased for the latter (15%, $p<0.001$). The loss of differentiation was also increased by SIK2 loss in general (SIK2$^{\Delta 41}$, 1% positive in 168 flies; 17% for SIK2-KD). The results of SIK2 loss-of-function, therefore, favored both proto-oncogenic and suppressive properties of the eye tissue depending on the tumorigenic context.

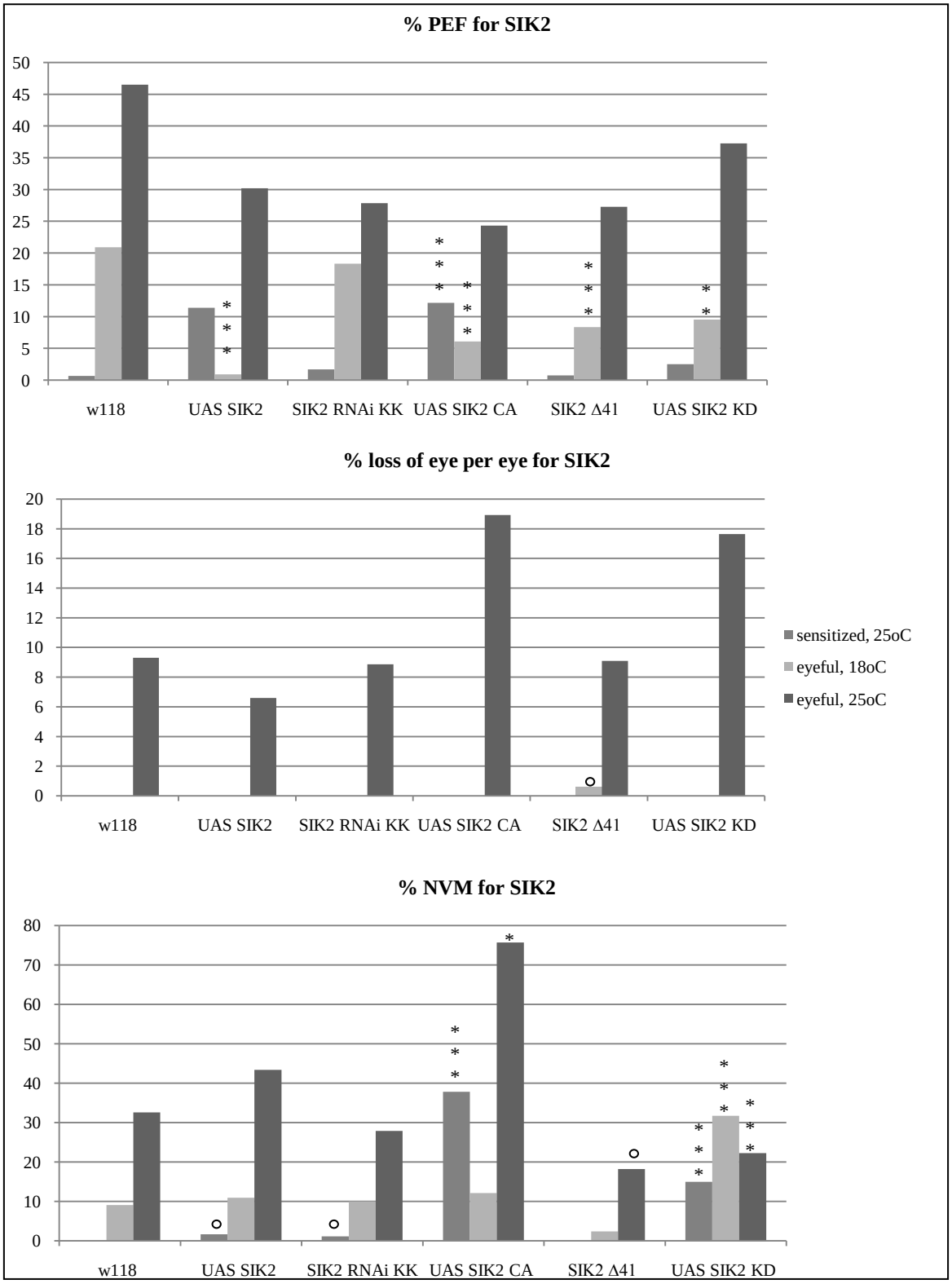

Figure 4.12. Changes of eye over-growth, tissue loss and metastasis in *sensitized* and *eyeful* for SIK2 (Number of flies counted are given in the x-axis. p values are *:0.1, **:0.01, ***:0.001, x: high lethality, o: low number of samples prevented proper statistical evaluation for high impact cases).

Control experiments were performed using ey-Gal4, the driver we used in the two backgrounds, *sensitized* and *eyeful*, at the two temperatures, 18°C and 25°C. Without the synergistic effects of Notch signaling and epigenetic alterations, SIKs seemed unable to induce any major morphological impact on the system (data not shown). Therefore, in addition to the ey-Gal4 driver, a stronger and longer active driver specific to photoreceptors, lGMR-Gal4, was introduced along with UAS-Dicer2, which has been shown to enhance RNA interference in neurons. As a result, interestingly, stronger induction of SIKs produced growth related phenotypes (Figure 4.13). Although, manipulation of the fly SIK2 induced eye growth significantly, frequencies of SIK2 effects remained very low (SIK2 KK RNAi, 1 out of 164 fly eyes <1%). In contrast, tissue size decrease was observed more frequently in all SIK2 lines. The highest score was generated by again SIK2 KK RNAi (61%, $p<0.001$). Wild type SIK2 over-expression led to decrease in the tissue size of %4 of eyes screened, whereas stronger activation of SIK2 signaling via SIK2-CA escalated the rate to 12% ($p<0.001$ for both cases). Of note, SIK2-dependent severe eye size decreases were observed only in ventral side of the analyzed fly eyes (Figure 4.14; also valid for SIK3).

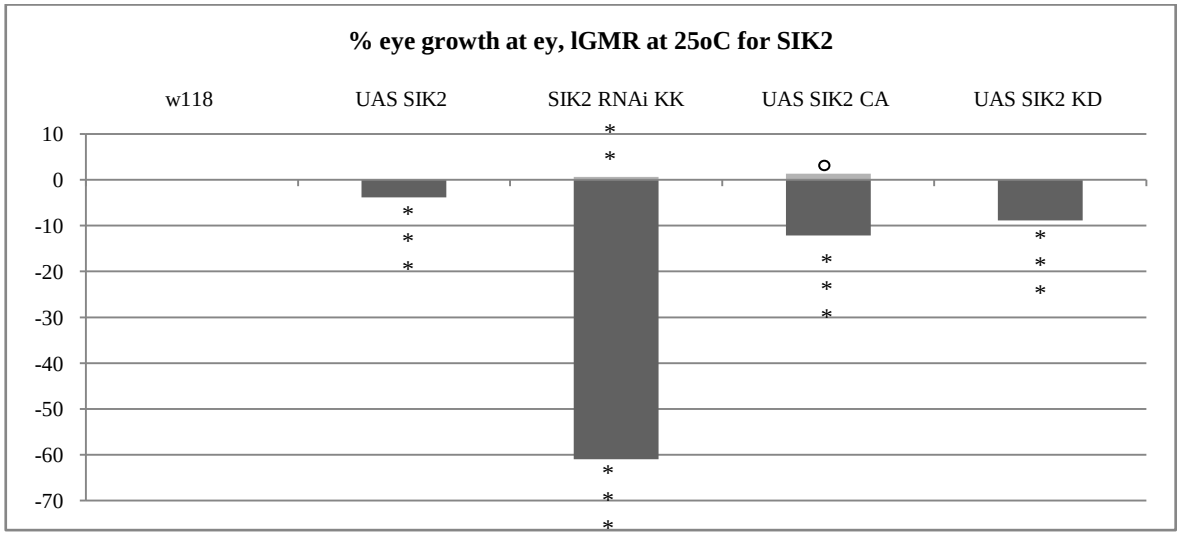

Figure 4.13. SIK2 related eye growth under ey-Gal4 and lGMR-Gal4.

Figure 4.14. SIK-induced decrease in eye size.

The wild type SIK3 expression in tumorigenesis backgrounds led to slight decreases in *eyeful* at 18°C and *eyeful* at 25°C in Figure 4.15 (%PEF 11, $p<0.1$; 30 respectively). The metastasis also did not changed significantly in all three backgrounds subsequent to SIK3 induction via ey-GAL4; although %NVM did increase to 43 from the control levels of 33. In contrast, constitutively active SIK3, thus stronger SIK3 signaling, greatly enhanced tumorigenesis phenotypes. In *sensitized* at 25°C background, both tumorous growth and metastasis increased significantly with SIK3-CA expression (%PEF 9, %NVM 11, $p<0.001$ for both). In *eyeful* experiments, SIK3-CA was proved to be lethal for the flies in the *eyeful* at 25°C, while few survivors (n: 2) could be counted. These survivors were negative for eye folding and visible metastatic due to the failure of eye tissue differentiation. In %25 of cases, only 1 out of 4 eyes was fully developed in the adult flies. On the other hand, in the lower temperature (*eyeful* at 18°C), the loss of differentiation rates were low as 25% ($p<0.001$). The survivors showed enhanced metastasis rate, though overgrowth was not affected (%NVM 50, $p<0.001$). It is probable that optimal levels of SIK3 could repress tumorigenesis, while the loss of PKA inhibition and consequently amplified SIK3 signaling would favor migration of tumors.

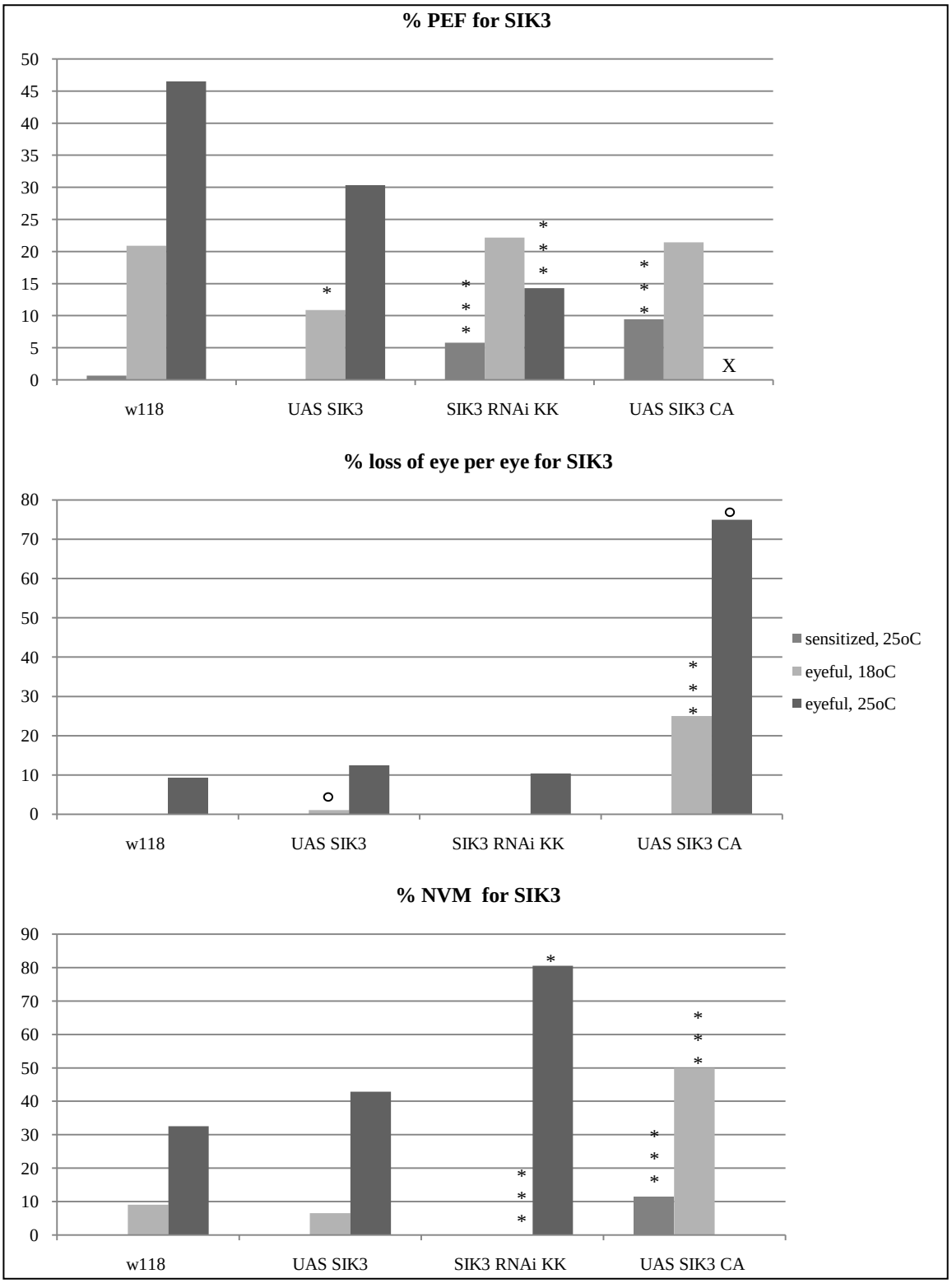

Figure 4.15. Changes of eye over-growth, tissue loss and metastasis in *sensitized* and *eyeful* for SIK3.

The only available line to mimic loss of SIK3 in cancers, the SIK3 KK line increased growth to 6 PEF% in *sensitized* at 25°C ($p<0.001$), while not producing any metastasis for that background (Figure 4.15). In the lower temperatures, *eyeful* at 18°C, the increase in tumorous growth was nominal; in comparison, the migration of tumors was abolished significantly (0 %NVM in 88 flies, $p<0.001$). In the potent *eyeful* background at 25°C, excessive folding was seemed to be inhibited, yet this could be a simple result of amplified metastasis rates due to loss of SIK3 (14 %PEF, $p<0.001$; 81 %NVM, $p<0.1$). Due to high discrepancy in the results, particularly in *eyeful* at 25°C, SIK3 knockdown should be repeated before any well-built conclusions could be proposed.

Similar to SIK2, in general, the alteration in SIK3 signaling decreased the tissue size in a developmental context (Figure 4.16). The presence of lGRM-Gal4 driver, in addition to ey-Gal4, and UAS-Dicer2, generated smaller eye tissue with expression of wild type SIK3 and SIK3-CA. Only the latter was significant in statistical terms (8%, $p<0.001$).

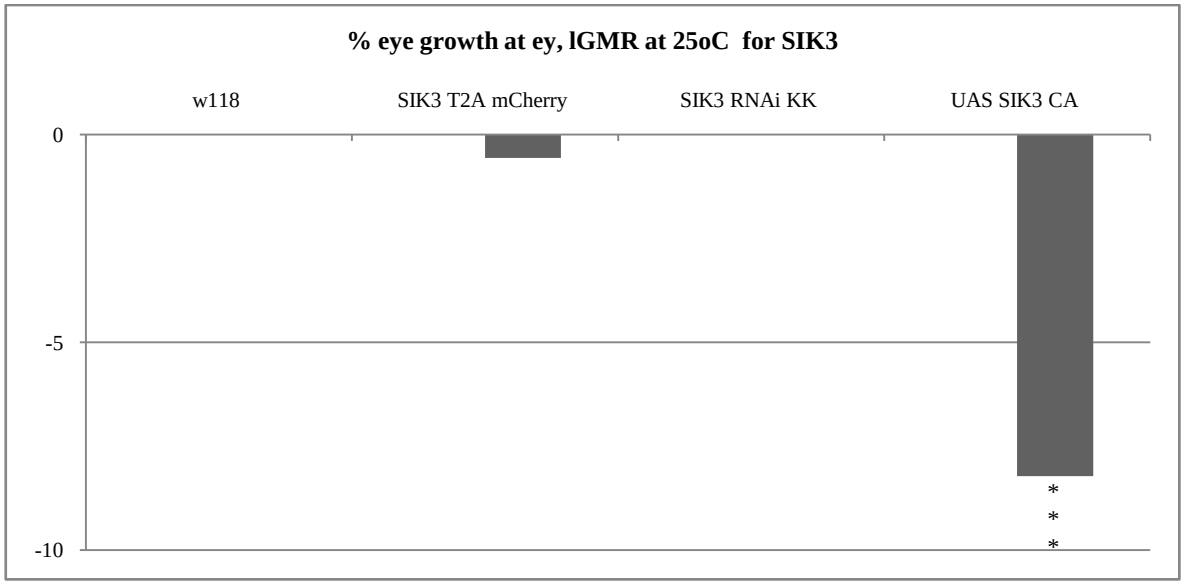

Figure 4.16. SIK3 related eye growth under ey-Gal4 and lGMR-Gal4.

Color changes in the examined specimens reflect alterations in gene expression levels affecting the complex network of pigment determination in the fly eye. The highest statistically significant score in eye color change was generated by the fly SIK3-CA in the *sensitized* background at 25°C (%38, p<0.001). Moreover, almost all eyes of the *eyeful* progeny raised at 25°C of fly SIK3-CA survivors showed fluctuations. SIK3-CA-induced eye color changes were observed along the DV axis of the eye (Figure 4.17, eye color change).

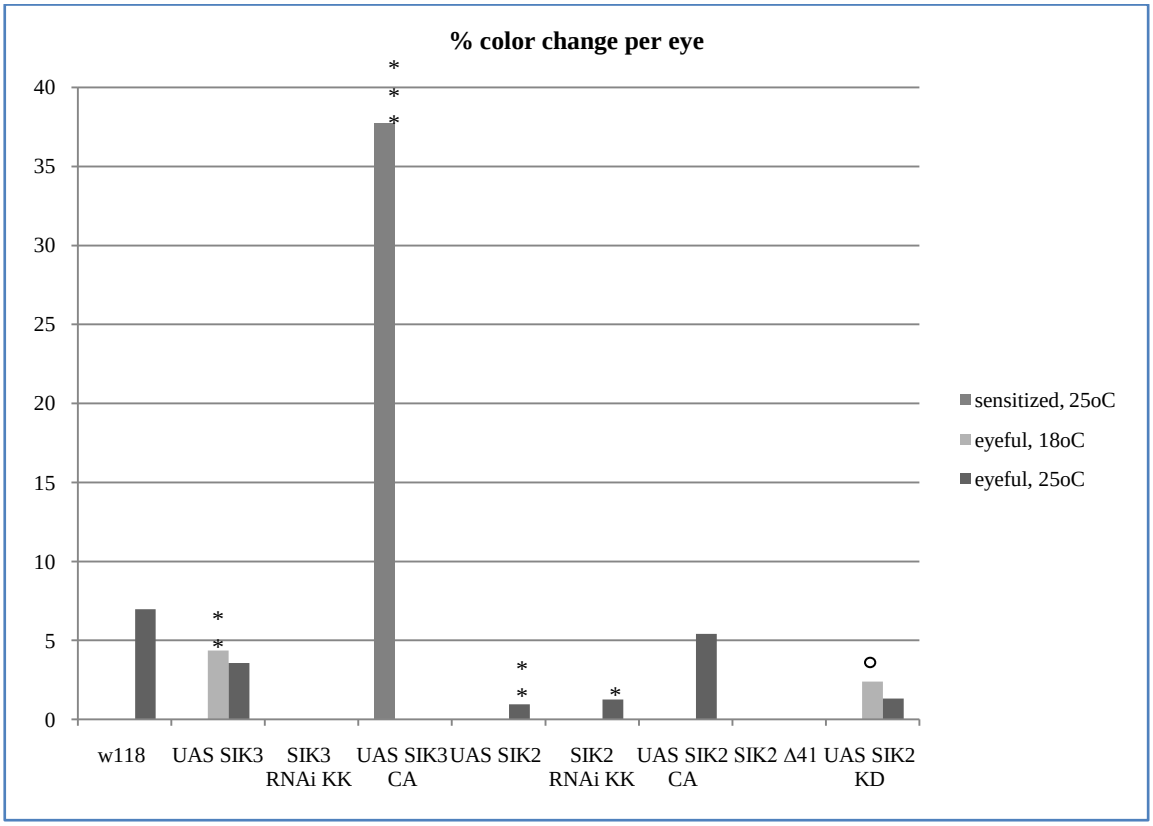

Figure 4.17. Eye color changes in tumorigenesis backgrounds.

4.3.3. Both Cell Division and Death Showed an Increase with Activation of SIKs

To evaluate the effect of SIK members on the proliferation rate of cells changes in mitotic rates upon SIK modulation were visualized and counted using an antibody against phospho-Histone H3. L3 larval imaginal eye discs of the *eyeful* background were dissected, stained and the numbers of cells positive for phospho-Histone H3 were determined (Figure 4.18). In all cases, cell division rates increased highly significantly (p<0.001). Compared to control w118 line count that summed up to 160 pH3 cells in average, the highest median

rate was achieved by fly SIK2-CA at cell count 360, which is closely followed by the fly SIK2 KK RNAi line, at 354. The average cell count for SIK3-CA was 246, for SIK3 RNAi 263. In other words, across the eye-antennal disc, the mitosis rate was almost doubled for SIK2 manipulations. This phenomenon was clear also when the sizes of the discs themselves were compared: due to high mitosis rates, discs taken from flies, where SIK2 was upregulated, were larger than those generated from progeny of w118 and *eyeful* control.

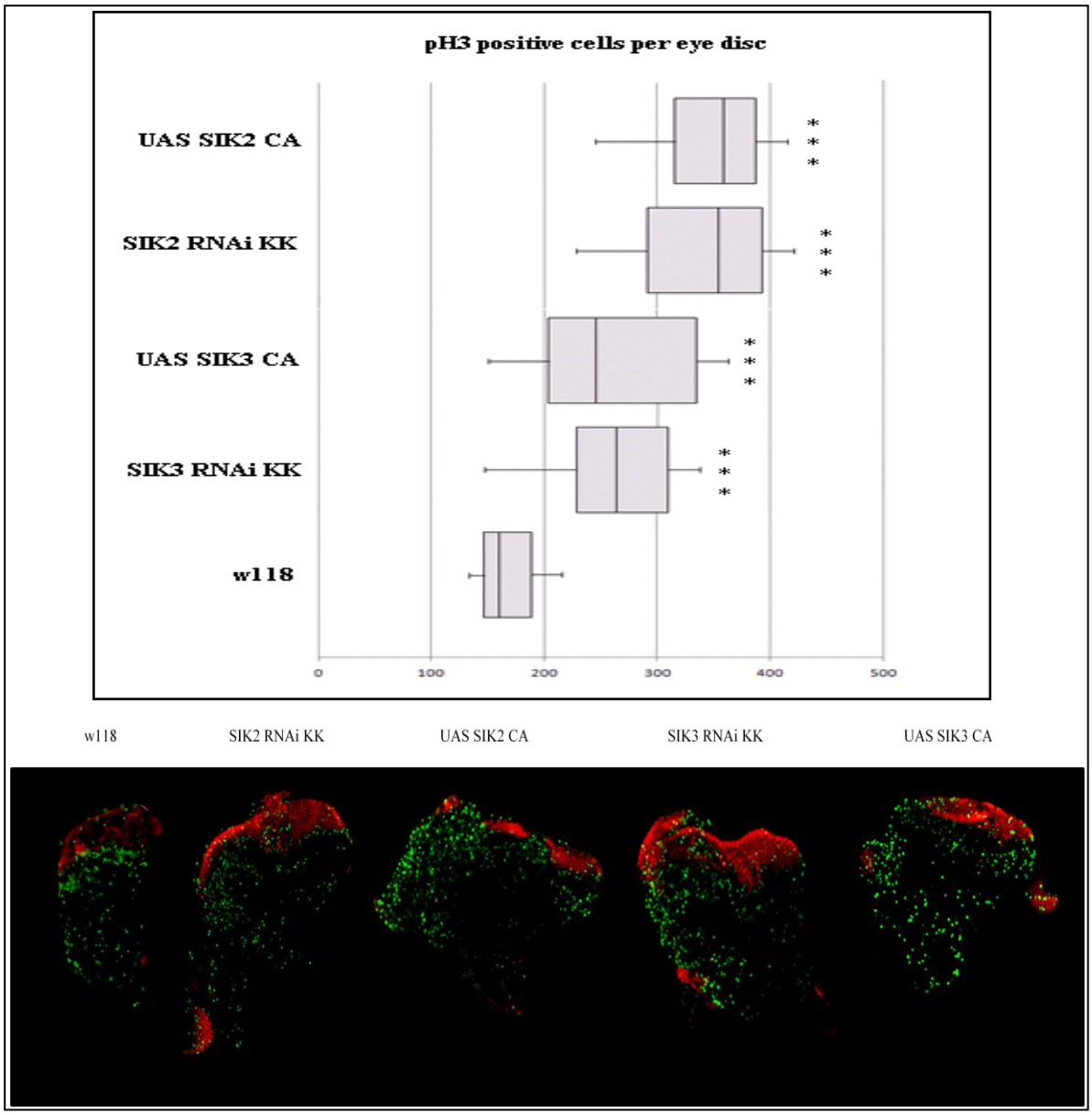

Figure 4.18. Cell division in *eyeful* with fly SIK reverse genetics (Green: phospho-Histone H3, Red: ELAV).

Cell death is another parameter in defining tissue size. To investigate if manipulation of SIK expression levels contributes to changes in cell death rates imaginal discs were stained by an antibody against cleaved Caspase 3.

The *Eyeful* control eye disc showed minimal cell death in cleaved Caspase 3 immunohistochemistry, mostly focused in the anterior of the MF; the frequency of death cells however was higher than in wild type discs, which are cell death resistant in the L3 stage (Figure 4.19 and Figure 4.20, Data not shown.). Due to the rather heterogeneous pattern of Caspase staining, it was impossible to count individual Caspase positive cells. Furthermore, total fluorescence per disc area could not be used in calculating changes in signal density since fluorescence microscopy was unable to discard intensity differences occurred due to the three dimensional cell position in eye discs. Nevertheless, the fly SIK2-CA mediated increased cell death observed in Figure 4.19 could be easily compared to control discs. SIK2 RNAi seemed to increase this rate as well; however, its significance cannot be assessed at the moment.

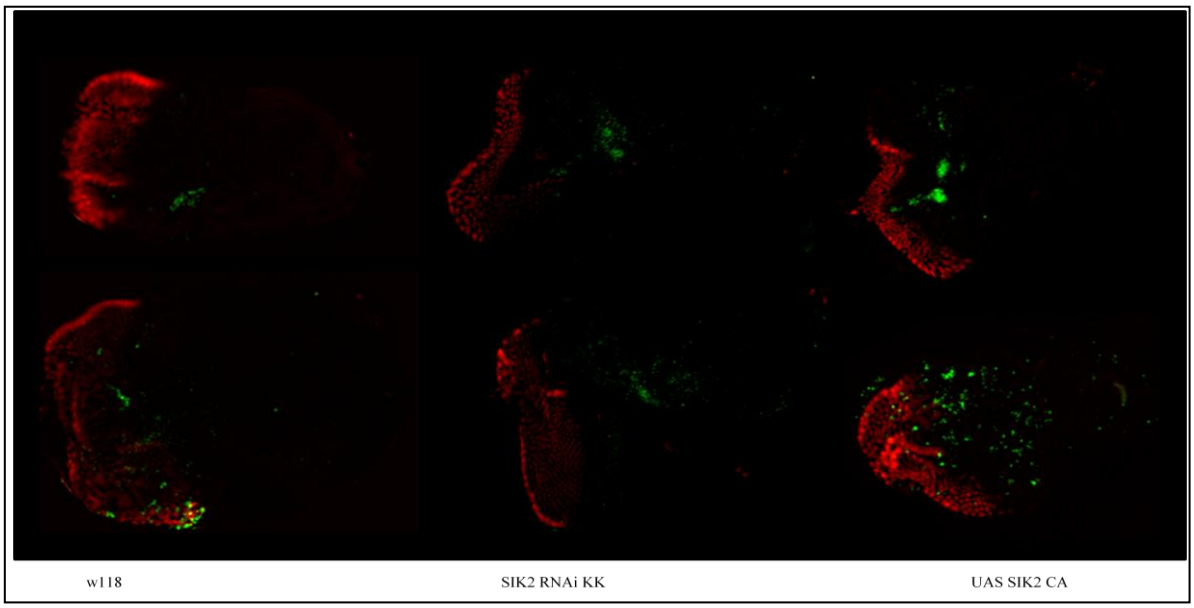

Figure 4.19. SIK2 induced cell death (Green: Cleaved Caspase 3, Red: ELAV).

A similar observation was made with fly SIK3 (Figure 4.16). SIK3 loss through knockdown seemed to increase cell death slightly, while fly SIK3-CA induction was very strong.

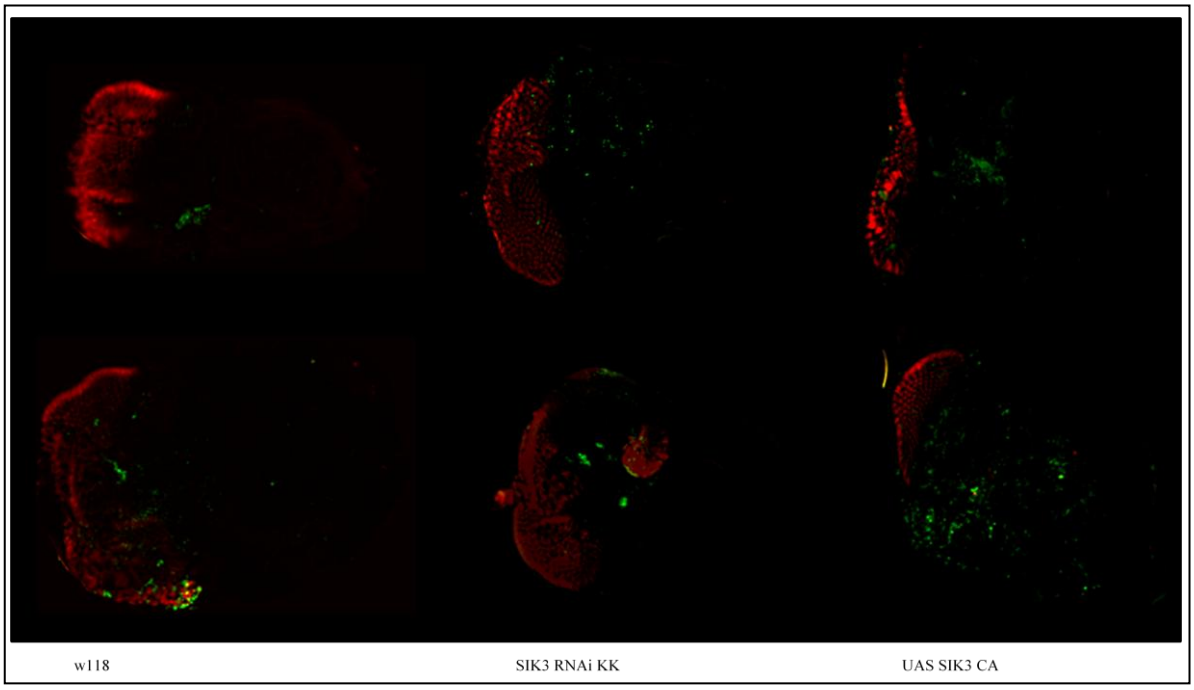

Figure 4.20. SIK3 induced cell death (Green: Cleaved Caspase 3, Red: ELAV).

4.3.4. De-regulation of SIK Signaling Altered Morphogenetic Furrow Initiation and Progress

Mitosis in imaginal discs happens in two waves, which can be visualized by anri-phosphohistone H3 staining. The presence of these two mitotic waves could be still observed in most *eyeful* control discs, anterior to ELAV positive PR cells, which also marked morphogenetic furrow progression (Figure 4.14). On the other hand, in different SIK manipulated backgrounds, mitotic waves almost disappeared as indicated by widespread ph-H3 stainings. Furthermore, MF initiation was disturbed in several cases. In Figure 4.18, the fly SIK2-CA disc harbored three distinct morphogenetic furrows and ectopic neuronal differentiation could be observed at ELAV positive staining in several other cases (Figure 4.18 and Figure 4.20).

Another interesting observation was that eye-antennal discs in which fly SIK3-CA was over-expressed showed imbalance in size differences between the two compartments. In contrast to other experimental groups and control discs, eye discs of fly SIK3-CA were smaller in size whereas antennal disc size was increased. The SIK3-CA disc in the second row of Figure 4.20 is a good example of this. In total, half of the discs observed exhibited a similar reversal of disc size. Accordingly, Adult SIK3 CA flies showed increased

duplications of antenna, antenna-like appendages, in addition to distortions in bristle patterns (Figure 4.21).

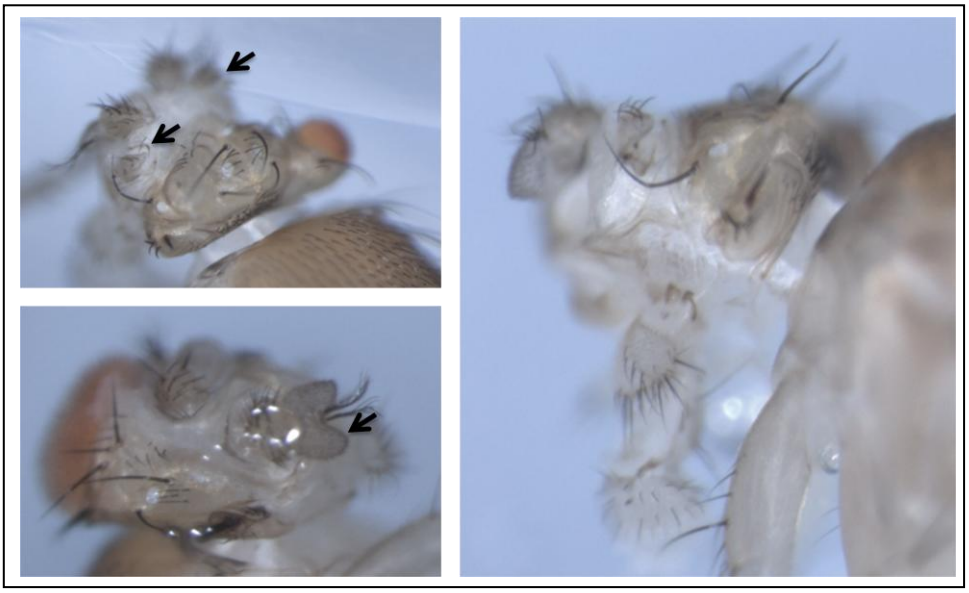

Figure 4.21. Antennal expansion and loss of differentiaon in SIK3 CA expressed discs in *sensitzed* and *eyeful*. Arrows represents antannel expansions.

4.4. Migration Assays

Fluctuations in *sensitized* and *eyeful* necessitated control experiments to visualize SIKs role in migration. Glia migration onto eye disc was a prime choice, since it was used as an eye disc model for migration, while the wing model enabled to see effects of fly SIKs in a different tissue.

4.4.1. Glial Migration was Modulated by SIK2 Fly Activity

In order to expand our perspective on the role of SIKs in tumor migration and to utilize simpler models, we employed glia migration as a secondary model. Retinal basal glia (RBG), the glia from the optic lobe of central nervous system, migrates onto the eye disc in the early larval 3 stage. This process is guided mostly by FGF signaling and can be manipulated by either pan-glial driver repo-Gal4 or RBG specific Mz97 driver.

Subsequent to dissection and staining of L3 discs, repo-positive glial cells were counted and plotted against number of PR rows (Figure 4.22). While neither over-

expression nor knockdown of SIKs did not change the size of PRs and glia and the morphology of the eye disc in general. However, a link between fly SIK2 manipulation and glial migration was evident. Over-activation of SIK signaling resulted in an increase of glial in eye discs; in contrast loss of SIK2 signaling decreased these rates. Loss of SIK3 also decreased glial numbers, although its effects were not as clear. Fly SIK3-CA did not alter glial migration.

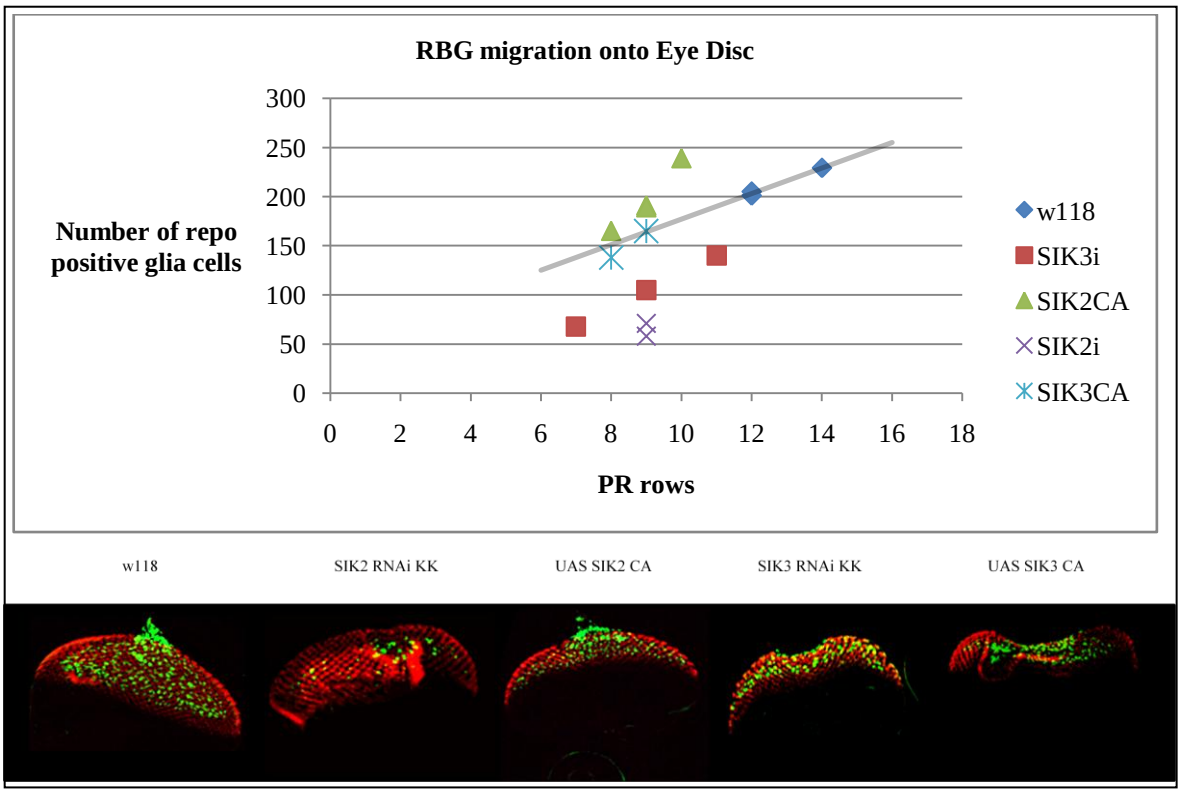

Figure 4.22. Effects of fly SIKs on modulation of glia migration onto eye disc (Green: Repo, Red: ELAV).

Of note, fly SIK2 RNAi proved to be lethal in the late pupal stage for *Drosophila*, as no flies survived into eclosion. However, using the Mz97-Gal4 driver, this lethality was not observed.

4.4.2. Ptc-Gal4 positive cells are lost under constitutive activation of SIK

The other migration model we employed was the wing model, which enabled us of switching the medium of the experiments with the aim of avoiding any tissue specific artifacts. In the developing wing, the anterior posterior (AP) boundary can be marked with

Ptc-Gal4 driven GFP expressing cells. Any manipulation able to alter migratory capabilities of these epithelial cells would be visualized via changes in GFP pattern.

SIK modulation in wing discs did not alter the migration of Ptc-Gal4 positive cells, except in case of fly SIK3-CA over-expression (Figure 4.23). Interestingly, rather than affecting the migration pattern, in fly SIK3-CA case, the signal was lost completely in the area dedicated to form the notum in adult flies. Moreover, in the wing proper, the AP axis marked by Ptc-Gal4 was disturbed.

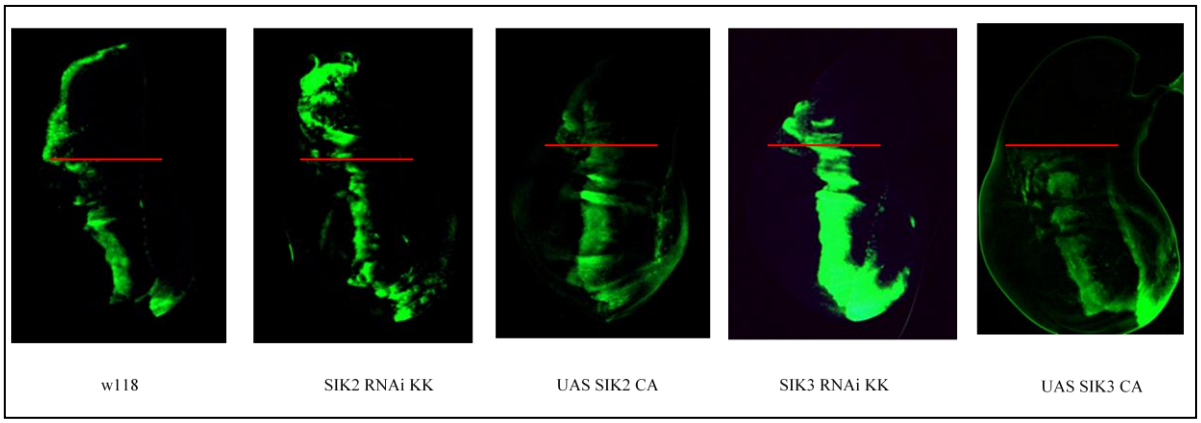

Figure 4.23. AP boundary changes upon manipulation of fly SIKs (Green: Ptc-Gal4 positive cells). The red lines represent boundary between the notum (upper) and the wing proper (lower).

5. DISCUSSION

The involvement of Salt Inducible Kinases in important signaling hubs presents this family of kinases as an interesting node of study in cancer research. Several studies linked SIKs to the regulation of both to cellular and systematic controls of energy metabolism. The earliest reports showed a contribution of SIK to the direct inhibition of insulin signaling via phosphorylation of intermediate cascade members during re-feeding and transcriptional modulation of ACTH signaling upon hormone stimulation by translocating transcriptional coactivators from the nucleus and thus highlighting SIK as a gluconeogenic and lipogenic program modulator, while more recent studies present SIK as a factor in survival under metabolic stress conditions (Berdeaux *et al.* 2007). The role of SIKs in the evaluation of structural information is scant. In *Drosophila* loss of SIKs alter adherens junction distribution and consequently cell morphology (Amin *et al.* 2009). An indirect, albeit a more relevant link between SIKs and structural monitoring comes from cell culture studies where loss of SIK sensitizes cells to escape from detachment-induced cell death because of p53 activation failure in these cells, either proposing an interaction with integrins or Focal Adhesion Kinase (Gilmore 2005; Cheng *et al.* 2009). Highly possible targets of SIK in relation to cell structure will increase in the near future, as exemplified by phosphorylation of tau and transcriptional control of major EMT determinants (Eneling *et al.* 2012; Yoshida and Goedert 2012). Other major signaling targets of SIK include FGF and TGF-β cascades, which are major developmental players as well as frequent cancer targets (Kowanetz *et al.* 2008; Küser 2012). A developmental requirement of SIKs is emphasized in null mutants. In mice, SIK3 mutants show chondrocyte hypertrophy, while SIK1 was shown to be essential for cardiomyogenesis (Romito *et al.* 2010; Sasagawa *et al.* 2012). In flies, SIK3 mutants are not viable (Wang *et al.* 2011). At the cellular level, SIK2 is required for cell cycle progression in parallel to Akt signaling, while loss of SIK2 in liver leads to its hypertrophy (Yoon *et al.* 2009; Ahmed *et al.* 2010).

SIKs are members of the AMPK related kinase group, AMPK-RKs, which are an evolutionarily linked group of proteins known to be activated by master tumor suppressor Lkb1 (Bright *et al.* 2009). Due to overlapping targets, thus similar functions and upstream activators, the existence of a compensation among members has been proposed (Shaw

2009). Unfortunately, synergistic dynamics of AMPK-RKs has not been studied systematically; moreover, most SIK studies did not always consider this possibility in their experiments. The ubiquitously expressed of all three SIKs, SIK3 is the least studied member; even though it has been present in every experimental context. A notable exception in the literature is a study by Sasaki *et al.*, 2011 that showed the absence of compensation in their mouse ischemia model; while one of the most recent publications, Liu *et al.*, 2001, provided that, although SIK1 mRNA increased upon stimulation as expected, SIK1 loss did not alter CRTC phosphorylation due to increases in SIK2 mRNA levels (Liu *et al.* 2011; Sasaki *et al.* 2011). In *Drosophila*, inhibition of AMPK-RKs could not mimic the loss of Lkb1 completely, suggesting an overall shared role in epithelial integrity (Amin *et al.* 2009). Data obtained in this study, also hinted in several cases towards the existence of such compensation. Experimentally, when both mRNA and protein levels were inquired via semi-quantitative RT-PCR and Western blot analysis respectively, at least SIK3 levels changed in response to manipulations of SIK2 expression levels (Figure 4.9 and Figure 4.10). Interestingly, loss of SIK2 mRNA resulted in an increase of SIK3 levels, while in Western blot analyses; SIK2 over-expression caused a stronger signal of SIK3 protein. Similar effects in gain and loss of function studies of a particular fly SIK would be observed throughout this study. The other evidence on possible compensation is demonstrated in Table 4.6, where somatic mutations in several members of AMPK-RKs were found in colorectal carcinoma were shown to co-occur. Although, mutation co-occurrence and patient survival correlation is not shown in our study, it would be a remarkable observation in case of a poorer prognosis when targeting multiple members of AMPK-RKs exclusively.

Physiological relevance of SIKs and importance of the task they perform could be evaluated with their conservation throughout evolution. Even though, as explained above, compensation is present among members, SIKs have been under natural selection since their introduction to Animalia (Figure 4.5). Contrary to the established notion, discovery of fly SIK2 as homolog of both human SIK1 and SIK2 by phylogenetic and protein structure analyses in Figure 4.1 and Figure 4.2 opened the possibility to calculate amino acid substitution rates of synonymous over non-synonymous nucleotides after SIK1 and SIK2 branches diverged possibly in Euteleostomi. On the contrary, cladograms in Figure 4.5 showed that, indeed, synonymous substitutions occurred less due to evolutionary

constraints when compared to non-synonymous mutations. As a practical suggestion of this finding, human SIK1 could be used in the following phases of our study. Other human SIKs have been prepared to be expressed in the tumorigenesis models we utilized, which would be the first actual study to prove an evolutionary link between human and fly SIK proteins functionally. Addition of human SIK1 might provide data in the evolutionary divergence of these two human genes.

Even protein domain and motif searches using publicly available tools like SMART and Scansite did not produce any conclusive evidence. Scansite results showed new possible branches of the SIK interactome (Figure 4.3 and Table 4.1). An abundance of suggestions for SH2 & SH3 interactors forced us to use the high stringency criteria, even causing elimination of published targets and effectors of SIKs. Still, many proteins with SH binding motifs having roles in cancer and cytoskeleton regulation were found on Table 4.1 for human SIK1 and SIK2. Phosphorylation by Src of fly SIK3 hints towards a role in tumor formation. Proposed interactions in publications regarding Erk and DNA damage kinases could be found also (Matsuoka *et al.* 2007; Küser 2012).

An enquiry on SIKs in cancer databases reinforced the idea that SIKs have a role in cancer. In the first set of data, collected from three different sources, mutations of SIKs were found to be present in a variety of cancer types, although overall SIK mutation frequencies were below 5% (Table 4.3). Most of these substitutions were located on kinase domains, which were predicted to be functionally important by two independent methods utilizing homology data of known protein isoforms (Table 4.4). When contributions of these mutations on colorectal carcinoma were investigated, SIK2 and SIK3 produced opposite results (Table 4.6). SIK2 caused shorter lifespan for the SIK2 mutation-carrying group, while SIK3 patients had a better prognosis. Their effects on target protein phosphorylation and expression levels were not clear; while phosphorylation effects mostly reinforced oncogenic effects, expression changes favored suppression. One should note that these changes should be evaluated in a larger network of cell signaling in order to predict the actual contribution. Although it is hard to define the effects of SIKs in overall signaling, the changes listed on Table 4.6, at least, hinted towards that SIKs could interact with several pathways that are important in survival and development, which included members like Akt, Notch, and Bcl2. Another line of evidence of SIK in cancers came from

analysis of publicly available expression level data of SIKs in tumor samples. Copy number studies and mRNA expression analyses showed that the general behavior in cancers is loss of SIKs, although several exceptions could be observed (Table 4.4 and Table 4.5).

The *in vivo* model employed for evaluation of SIKs in cancers used in this study utilizes two backgrounds, namely *sensitized* and *eyeful* (Ferres-Marco *et al.* 2006; Bossuyt *et al.* 2009). With the help of the the well-established Gal4-UAS system the Notch pathway is upregulated in the *sensitized* background, while in the *eyeful* background two a additional genes of the Polycomb group are upregulated. These backgrounds thus produce one of the complex tumorigenesis models available in the *Drosophila* community as both developmental and epigenetic aspects of cancer formation could be modeled faithfully. However, in the course of the experiments variance in temperature-dependent efficiency of the Gal4-UAS system and the universality of epigenetics in maintenance of gene expression confronted us with difficulties. Thus, variations in phenotypes proved difficult in the correlation and normalization of different experimental data sets. As a result, we used the experimental setups in our study: *sensitized* at 25°C, *eyeful* at 25°C, and *eyeful* at 18°C which is a weaker background with the aim to decrease GAL4-UAS efficiency and thus producing lower penetrance in w118 control lines. Meanwhile a lower temperature of induction gave the opportunity so screen whether the function of SIKs in the tumor context had a concentration-dependent effect (Figures 4.12-15).

In a recent study human SIK2 was proposed as a possible proto-oncogene in ovary cancer cell lines following the evidence that SIK2 is required for cell cycle progression and the proliferation rate of tumor cells in culture declined as result of to SIK2 knockdown (Ahmed *et al.* 2010). On the other hand, *in vivo* studies in the cancer context have been neglected so far. In our *in vivo* fly model, in Figure 4.12, we utilized three different methods to achieve SIK2 loss-of-function: RNAi knockdown (KK line), null mutant (Δ41), kinase dead mutant (fly SIK2 KD). Interestingly, null mutants of SIK2, which do not produce SIK2 protein, would be expected to produce the strongest loss-of-function phenotypes. However, loss of SIK2 did not generate statistically significant results, except in the *eyeful* background at 18°C where tumor growth diminished. Due to the relatively long process of null mutant generation in *Drosophila*, fly lines could generate

compensation against loss of genes crucial in survival. It is possible to perform these experiments by out-crossing the genomic locus of SIK deficiency. SIK2 knockdown did not contribute to the phenotypes, except metastases could be observed at *sensitized* in low frequencies, indicating low amounts of SIK2 were still functional. The efficiency of SIK2 knockdowns could be increased via introduction of UAS-Dicer2, a common approach applied in *Drosophila* genetics. The over-expression of SIK2 fly KD induced both increase and decrease of potency of tumors according to the background and temperature. As a result, it is not clear to state the impact of loss of SIK2 in fly cells, while one could propose that alterations in SIK2 kinase activity could enhance susceptibility of tumor cells to further changes. On the other hand, over-expressions of SIK wild type and constitutively active forms did produce clear cut results. Both fly lines did manage to decrease tumorous growth under lower expression conditions of *eyeful* at 18°C background, while metastasis levels remained unchained. Either the higher potency of *sensitized* and *eyeful* backgrounds or higher levels of expression provided by more efficiency Gal4-UAS system, however, greatly increased both growth and migration of the tumors for SIK2 gain. Therefore, one could argue that higher any cell deviates from optimal SIK2 signaling levels, stronger tumorigenesis becomes.

The least studied SIKs among all three proteins, SIK3 were proposed to be a tumor marker in ovarian cancers as it was found to over-expressed in high grade tumors and its loss decreased malignancy in immunologically deprived mice (Charoenfuprasert *et al.* 2011). When we observe expressed SIK3 variants in our model, in parallel to literature, over-expression of SIK3s in most cases increased tumor phenotypes (Figure 4.15). Although, wild type SIK3 decreased slightly growth ($p<0.1$) and eye loss in *eyeful* at 18°C, no significant contribution were observed in other backgrounds. On the other hand, SIK3 fly CA enhanced significantly eye growth and metastasis in *sensitized*; at low temperatures of *eyeful*, SIK3 caused higher metastasis rates and induced loss of differentiation in the *Drosophila* eye tissue. The loss of SIK3 produced mixed results: in case low levels of SIK3 RNAi induction, metastasis did not occur; however, SIK3 loss induced excessive growth in *sensitized* and numerous metastases in *eyeful* at 25°C. This discrepancy in loss of SIK3 could be an artifact of the experimental group presented in Figure 4.15. The earlier crosses with SIK3 KK RNAi had not produced such strong impact on tumorigenesis (Data not shown). Moreover, as in the following experiments in different contexts presented with

Figure 4.18 and Figure 4.20, SIK3 loss of function gave the weakest results, which reinforces the idea as SIK3 results being artifact. Nevertheless, activation of SIK3 signaling increases tumor phenotypes and SIK3 could be considered as an oncogene. However, as mild expression slightly decreases eye growth, one could propose that SIK3 concentration in a cell is important in its functionality as SIK2.

Simultaneous increase in cell division and death is a possible phenomenon in cancers (Guo and Hay 1999; Debacq 2002; Yokohori *et al.* 2004). Driven by oncogenes, some cells could facilitate mechanisms induce proliferation; whereas, either forced by remaining surveillance checkpoints or simply oncogenic expression toxicity, others die eventually. Due to third instar larval (L3) stage being as the focal point of ey-Gal4 expression strength and ease of experimentation, we dissected L3 larvae with the aim of evaluating changes in cell survival. The initial and most striking observation came from cell proliferation assay (Figure 4.18). In all cases of SIK fly manipulation, both loss and gain-of-function, tissue size dramatically increased in correlation to statistically significant mitosis rate gains when compared to eyeful w118 controls. Moreover, contribution of SIKs to cell division differed in extent between to genes: SIK2 fly protein manipulations were stronger in effect when compared to SIK3 fly genes. The differential contributions were highly probably due to different roles assumed by SIK fly proteins in cancer and proliferation contexts. The western results showed that SIKs over-expression produced in equal amounts by the same driver; therefore, it is safe to assume the absence of positional effects on a particular line and advantage over the other lines in efficiency (Figure 4.7). Due to the use KK lines for RNA interference, the potency of SIK RNAi lines are expected to be in equivalent amounts (Venken *et al.* 2006; Dietzl *et al.* 2007). The differences in strength between SIKs could be found in cell death also (Figure 4.19 and Figure 4.20). The cell death rates escalated subsequent to SIK fly manipulations, though in lower amounts for loss-of-function. These effects of SIK on cell survival were not unexpected. Several interactors listed above links SIKs with cell surveillance, cell division and survival, under normal or stress conditions. Meanwhile, these experiments provided the strongest evidence that levels of SIKs are important in its function and both gain and loss-of-function could hinder SIK signaling. An additional important aspect to be addressed in future experiments would be wild type over-expression studies to test further this claim. It is probable that wild type SIK over-expression would either decrease rates of division or increase cell

death, both to much less extent in comparison of constitutively active over-expressions, according to Figures 4.18-20. Furthermore, over-expression dependent toxicity in *eyeful* tumors could be evaluated using a weaker driver.

The force molds eye-antennal disc into committed state morphogenetic furrow, which is accompanied by two mitotic waves, could be influenced more than 75 proteins including major morphogens, JAK-STAT, Wnt, Hedgehog, Dpp signaling as well as other developmentally crucial pathways, as Notch signaling according to Flybase, a database of *Drosophila* genes (Dominguez and Casares 2005; McQuilton *et al.* 2011). These proteins work as coherent force, in parallel and opposite ways to ensure morphogenetic furrow stability and prevent ectopic furrows. In immunostainings of SIK fly proteins clearly showed that any alterations in SIK signaling in tumor backgrounds could indeed alter these fine patterns. In Figure 4.18, although mitosis rates were increased to wild type eye discs, still in the control *eyeful* eye discs, w118 line, a uniform morphogenetic furrow could be visualized at the furthest anterior end of ELAV positive cells. These were accompanied by two mitotic waves which represented by two distinct pH3 (Green) staining. On the other hand, in SIK fly manipulations, it was impossible to locate these waves of pH3 staining. Since control discs could retain these patterns even in the case of enlargement of the disc, their loss could not be explained by the simple morphological changes in epithelia of the discs. Highly possibly, these were indigenous consequences upon SIK manipulations of signaling alterations governing cell cycle transitions, primarily Notch and EGFR pathways (Doroquez and Rebay 2006). The more striking phenotype observed in SIK discs were related to morphogenetic furrow itself. The uniformity of ELAV stainings of control w118 discs were lost and several individual furrows could be marked with these ELAV positive clusters as in exemplified by SIK2 fly CA disc. Even in the case furrows could be found in regular form, additional discs far from the furrow could be found ectopically. While the disc proper is thought to receive crucial signals for furrow initiation from the peripodial membrane, more-than-one furrow initiation could be explained by the interference of SIKs in these signals. This could be further analyzed via use of peripodial membrane specific driver, c311-Gal4 (Manseau *et al.* 1997). In case of ectopic ELAV stainings, however, these clusters were far from the core cluster, thus hinting independent formation without any information from the peripodial membrane. Since the role of epigenetics in Unpaired expression of JAK/STAT signaling, furrow formation in other words, is known, a probable

explanation for ectopic furrows was involvement of SIKs in histone deacetylation and following gene expression control (Tsai *et al.* 2007).

Increase in eye disc size due SIK over-expressions, however, represents their earlier effect on discs, independent of morphogenetic furrow and mitotic waves. Principally, Eyeless expression confers eye disc growth (Dominguez and Casares 2005). However, it is not safe to assume this observation as a fact, unless eye disc area of control and SIK discs were compared statistically. The eye disc sizes itself were subject to fluctuate in the control w118 lines, which could be observed in adult eye sizes (20% PEF in *sensitized* at 18°C, in Figure 4.14 and Figure 4.15). In immunostainings with SIKs, experimental group discs also were larger in size for some cases. Additional statistics were also required for the prevalence assessment of other phenotypes, namely induction of additional morphogenetic furrows, ectopic morphogenetic furrow induction in the anterior eye disc, and loss of mitotic waves. On the other hand, from a developmental perspective, SIK manipulations by themselves restrict eye growth when over-expressed in higher amounts for long durations by strong drivers as in case of ey-GAL4 combined lGMR-GAL4 driver (Figures 4.13 and Figure 4.16). Interestingly, SIKs induced growth reduced was restricted to dorsal part of the eye, as in eye color changes occurred in tumor backgrounds, which hinted that SIK phenotypes alter according to DV axis and thus indicating to possible interactions with genes defining this borders, such as Notch, Iro-C. (Figure 4.12 and Figure 4.15) (McNeill *et al.* 1997).

Tumorigenesis analyses of SIKs showed that fate transitions could occur by constitutive over-expression of SIK3 protein since several ectopic antennae emerged in the eye field of survivor flies (Figure 4.17). This observation was supported during immunohistochemistry analyses which showed enormous increases of the antennal region at the expense of the eye domain in half of the discs dissected (As an example, please refer to Figures 4.18-20). The division of the eye-antennal discs into two respective domains is primarily maintained by retinal determination genes. The most acknowledged event in eye-versus-antennal fate choice is restriction of Eyeless expression to the eye discs as Cut expression supersedes Eyeless in antennal disc. Additionally, the universal iterative use of Notch and EGFR pathways has been implicated in this determination process (Kumar 2001). It is possible to argue that SIK3 CA could interact either of these pathways.

Characterization of expression pattern of these genes via antibody staining could provide the candidate interactor for SIK3. The primary target would be the Notch signaling since antennal transformations induced by SIK3 did not required epigenetic manipulations as SIK3 CA could transform the tissues even in *sensitized* background. Notch signaling could be modulated in various nodes: SIK3 could interact with Notch ligands which are known to be expressed differentially between the eye and antennal discs or phosphorylate coactivators of Notch transcription (Kumar 2001).

Increase in metastasis rate with SIK manipulation in tumorigenesis backgrounds prompted the question on ability of SIKs to influence migration in other contexts. Of two experimental setups we employed, the primary model was a chance to link with Kuser *et al.,* 2012: glial migration model, where retinal basal glia migrate onto eye disc (Küser 2012). Counting number of differentiated PR rows via ELAV staining, thus monitoring progression rates of MF, and we could assess any changes in migration rates after correlating glia cell number and MF progress (Figure 4.22) (Franzdottir *et al.* 2009). SIK2 fly CA over-expression increased numbers of glia, whereas loss of SIK2 in those cells decreased, which could be seen in loss of SIK3, too. This suggests a positive role in SIK2 migration, in parallel to increase in metastasis driven by SIK2 in *sensitized* and *eyeful* at 25°C. One issue remains to be addressed in this experiment, the state of glia migration in optic stalk, the bridge that connects the source of glia, optic lobe, and the target eye disc. Upregulation of FGF signaling, as in case of constitutive activation of Hearthless, can induce migration; however, glia cannot reach eye disc and remains stalled in the optic stalk. This is reminiscent of SIK2 loss phenotype, as very few glia were detected in the disc. If SIK2 knockdown causes higher migration, yet decreased presence of glia, one can assume that intervention to SIK signaling in both ways could produce same outcomes, once again.

Glial migration model we employed here could be expanded in order to discover SIK involvement specifically in glial cancers. Several synergistic glial cancer models have been published in *Drosophila* literature. Witte *et al.,* 2009 used the same RBG migration to model glioma, as well as others focused on fly CNS for modeling (Read *et al.* 2009; Witte *et al.* 2009). Using SIK2 in these models could strengthen our claim, in addition to present new interaction partners from these models to SIK2.

Similar to SIK3 fly CA induced death, SIK2 fly loss also detrimental to flies causing late pupal lethality. Similar results have been suggested: for example over-expression of EGF-R and Raf causes in the same developmental time point due to excessive glia numbers; or knockdown of Intergrin subunits also produce lethality (Read *et al.* 2009; Xie and Auld 2011). It is important note that, neither SIK2 over-expression nor SIK3 manipulations caused similar phenotypes. In addition, RBG specific glial drivers did not induced death, thereby making other glial as the culprit.

The other model employed was wing model (Figure 4.23) (Vidal *et al.* 2006). Interestingly, except SIK3 CA, we did not get major changes in pattern of Ptc-Gal4 staining. Even if major signaling pathways are shared between eye and imaginal disc, this result simply could be an effect of context difference between two tissues. As we induced changes in SIKs at whole AP axis by Ptc-Gal4, it is possible to see changes in migration if we express these genes clonally in a finer resolution. Of note, Src oncogene promotes ectopic migration in wing discs (Vidal *et al.* 2010). Scansite results in Table 4.1 predicted Src as SIK interactor, therefore it is possible to tap a hidden potential in case of Src and SIK combination.

SIK3 fly CA, on the other hand, produced quite remarkable result as Ptc-Gal4 staining was lost on wing disc area dedicated to notum. One explanation is SIK3 fly CA expression interacts with EGF-R, the major driving force in notum, and abolishes Ptc expression (Klein 2001). The other reason is death of these cells, which would predict morphological defects in the adult. Unfortunately so far, no data is available on Ptc driven SIK3 CA over-expressed wing discs. Even then, it is important to emphasize that *Drosophila* imaginal discs are known to proliferate under compensatory growth conditions, therefore it is possible to overlook the impact of possible SIK3 CA induced cell death when adult notum could emerge after eclosion. One way to overcome this compensation is clonally labeling cells and subsequently trace their origin.

The first member of SIKs to be directly associated with cancer, SIK1 was presented as a tumor suppressor. However, as SIK1, despite being a member of AMPK related kinase group, an important downstream element of tumor suppressor Lkb1 driven signaling events, SIK2 and SIK3 were shown to have oncogenic effects in their respective caner

contexts, which posed a riddle for the scientific community. Our study, aiming to model *Drosophila* SIKs *in vivo* comprehensively, showed that *Drosophila* SIKs are oncogenes; though further over-expression studies of human SIKs, including SIK1 which found to be evolutionarily linked to fly SIK2 in this work, should be carried out to expand this statement to human SIKs. When lethality of SIK3 gain in flies reduced, tumor phenotypes greatly were enhanced among survivor flies. However, this statement could simply be an oversimplification. We have shown that SIK2 activity varied according to expression induction strength and tumor background potency, a fact which could be appropriate for SIK3 also to a lesser extent. Optimal amounts of SIK2 could repress anomalous growth. Interestingly, in most cases, loss and gain-of-function SIK2 manipulations produced same results regarding tissue growth, cell death and proliferation, glial migration. Considering that SIKs are lost in human cancers, over-expression studies could be proposed as substitutes of loss-of-function studies which are hampered possible compensation mechanisms, which could be overcome via multiple interferences of SIK and other AMPK-RK proteins in future experiments.

As the first goal of the study to evaluate SIKs in our synergistic *Drosophila* eye cancer model, we have provided additional aspects to the study. We have shown accounts of *Drosophila* SIKs on development. SIK2 were found to be a positive regulator of glia migration, thus possible interactors of FGF signaling. SIK3 might have a role in fate determination between eye and antennal discs while influencing Notch signaling, among other candidate pathways. Furthermore, we have generated new tools. As we present a novel cleavable tag 2A to *Drosophila* community, we have established one of the first *Drosophila* disease models in Turkish scientific society.

APPENDIX A: IMMUNOHISTOCHEMISTRY FOR SIK IN EYE DISCS

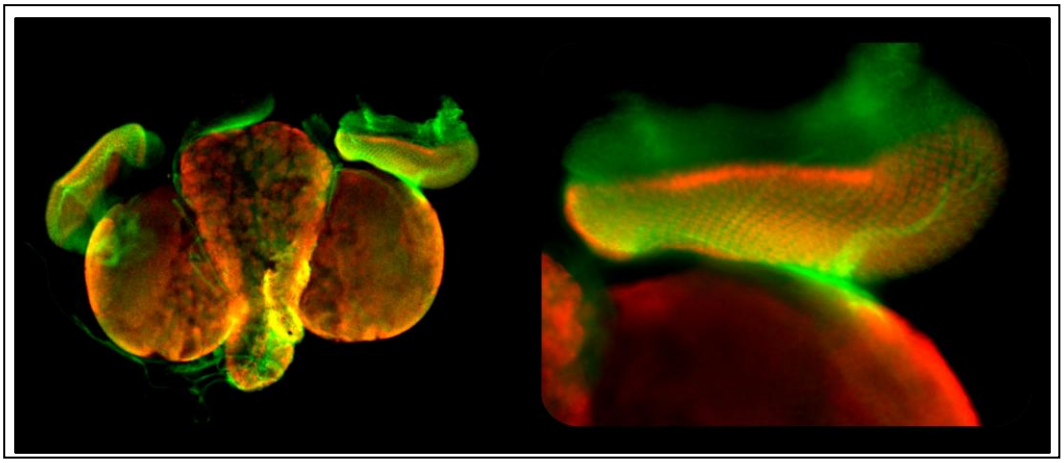

Figure A.1. Stainings in fly eye disc attached brain using anti-human SIK2 (eye disc under focus on right; Green: SIK2, Red: ELAV).

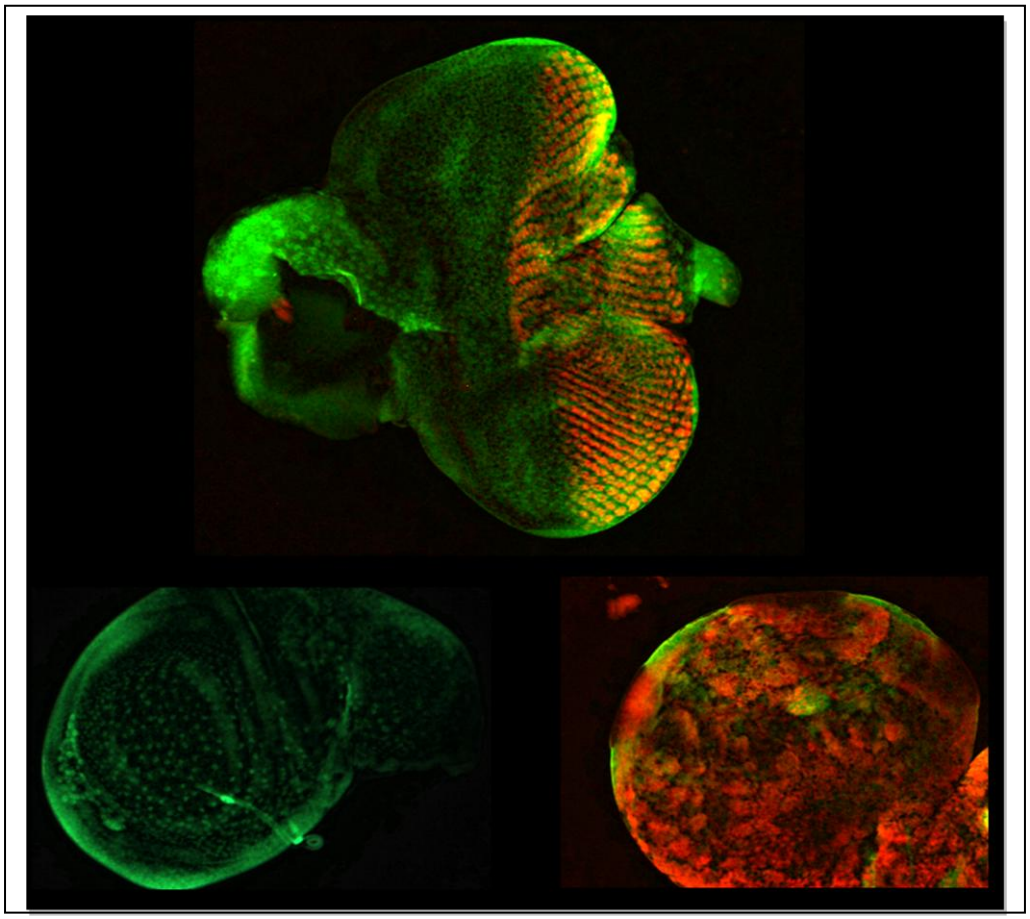

Figure A.2. Stainings in fly wing (lower left), eye disc (upper) and optic lobe of larval brain (lower right) using human anti-SIK3 antibody (Green: SIK2, Red: ELAV).

APPENDIX B: Cloning of SIK Constructs

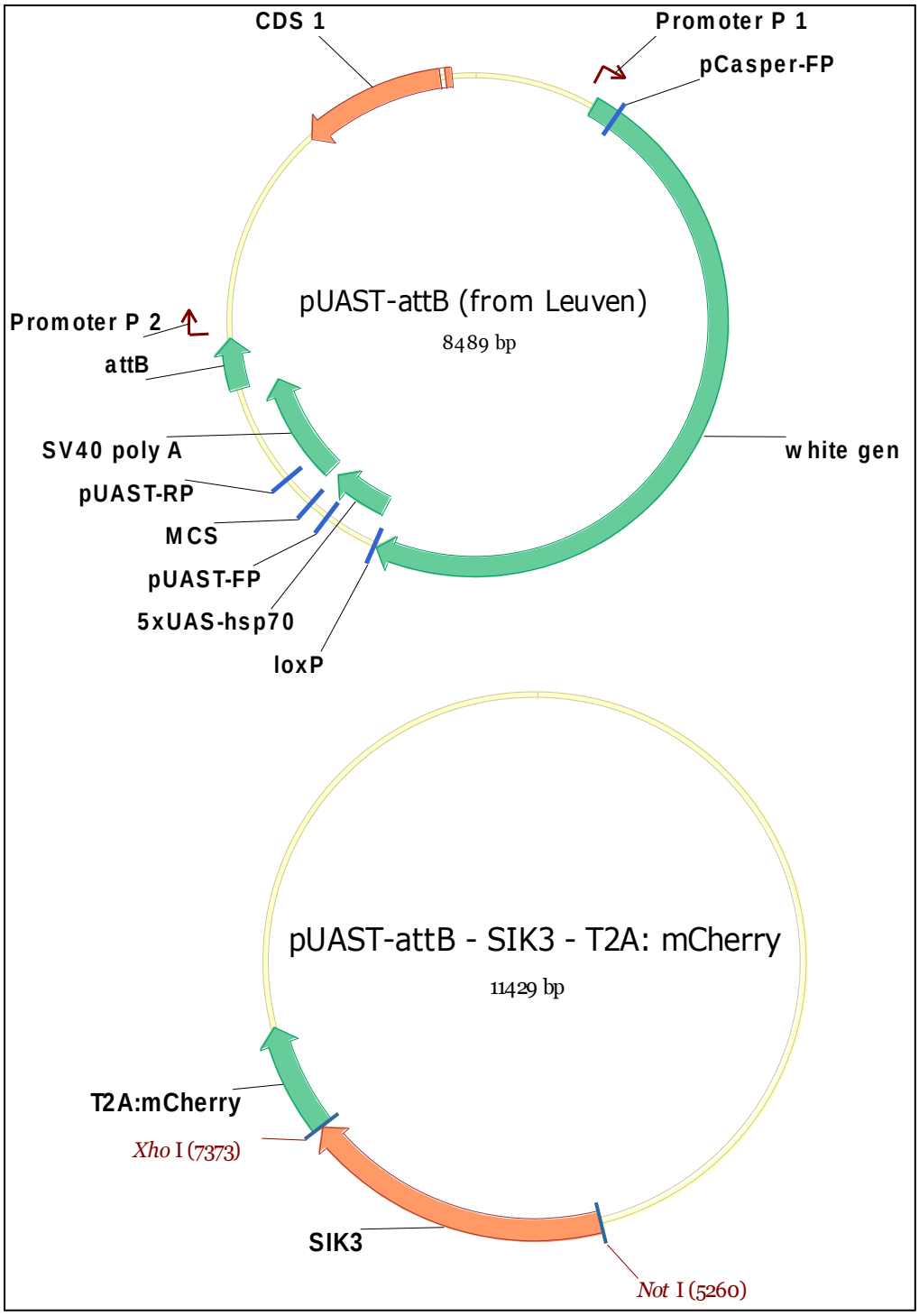

Figure B.1. Original pUAST-attB vector into which fly SIK3 was cloned resulting in the construct pUAST- attB- SIK3::T2A::mCherry.

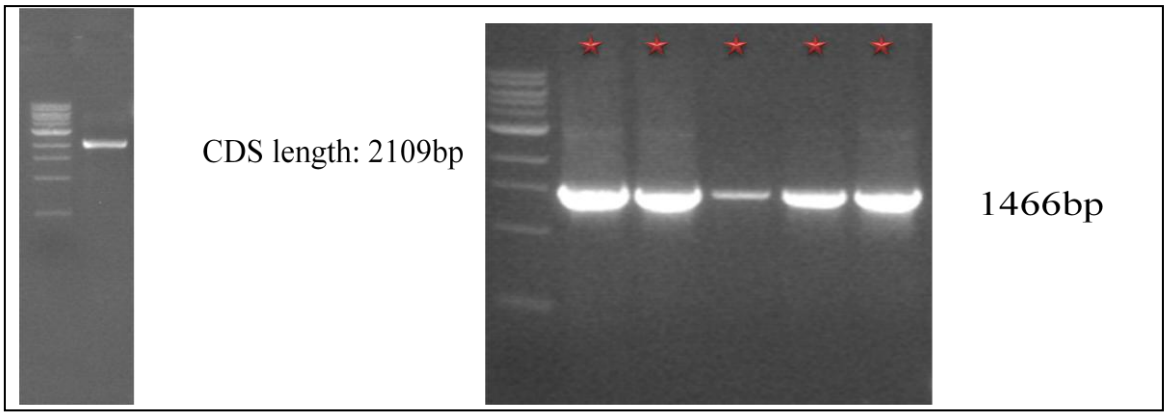

Figure B.2. Initial PCR amplification of fly SIK3 with Advantage Polymerase and subsequent validation of pGEMT-EASY cloning with colony PCR.

Figure B.3. NotI and XhoI double digestions of SIK3 fly- pGEM-T-Easy and pUAST-attB-SIK3-::T2A::mCherry.

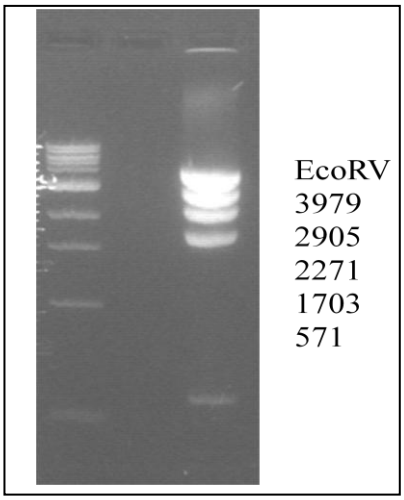

Figure B.4. Diagnostic digestion of pUAST-attB-SIK3-T2A::mCherry with EcoRV.

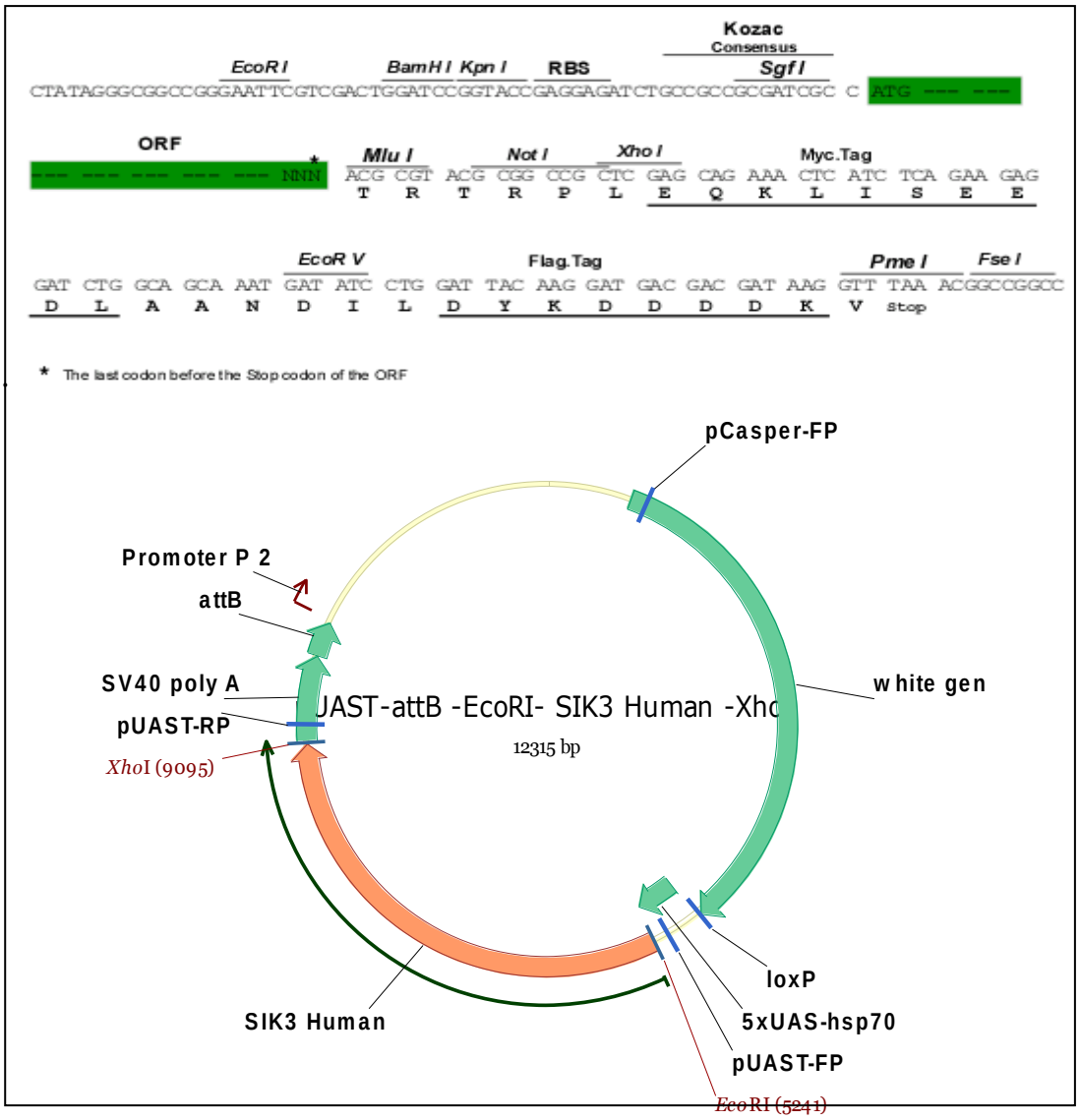

Figure B.5. pCMV6 multiple cloning site and map of human SIK3 in pUAST.

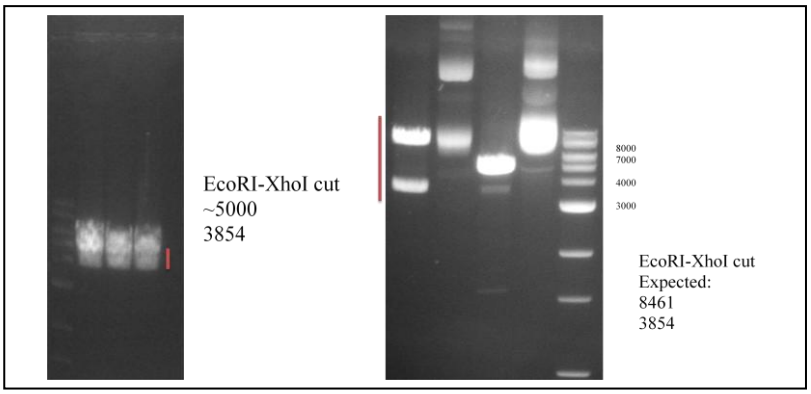

Figure B.6. Retake of human SIK3 from pCMV6 background. Double digest of pUAST-human SIK3 clone. The second and fourth lanes are undigested DNA of the clones.

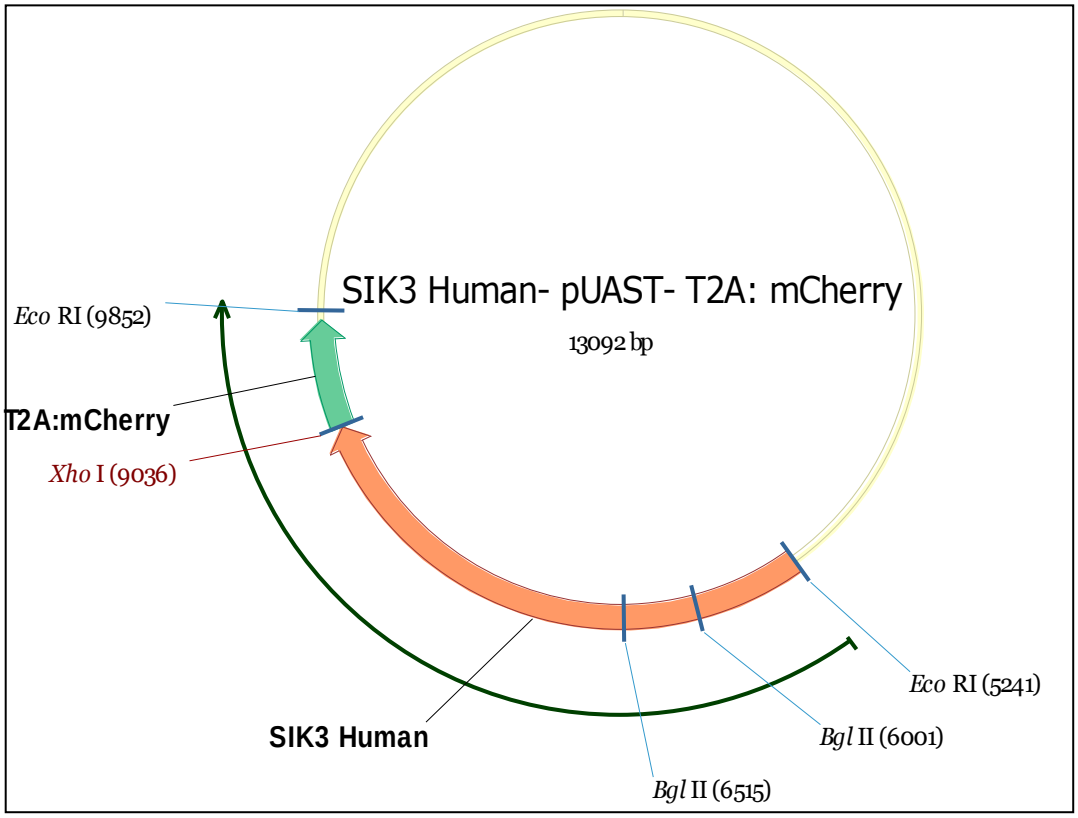

Figure B.7. Map of SIK3 human with T2A::mCherry. Green arrow represents fusion mRNA, which could produce two different proteins, SIK3 and T2A::mCherry.

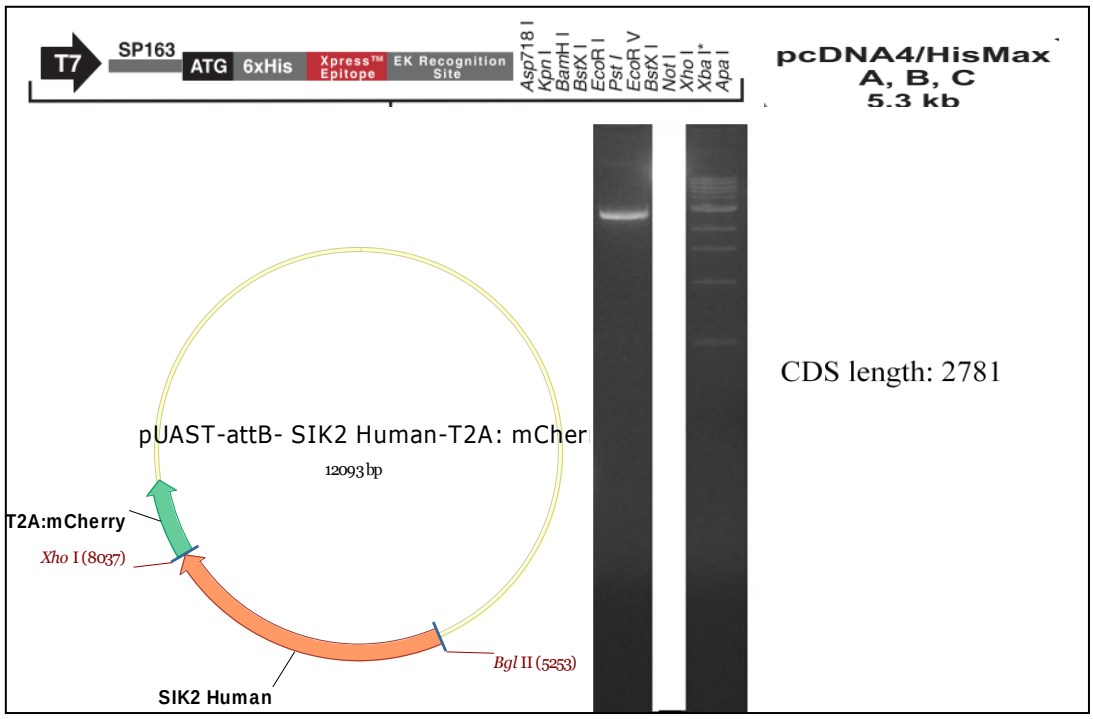

Figure B.8. Cloning of SIK2 human to pUAST-T2A::mCherry.

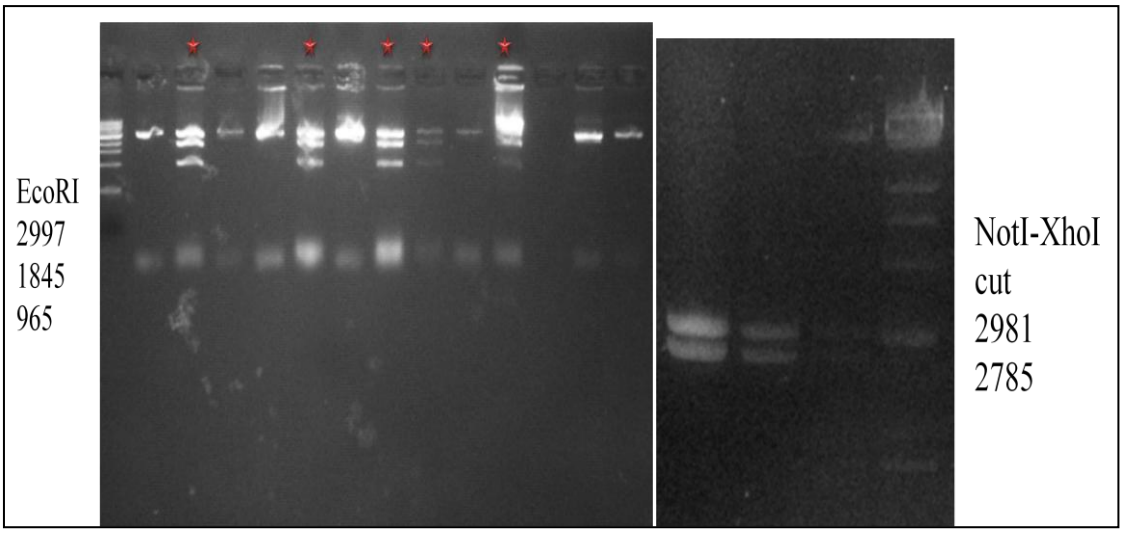

Figure B.9. Cloning of human SIK2 into pGEM-T-Easy and subsequent double digestion.

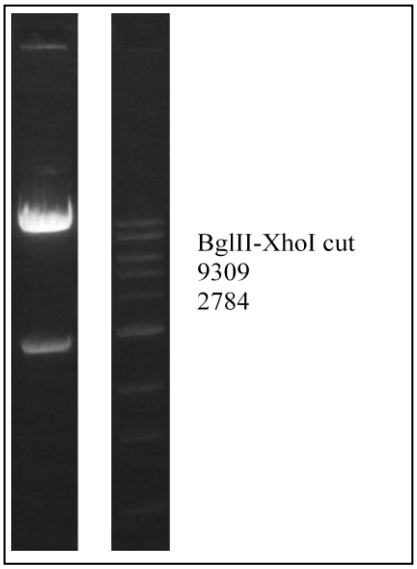

Figure B.10. Diagnostic digest for human SIK2 cloned into pUAST.

APPENDIX C: Chemicals, Supplies and Equipments

Equiment	Manufacturer
Autoclave	Astell Scientific Ltd., UK
Centrifuges	Eppendorf, Germany (Centrifuge 5424, 5417R)
Cold Room	Birikim Elektrik Soğutma, Turkey
Confocal Microscope	Leica Microsystems, USA (TCS SP5)
Cryostat	Leica Microsystems, USA (CM3050S)
Dissecting Forceps	Roboz, USA
Electronic Balances	Sartorius, Germany (TE412)
Electrophoresis Equipment	Bio-Rad Labs, USA (ReadySub-Cell GT Cells)
Fluorescence Stereomicroscope	Leica Microsystems, USA(MZ16FA)
Freezers	Arçelik, Turkey Thermo Electron Corp., USA (Thermo Forma 723)
Gel Documentation System	Bio-Rad Labs, USA (Gel Doc XR)
Heating Block	Fisher Scientific, France (Dry-bath incubator)
Heating magnetic stirrer	IKA, China (RCT Basic)
Incubator	Weiss Gallenkamp, UK (Incubator Plus Series
Inverted Microscope	Zeiss, USA (Axio Observer, Z1)
Laboratory Bottles	Isolab, Germany
Micropipettes	Eppendort, Germany
Microwave oven	Vestel, Turkey
Nanodrop	Thermo Scientific, USA
pH meter	WTW, Germany (Ph330i)
Refrigerators	Arçelik, Turkey
Rotamax	Heidolph, Germany
Stella	
Stereo Microscope	Olympus, USA (SZ61)
Thermal Cycler	Biorad, USA (c1000 Thermal Cycler)
Vortex Mixer	Scientific Industries, USA (Vortex Genie2)
Water Bath	Grant Instruments, UK (JB Aqua 12)

Disposable Materials	Manufacturer
Culture tubes, 14 ml	Greiner Bio One, Belgium
Fisherbrand Microscope Cover Glass	Fisher Scientific, UK (12-545-F)
Fisherbrand Superfrost®/Plus Microscope Slides	Fisher Scientific, UK (12-550-15)
Filter Tips	Greiner Bio-One, Belgium
Microtubes	Citotest Labware Manufacturing, China
PCR Tube Strips	Bio-Rad, USA(TBS0201)
Petri dish : Greiner Bio	One, Belgium
Pipette tips	VWR, USA

Enzymes, Kits & Solutions	**Manufacturer**
1kb DNA Ladder	New England Biolabs, USA (N3232L)
5X GoTaq Colorless Flexi Buffer	Promega, USA (M890A)
Acrylamide	Sigma-Aldrich, USA (A3574)
Advantage® 2 Polymerase Mix	Clontech, USA (639201)
Ampicillin	Sigma-Aldrich, USA (A9518)
APS	Fisher, USA (A/P470/46)
Bovine Serum Albumin	Promega, USA (R396E)
DTT	Fisher, USA (BP172-25)
Ethanol Absolute Chromasolv	Sigma-Aldrich, USA (34870).
Ethidium Bromide Solution 10 mg/ml	Sigma Life Sciences, USA (E1510-1ML)
Glycerol, for molecular biology	Sigma-Aldrich, USA (G5516-500ML)
Glycine	Fisher, USA (BP381-500)
GoTaq Flexi DNA Polymerase	Promega, USA (M830B)
LB Agar	Sigma Life Sciences, USA (SL08394)
Kanamycin	Sigma-Aldrich, USA (K4000)
LB Broth EZMix™ Powder	Sigma-Aldrich, USA (L7658-1KG)
Lithium Chloride	Merck, Germany (1056790100)
Milk powder	Cell Signaling, USA (9999S)
Qiagen Magnesium Chloride, 25mM	Qiagen, USA (12145)
Plasmid Midi Kit (100)	Qiagen, USA (27106)
QIAprep Spin Miniprep Kit (250)	Qiagen, USA (27106)
QIAquick PCR Purification Kit (250)	Qiagen, USA (28106)
Paraformaldehyde	Sigma-Aldrich, USA (P6148-1KG)
pGEM-T Easy Vector Systems	Promega, USA (A137A)
Potassium Acetete, for molecular biology	Sigma-Aldrich, USA (P119-100G)
Potassium Chloride	Sigma-Aldrich, USA (P9541-500G)
Phenol:Chloroform:Isoamyl alcohol	Sigma-Aldrich, USA (P2069)
SDS	Sigma-Aldrich, USA (L3771 – 100G)
SeaKem LE Agarose	Cambrex Bio Science, USA (50004)
Sodium Acetate	Sigma-Aldrich, USA (S8625)
Sodium Chloride, SigmaUltra	Sigma-Aldrich, USA (S7653-1KG)
SuperScript® First-Strand Synthesis System for RT-PCR	Invitrogen, USA (11904-018)
T4 DNA Ligase	New England Biolabs, USA (M0202S)
T4 DNA Ligase Reaction Buffer	New England Biolabs, USA (B0202)
TEMED	Fisher, USA (BP150-20)
Tissue-Tek	Sakura Finetek, USA (4583/ 25608-930)
Trizma Base	Sigma-Aldrich, USA (T6066)
Trizol	Invitrogen, USA (15596-026)
Tween 20	Sigma-Aldrich, USA (27,434-8)
TritonX	Roche, Germany (11 332 481 001)

:

REFERENCES

Ahmed, A. A., Z. Lu, N. B. Jennings, D. Etemadmoghadam, L. Capalbo, R. O. Jacamo, N. Barbosa-Morais, X. F. Le, P. Vivas-Mejia, G. Lopez-Berestein, G. Grandjean, G. Bartholomeusz, *et al.*, 2010, "Sik2 Is a Centrosome Kinase Required for Bipolar Mitotic Spindle Formation That Provides a Potential Target for Therapy in Ovarian Cancer", *Cancer Cell*, Vol. 18(2), pp. 109-21.

Al-Hakim, A. K., O. Goransson, M. Deak, R. Toth, D. G. Campbell, N. A. Morrice, A. R. Prescott and D. R. Alessi, 2005, "14-3-3 Cooperates with Lkb1 to Regulate the Activity and Localization of Qsk and Sik", *Journal of Cell Science*, Vol. 118(Pt 23), pp. 5661-73.

Amin, N., A. Khan, D. St Johnston, I. Tomlinson, S. Martin, J. Brenman and H. McNeill, 2009, "Lkb1 Regulates Polarity Remodeling and Adherens Junction Formation in the Drosophila Eye", *Proceedings of the National Academy of Sciences of the United States of America*, Vol. 106(22), pp. 8941-6.

Atkins, M. and G. Mardon, 2009, "Signaling in the Third Dimension: The Peripodial Epithelium in Eye Disc Development", *Developmental Dynamics*, Vol. 238(9), pp. 2139-48.

Attal, J., M. C. Theron, S. Rival, C. Puissant and L. M. Houdebine, 2000, "The Efficiency of Different Iress (Internal Ribosomes Entry Site) in Monocistronic Mrnas", *Molecular Biology Reports*, Vol. 27(1), pp. 21-6.

Augustinack, J. C., A. Schneider, E. M. Mandelkow and B. T. Hyman, 2002, "Specific Tau Phosphorylation Sites Correlate with Severity of Neuronal Cytopathology in Alzheimer's Disease", *Acta Neuropathologica*, Vol. 103(1), pp. 26-35.

Axelson, H., 2006, "Eyeing Tumorigenesis: Notch Signaling and Epigenetic Silencing of Rb in Drosophila", *Bioessays*, Vol. 28(7), pp. 692-5.

Baker, N. E. and S. Y. Yu, 1997, "Proneural Function of Neurogenic Genes in the Developing Drosophila Eye", *Current Biology*, Vol. 7(2), pp. 122-32.

Baonza, A. and M. Freeman, 2001, "Notch Signalling and the Initiation of Neural Development in the Drosophila Eye", *Development*, Vol. 128(20), pp. 3889-98.

Baonza, A., F. Roch and E. Martin-Blanco, 2000, "Der Signaling Restricts the Boundaries of the Wing Field During Drosophila Development", *Proceedings of the National Academy of Sciences of the United States of America*, Vol. 97(13), pp. 7331-5.

Basler, K. and G. Struhl, 1994, "Compartment Boundaries and the Control of Drosophila Limb Pattern by Hedgehog Protein", *Nature*, Vol. 368(6468), pp. 208-14.

Bass, B. P., K. Cullen and K. McCall, 2007, "The Axon Guidance Gene Lola Is Required for Programmed Cell Death in the Drosophila Ovary", *Developmental Biology*, Vol. 304(2), pp. 771-85.

Berdeaux, R., N. Goebel, L. Banaszynski, H. Takemori, T. Wandless, G. D. Shelton and M. Montminy, 2007, "Sik1 Is a Class Ii Hdac Kinase That Promotes Survival of Skeletal Myocytes", *Nature Medicine*, Vol. 13(5), pp. 597-603.

Bessa, J., B. Gebelein, F. Pichaud, F. Casares and R. S. Mann, 2002, "Combinatorial Control of Drosophila Eye Development by Eyeless, Homothorax, and Teashirt", *Genes & Development*, Vol. 16(18), pp. 2415-27.

Bettencourt-Dias, M., R. Giet, R. Sinka, A. Mazumdar, W. G. Lock, F. Balloux, P. J. Zafiropoulos, S. Yamaguchi, S. Winter, R. W. Carthew, M. Cooper, D. Jones, *et al.*, 2004, "Genome-Wide Survey of Protein Kinases Required for Cell Cycle Progression", *Nature*, Vol. 432(7020), pp. 980-7.

Bonchuk, A., S. Denisov, P. Georgiev and O. Maksimenko, 2011, "Drosophila Btb/Poz Domains Of "Ttk Group" Can Form Multimers and Selectively Interact with Each Other", *Journal of Molecular Biology*, Vol. 412(3), pp. 423-36.

Bossuyt, W., N. De Geest, S. Aerts, I. Leenaerts, P. Marynen and B. A. Hassan, 2009, "The Atonal Proneural Transcription Factor Links Differentiation and Tumor Formation in Drosophila", *PLoS Biology*, Vol. 7(2).

Bray, S., 1998, "Notch Signalling in Drosophila: Three Ways to Use a Pathway", *Seminars in Cell & Developmental Biology*, Vol. 9(6), pp. 591-7.

Bray, S. and F. Bernard, 2010, "Notch Targets and Their Regulation", *Current Topics in Developmental Biology*, Vol. 92 pp. 253-75.

Bricambert, J., J. Miranda, F. Benhamed, J. Girard, C. Postic and R. Dentin, 2010, "Salt-Inducible Kinase 2 Links Transcriptional Coactivator P300 Phosphorylation to the Prevention of Chrebp-Dependent Hepatic Steatosis in Mice", *The Journal of Clinical Investigation*, Vol. 120(12), pp. 4316-31.

Bright, N. J., C. Thornton and D. Carling, 2009, "The Regulation and Function of Mammalian Ampk-Related Kinases", *Acta Physiologica (Oxford, England)*, Vol. 196(1), pp. 15-26.

Bright, N. J., C. Thornton and D. Carling, 2009, "The Regulation and Function of Mammalian Ampk-Related Kinases", *Acta Physiol (Oxf)*, Vol. 196(1), pp. 15-26.

Brown, K. A., A. J. Ham, C. N. Clark, N. Meller, B. K. Law, A. Chytil, N. Cheng, J. A. Pietenpol and H. L. Moses, 2008, "Identification of Novel Smad2 and Smad3 Associated Proteins in Response to Tgf-Beta1", *Journal of Cellular Biochemistry*, Vol. 105(2), pp. 596-611.

Brumby, A. M. and H. E. Richardson, 2003, "Scribble Mutants Cooperate with Oncogenic Ras or Notch to Cause Neoplastic Overgrowth in Drosophila", *The EMBO Journal*, Vol. 22(21), pp. 5769-79.

Brumby, A. M. and H. E. Richardson, 2005, "Using Drosophila Melanogaster to Map Human Cancer Pathways", *Nature Reviews Cancer*, Vol. 5(8), pp. 626-39.

Cagan, R. L. and D. F. Ready, 1989, "The Emergence of Order in the Drosophila Pupal Retina", *Developmental Biology*, Vol. 136(2), pp. 346-62.

Cagan, R. L. and T. A. Reh, 2010, "Preface. Aspects of Eye Development: Advances over the Past Twenty Years", *Current Topics in Developmental Biology*, Vol. 93 pp. xi-xii.

Candaş, D., 2007, *Sik2 Is a Potential Mediator of Cross-Talk between Fgf and Pka Pathways*, M.S. Thesis, Boğaziçi University..

Chanut, F. and U. Heberlein, 1997, "Role of Decapentaplegic in Initiation and Progression of the Morphogenetic Furrow in the Developing Drosophila Retina", *Development*, Vol. 124(2), pp. 559-67.

Charoenfuprasert, S., Y. Y. Yang, Y. C. Lee, K. C. Chao, P. Y. Chu, C. R. Lai, K. F. Hsu, K. C. Chang, Y. C. Chen, L. T. Chen, J. Y. Chang, S. J. Leu, *et al.*, 2011, "Identification of Salt-Inducible Kinase 3 as a Novel Tumor Antigen Associated with Tumorigenesis of Ovarian Cancer", *Oncogene*, Vol. 30(33), pp. 3570-84.

Cheng, H., P. Liu, Z. C. Wang, L. Zou, S. Santiago, V. Garbitt, O. V. Gjoerup, J. D. Iglehart, A. Miron, A. L. Richardson, W. C. Hahn and J. J. Zhao, 2009, "Sik1 Couples Lkb1 to P53-Dependent Anoikis and Suppresses Metastasis", *Science Signaling*, Vol. 2(80), pp. ra35.

Cheng, J., M. Uchida, W. Zhang, M. R. Grafe, P. S. Herson and P. D. Hurn, 2011, "Role of Salt-Induced Kinase 1 in Androgen Neuroprotection against Cerebral Ischemia", *Journal of Cerebral Blood Flow and Metabolism*, Vol. 31(1), pp. 339-50.

Chi, C., H. Zhu, M. Han, Y. Zhuang, X. Wu and T. Xu, 2010, "Disruption of Lysosome Function Promotes Tumor Growth and Metastasis in Drosophila", *The Journal of Biological Chemistry*, Vol. 285(28), pp. 21817-23.

Cho, K. O., J. Chern, S. Izaddoost and K. W. Choi, 2000, "Novel Signaling from the Peripodial Membrane Is Essential for Eye Disc Patterning in Drosophila", *Cell*, Vol. 103(2), pp. 331-42.

Cho, K. O. and K. W. Choi, 1998, "Fringe Is Essential for Mirror Symmetry and Morphogenesis in the Drosophila Eye", *Nature*, Vol. 396(6708), pp. 272-6.

Choi, S., W. Kim and J. Chung, 2011, "Drosophila Salt-Inducible Kinase (Sik) Regulates Starvation Resistance through Camp-Response Element-Binding Protein (Creb)-Regulated Transcription Coactivator (Crtc)", *The Journal of Biological Chemistry*, Vol. 286(4), pp. 2658-64.

Debacq, C., B. Asquith, P. Kerkhofs, D. Portetelle, A. Burny, R. Kettmann and L. Willems, 2002, "Increased Cell Proliferation, but Not Reduced Cell Death, Induces Lymphocytosis in Bovine Leukemia Virus-Infected Sheep", *Proceedings of the National Academy of Sciences of the United States of America*, Vol. 99(15), pp. 10048-53.

Dentin, R., Y. Liu, S. H. Koo, S. Hedrick, T. Vargas, J. Heredia, J. Yates, 3rd and M. Montminy, 2007, "Insulin Modulates Gluconeogenesis by Inhibition of the Coactivator Torc2", *Nature*, Vol. 449(7160), pp. 366-9.

Dichtel-Danjoy, M. L., J. Caldeira and F. Casares, 2009, "Soxf Is Part of a Novel Negative-Feedback Loop in the Wingless Pathway That Controls Proliferation in the Drosophila Wing Disc", *Development*, Vol. 136(5), pp. 761-9.

Dickson, B., F. Sprenger and E. Hafen, 1992, "Prepattern in the Developing Drosophila Eye Revealed by an Activated Torso--Sevenless Chimeric Receptor", *Genes & Development*, Vol. 6(12A), pp. 2327-39.

Dietrich, J. B., H. Takemori, S. Grosch-Dirrig, A. Bertorello and J. Zwiller, 2012, "Cocaine Induces the Expression of Mef2c Transcription Factor in Rat Striatum through Activation of Sik1 and Phosphorylation of the Histone Deacetylase Hdac5", *Synapse*, Vol. 66(1), pp. 61-70.

Dietzl, G., D. Chen, F. Schnorrer, K. C. Su, Y. Barinova, M. Fellner, B. Gasser, K. Kinsey, S. Oppel, S. Scheiblauer, A. Couto, V. Marra, *et al.*, 2007, "A Genome-Wide Transgenic Rnai Library for Conditional Gene Inactivation in Drosophila", *Nature*, Vol. 448(7150), pp. 151-6.

Dominguez, M. and F. Casares, 2005, "Organ Specification-Growth Control Connection: New in-Sights from the Drosophila Eye-Antennal Disc", *Developmental Dynamics*, Vol. 232(3), pp. 673-84.

Dominguez, M. and J. F. de Celis, 1998, "A Dorsal/Ventral Boundary Established by Notch Controls Growth and Polarity in the Drosophila Eye", *Nature*, Vol. 396(6708), pp. 276-8.

Dominguez, M. and E. Hafen, 1997, "Hedgehog Directly Controls Initiation and Propagation of Retinal Differentiation in the Drosophila Eye", *Genes & Development*, Vol. 11(23), pp. 3254-64.

Doroquez, D. B. and I. Rebay, 2006, "Signal Integration During Development: Mechanisms of Egfr and Notch Pathway Function and Cross-Talk", *Critical Reviews in Bİochemistry and Molecular Biology*, Vol. 41(6), pp. 339-85.

Drewes, G., B. Trinczek, S. Illenberger, J. Biernat, G. Schmitt-Ulms, H. E. Meyer, E. M. Mandelkow and E. Mandelkow, 1995, "Microtubule-Associated Protein/Microtubule Affinity-Regulating Kinase (P110mark). A Novel Protein Kinase That Regulates Tau-Microtubule Interactions and Dynamic Instability by Phosphorylation at the Alzheimer-Specific Site Serine 262", *The Journal of Biological Chemistry*, Vol. 270(13), pp. 7679-88.

Du, J., Q. Chen, H. Takemori and H. Xu, 2008, "Sik2 Can Be Activated by Deprivation of Nutrition and It Inhibits Expression of Lipogenic Genes in Adipocytes", *Obesity (Silver Spring)*, Vol. 16(3), pp. 531-8.

Ellisen, L. W., J. Bird, D. C. West, A. L. Soreng, T. C. Reynolds, S. D. Smith and J. Sklar, 1991, "Tan-1, the Human Homolog of the Drosophila Notch Gene, Is Broken by Chromosomal Translocations in T Lymphoblastic Neoplasms", *Cell*, Vol. 66(4), pp. 649-61.

Eneling, K., L. Brion, V. Pinto, M. J. Pinho, J. I. Sznajder, N. Mochizuki, K. Emoto, P. Soares-da-Silva and A. M. Bertorello, 2012, "Salt-Inducible Kinase 1 Regulates E-Cadherin Expression and Intercellular Junction Stability", *FASEB Journal*, Vol.

Eneling, K., J. Chen, L. C. Welch, H. Takemori, J. I. Sznajder and A. M. Bertorello, 2011, "Salt-Inducible Kinase 1 Is Present in Lung Alveolar Epithelial Cells and Regulates Active Sodium Transport", *Biochemical and Biophysical Research Communications*, Vol. 409(1), pp. 28-33.

Feldman, J. D., L. Vician, M. Crispino, W. Hoe, M. Baudry and H. R. Herschman, 2000, "The Salt-Inducible Kinase, Sik, Is Induced by Depolarization in Brain", *Journal of Neurochemistry*, Vol. 74(6), pp. 2227-38.

Ferres-Marco, D., I. Gutierrez-Garcia, D. M. Vallejo, J. Bolivar, F. J. Gutierrez-Avino and M. Dominguez, 2006, "Epigenetic Silencers and Notch Collaborate to Promote Malignant Tumours by Rb Silencing", *Nature*, Vol. 439(7075), pp. 430-6.

Fischer, J. A., E. Giniger, T. Maniatis and M. Ptashne, 1988, "Gal4 Activates Transcription in Drosophila", *Nature*, Vol. 332(6167), pp. 853-6.

Flores, G. V., H. Duan, H. Yan, R. Nagaraj, W. Fu, Y. Zou, M. Noll and U. Banerjee, 2000, "Combinatorial Signaling in the Specification of Unique Cell Fates", *Cell*, Vol. 103(1), pp. 75-85.

Franzdottir, S. R., D. Engelen, Y. Yuva-Aydemir, I. Schmidt, A. Aho and C. Klambt, 2009, "Switch in Fgf Signalling Initiates Glial Differentiation in the Drosophila Eye", *Nature*, Vol. 460(7256), pp. 758-61.

Freeman, M., 1996, "Reiterative Use of the Egf Receptor Triggers Differentiation of All Cell Types in the Drosophila Eye", *Cell*, Vol. 87(4), pp. 651-60.

Furler, S., J. C. Paterna, M. Weibel and H. Bueler, 2001, "Recombinant Aav Vectors Containing the Foot and Mouth Disease Virus 2a Sequence Confer Efficient Bicistronic Gene Expression in Cultured Cells and Rat Substantia Nigra Neurons", *Gene Therapy*, Vol. 8(11), pp. 864-73.

Gibson, M. C. and G. Schubiger, 2000, "Peripodial Cells Regulate Proliferation and Patterning of Drosophila Imaginal Discs", *Cell*, Vol. 103(2), pp. 343-50.

Gilmore, A. P., 2005, "Anoikis", *Cell Death and Differentiation*, Vol. 12 (2), pp. 1473-7.

Giniger, E., K. Tietje, L. Y. Jan and Y. N. Jan, 1994, "Lola Encodes a Putative Transcription Factor Required for Axon Growth and Guidance in Drosophila", *Development*, Vol. 120(6), pp. 1385-98.

Giza, C. C., M. L. Prins, D. A. Hovda, H. R. Herschman and J. D. Feldman, 2002, "Genes Preferentially Induced by Depolarization after Concussive Brain Injury: Effects of Age and Injury Severity", *Journal of Neurotrauma*, Vol. 19(4), pp. 387-402.

Gladstone, M. and T. T. Su, 2011, "Chemical Genetics and Drug Screening in Drosophila Cancer Models", *Journal of Genetics and Genomics*, Vol. 38(10), pp. 497-504.

Goto, S. and S. Hayashi, 1997, "Specification of the Embryonic Limb Primordium by Graded Activity of Decapentaplegic", *Development*, Vol. 124(1), pp. 125-32.

Grillo, M., M. Furriols, J. Casanova and S. Luschnig, 2010, "Control of Germline Torso Expression by the Btb/Poz Domain Protein Pipsqueak Is Required for Embryonic Terminal Patterning in Drosophila", *Genetics*, Vol. 187(2), pp. 513-21.

Guo, M. and B. A. Hay, 1999, "Cell Proliferation and Apoptosis", *Current Opinion in Cell Biology*, Vol. 11(6), pp. 745-52.

Hanahan, D. and R. A. Weinberg, 2011, "Hallmarks of Cancer: The Next Generation", *Cell*, Vol. 144(5), pp. 646-74.

Hart, A. C., H. Kramer, D. L. Van Vactor, Jr., M. Paidhungat and S. L. Zipursky, 1990, "Induction of Cell Fate in the Drosophila Retina: The Bride of Sevenless Protein Is Predicted to Contain a Large Extracellular Domain and Seven Transmembrane Segments", *Genes & Development*, Vol. 4(11), pp. 1835-47.

Hashimoto, Y. K., T. Satoh, M. Okamoto and H. Takemori, 2008, "Importance of Autophosphorylation at Ser186 in the a-Loop of Salt Inducible Kinase 1 for Its Sustained Kinase Activity", *Journal of Cellular Biochemistry*, Vol. 104(5), pp. 1724-39.

Heberlein, U., C. M. Singh, A. Y. Luk and T. J. Donohoe, 1995, "Growth and Differentiation in the Drosophila Eye Coordinated by Hedgehog", *Nature*, Vol. 373(6516), pp. 709-11.

Heberlein, U., T. Wolff and G. M. Rubin, 1993, "The Tgf Beta Homolog Dpp and the Segment Polarity Gene Hedgehog Are Required for Propagation of a Morphogenetic Wave in the Drosophila Retina", *Cell*, Vol. 75(5), pp. 913-26.

Heitzler, P., M. Bourouis, L. Ruel, C. Carteret and P. Simpson, 1996, "Genes of the Enhancer of Split and Achaete-Scute Complexes Are Required for a Regulatory Loop between Notch and Delta During Lateral Signalling in Drosophila", *Development*, Vol. 122(1), pp. 161-71.

Horike, N., A. Kumagai, Y. Shimono, T. Onishi, Y. Itoh, T. Sasaki, K. Kitagawa, O. Hatano, H. Takagi, T. Susumu, H. Teraoka, K. Kusano, *et al.*, 2010, "Downregulation of Sik2 Expression Promotes the Melanogenic Program in Mice", *Pigment Cell & Melanoma Research*, Vol. 23(6), pp. 809-19.

Horike, N., H. Takemori, Y. Katoh, J. Doi and M. Okamoto, 2002, "Roles of Several Domains Identified in the Primary Structure of Salt-Inducible Kinase (Sik)", *Endocrine Research*, Vol. 28(4), pp. 291-4.

Hsiao, F. C., A. Williams, E. L. Davies and I. Rebay, 2001, "Eyes Absent Mediates Cross-Talk between Retinal Determination Genes and the Receptor Tyrosine Kinase Signaling Pathway", *Developmental Cell*, Vol. 1(1), pp. 51-61.

Huang, D. H., Y. L. Chang, C. C. Yang, I. C. Pan and B. King, 2002, "Pipsqueak Encodes a Factor Essential for Sequence-Specific Targeting of a Polycomb Group Protein Complex", *Molecular and Cellular Biology*, Vol. 22(17), pp. 6261-71.

Huang, P. H., C. H. Chen, C. C. Chou, A. M. Sargeant, S. K. Kulp, C. M. Teng, J. C. Byrd and C. S. Chen, 2010, "Histone Deacetylase Inhibitors Stimulate Histone H3 Lysine 4 Methylation in Part Via Transcriptional Repression of Histone H3 Lysine 4 Demethylases", *Molecular Pharmacology*, Vol. 79(1), pp. 197-206.

Hummel, T., S. Attix, D. Gunning and S. L. Zipursky, 2002, "Temporal Control of Glial Cell Migration in the Drosophila Eye Requires Gilgamesh, Hedgehog, and Eye Specification Genes", *Neuron*, Vol. 33(2), pp. 193-203.

Igaki, T., R. A. Pagliarini and T. Xu, 2006, "Loss of Cell Polarity Drives Tumor Growth and Invasion through Jnk Activation in Drosophila", *Current Biology*, Vol. 16(11), pp. 1139-46.

Ikushima, H. and K. Miyazono, 2012, "Tgf-Beta Signal Transduction Spreading to a Wider Field: A Broad Variety of Mechanisms for Context-Dependent Effects of Tgf-Beta", *Cell and Tİssue Research*, Vol. 347(1), pp. 37-49.

Jaleel, M., F. Villa, M. Deak, R. Toth, A. R. Prescott, D. M. Van Aalten and D. R. Alessi, 2006, "The Ubiquitin-Associated Domain of Ampk-Related Kinases Regulates Conformation and Lkb1-Mediated Phosphorylation and Activation", *The Biochemical Journal*, Vol. 394(Pt 3), pp. 545-55.

Jefcoate, C. R., J. Lee, N. Cherradi, H. Takemori and H. Duan, 2011, "Camp Stimulation of Star Expression and Cholesterol Metabolism Is Modulated by Co-Expression of Labile Suppressors of Transcription and Mrna Turnover", *Molecular and Cellular Endocrinology*, Vol. 336(1-2), pp. 53-62.

Katanaev, V. L. and M. V. Kryuchkov, 2012, "The Eye of Drosophila as a Model System for Studying Intracellular Signaling in Ontogenesis and Pathogenesis", *Biochemistry*, Vol. 76(13), pp. 1556-81.

Katoh, M., 2004, "Identification and Characterization of Human Foxn5 and Rat Foxn5 Genes in Silico", *International Journal of Oncology*, Vol. 24(5), pp. 1339-44.

Katoh, Y., H. Takemori, N. Horike, J. Doi, M. Muraoka, L. Min and M. Okamoto, 2004, "Salt-Inducible Kinase (Sik) Isoforms: Their Involvement in Steroidogenesis and Adipogenesis", *Molecular and Cellular Endocrinology*, Vol. 217(1-2), pp. 109-12.

Kenyon, K. L., S. S. Ranade, J. Curtiss, M. Mlodzik and F. Pignoni, 2003, "Coordinating Proliferation and Tissue Specification to Promote Regional Identity in the Drosophila Head", *Developmental Cell*, Vol. 5(3), pp. 403-14.

Kimura, M., 1980, "A Simple Method for Estimating Evolutionary Rates of Base Substitutions through Comparative Studies of Nucleotide Sequences", *Journal of Molecular Evolution*, Vol. 16(2), pp. 111-20.

Klein, T., 2001, "Wing Disc Development in the Fly: The Early Stages", *Current Opinion in Genetics & Development*, Vol. 11(4), pp. 470-5.

Kowanetz, M., P. Lonn, M. Vanlandewijck, K. Kowanetz, C. H. Heldin and A. Moustakas, 2008, "Tgfbeta Induces Sik to Negatively Regulate Type I Receptor Kinase Signaling", *The Journal of Cell Biology*, Vol. 182(4), pp. 655-62.

Krejci, A., F. Bernard, B. E. Housden, S. Collins and S. J. Bray, 2009, "Direct Response to Notch Activation: Signaling Crosstalk and Incoherent Logic", *Science Signaling*, Vol. 2(55), pp. ra1.

Krupp, J. J., L. E. Yaich, R. J. Wessells and R. Bodmer, 2005, "Identification of Genetic Loci That Interact with Cut During Drosophila Wing-Margin Development", *Genetics*, Vol. 170(4), pp. 1775-95.

Kumar, J. P., 2001, "Signalling Pathways in Drosophila and Vertebrate Retinal Development", *Nature Reviews Genetics*, Vol. 2(11), pp. 846-57.

Kumar, J. P. and K. Moses, 2001, "Egf Receptor and Notch Signaling Act Upstream of Eyeless/Pax6 to Control Eye Specification", *Cell*, Vol. 104(5), pp. 687-97.

Kurata, S., M. J. Go, S. Artavanis-Tsakonas and W. J. Gehring, 2000, "Notch Signaling and the Determination of Appendage Identity", *Proceedings of the National Academy of Sciences of the United States of America*, Vol. 97(5), pp. 2117-22.

Küser, G., 2006, *Identification of Candidate Substrates of Sik2 in Vitro*, M.S. Thesis, Boğaziçi University.

Küser, G., 2012, *Sik2: A Key Player in Fgf2-Induced Proliferation and Insulin- Induced Surivival/Hyperglycemia-Dependent Apoptosis in Müller Cells*, Ph.D. Thesis, Boğaziçi University.

Lanjuin, A. and P. Sengupta, 2002, "Regulation of Chemosensory Receptor Expression and Sensory Signaling by the Kin-29 Ser/Thr Kinase", *Neuron*, Vol. 33(3), pp. 369-81.

Lim, H. Y. and A. Tomlinson, 2006, "Organization of the Peripheral Fly Eye: The Roles of Snail Family Transcription Factors in Peripheral Retinal Apoptosis", *Development*, Vol. 133(18), pp. 3529-37.

Liu, Y., V. Poon, G. Sanchez-Watts, A. G. Watts, H. Takemori and G. Aguilera, 2011, "Salt-Inducible Kinase Is Involved in the Regulation of Corticotropin-Releasing Hormone Transcription in Hypothalamic Neurons in Rats", *Endocrinology*, Vol. 153(1), pp. 223-33.

Lizcano, J. M., O. Goransson, R. Toth, M. Deak, N. A. Morrice, J. Boudeau, S. A. Hawley, L. Udd, T. P. Makela, D. G. Hardie and D. R. Alessi, 2004, "Lkb1 Is a Master Kinase That Activates 13 Kinases of the Ampk Subfamily, Including Mark/Par-1", *The EMBO Journal*, Vol. 23(4), pp. 833-43.

Lonn, P., M. Vanlandewijck, E. Raja, M. Kowanetz, Y. Watanabe, K. Kowanetz, E. Vasilaki, C. H. Heldin and A. Moustakas, 2012, "Transcriptional Induction of Salt-Inducible Kinase 1 by Transforming Growth Factor Beta Leads to Negative Regulation of Type I Receptor Signaling in Cooperation with the Smurf2 Ubiquitin Ligase", *The Journal of Biological Chemistry*, Vol. 287(16), pp. 12867-78.

MacDonald, J. W. and D. Ghosh, 2006, "Copa--Cancer Outlier Profile Analysis", *Bioinformatics*, Vol. 22(23), pp. 2950-1.

Maduzia, L. L., A. F. Roberts, H. Wang, X. Lin, L. J. Chin, C. M. Zimmerman, S. Cohen, X. H. Feng and R. W. Padgett, 2005, "C. Elegans Serine-Threonine Kinase Kin-29 Modulates Tgfbeta Signaling and Regulates Body Size Formation", *BMC Developmental Biology*, Vol. 5 pp. 8.

Manseau, L., A. Baradaran, D. Brower, A. Budhu, F. Elefant, H. Phan, A. V. Philp, M. Yang, D. Glover, K. Kaiser, K. Palter and S. Selleck, 1997, "Gal4 Enhancer Traps Expressed in the Embryo, Larval Brain, Imaginal Discs, and Ovary of Drosophila", *Developmental Dynamics*, Vol. 209(3), pp. 310-22.

Martinez, A. M., B. Schuettengruber, S. Sakr, A. Janic, C. Gonzalez and G. Cavalli, 2009, "Polyhomeotic Has a Tumor Suppressor Activity Mediated by Repression of Notch Signaling", *Nature Genetics*, Vol. 41(10), pp. 1076-82.

Matsuoka, S., B. A. Ballif, A. Smogorzewska, E. R. McDonald, 3rd, K. E. Hurov, J. Luo, C. E. Bakalarski, Z. Zhao, N. Solimini, Y. Lerenthal, Y. Shiloh, S. P. Gygi, *et al.*, 2007, "Atm and Atr Substrate Analysis Reveals Extensive Protein Networks Responsive to DNA Damage", *Science*, Vol. 316(5828), pp. 1160-6.

Maves, L. and G. Schubiger, 1998, "A Molecular Basis for Transdetermination in Drosophila Imaginal Discs: Interactions between Wingless and Decapentaplegic Signaling", *Development*, Vol. 125(1), pp. 115-24.

Maves, L. and G. Schubiger, 2003, "Transdetermination in Drosophila Imaginal Discs: A Model for Understanding Pluripotency and Selector Gene Maintenance", *Current Opinion in Genetics & Development*, Vol. 13(5), pp. 472-9.

McNeill, H., C. H. Yang, M. Brodsky, J. Ungos and M. A. Simon, 1997, "Mirror Encodes a Novel Pbx-Class Homeoprotein That Functions in the Definition of the Dorsal-Ventral Border in the Drosophila Eye", *Genes & Development*, Vol. 11(8), pp. 1073-82.

McQuilton, P., S. E. St Pierre and J. Thurmond, 2011, "Flybase 101--the Basics of Navigating Flybase", *Nucleic Acids Research*, Vol. 40(Database issue), pp. D706-14.

Mukherjee, T., I. Choi and U. Banerjee, 2012, "Genetic Analysis of Fibroblast Growth Factor Signaling in the Drosophila Eye", *G3 (Bethesda, Md.)*, Vol. 2(1), pp. 23-8.

Murakami, S., D. Umetsu, Y. Maeyama, M. Sato, S. Yoshida and T. Tabata, 2007, "Focal Adhesion Kinase Controls Morphogenesis of the Drosophila Optic Stalk", *Development*, Vol. 134(8), pp. 1539-48.

Muraoka, M., A. Fukushima, S. Viengchareun, M. Lombes, F. Kishi, A. Miyauchi, M. Kanematsu, J. Doi, J. Kajimura, R. Nakai, T. Uebi, M. Okamoto, *et al.*, 2009, "Involvement of Sik2/Torc2 Signaling Cascade in the Regulation of Insulin-Induced Pgc-1alpha and Ucp-1 Gene Expression in Brown Adipocytes", *American Journal of Physiology Endocrinology and Metabolism*, Vol. 296(6), pp. E1430-9.

Nagaraj, R. and U. Banerjee, 2007, "Combinatorial Signaling in the Specification of Primary Pigment Cells in the Drosophila Eye", *Development*, Vol. 134(5), pp. 825-31.

Nagel, S., E. Leich, H. Quentmeier, C. Meyer, M. Kaufmann, M. Zaborski, A. Rosenwald, H. G. Drexler and R. A. Macleod, 2010, "Amplification at 11q23 Targets Protein Kinase Sik2 in Diffuse Large B-Cell Lymphoma", *Leukemia & Lymphoma*, Vol. 51(5), pp. 881-91.

Obenauer, J. C., L. C. Cantley and M. B. Yaffe, 2003, "Scansite 2.0: Proteome-Wide Prediction of Cell Signaling Interactions Using Short Sequence Motifs", *Nucleic Acids Research*, Vol. 31(13), pp. 3635-41.

Oldham, S. and E. Hafen, 2003, "Insulin/Igf and Target of Rapamycin Signaling: A Tor De Force in Growth Control", *Trends in Cell Biology*, Vol. 13(2), pp. 79-85.

Özcan, F., 2003, *Identification of a Putative Serine/Threonine Kinase Implicated in Fgf Signal Transduction and Its Compatibility with an Fgf Pathway Simulation Model*, Ph.D. Thesis, Bogaziçi University.

Palomero, T., M. L. Sulis, M. Cortina, P. J. Real, K. Barnes, M. Ciofani, E. Caparros, J. Buteau, K. Brown, S. L. Perkins, G. Bhagat, A. M. Agarwal, *et al.*, 2007, "Mutational Loss of Pten Induces Resistance to Notch1 Inhibition in T-Cell Leukemia", *Nature Medicine*, Vol. 13(10), pp. 1203-10.

Panin, V. M., V. Papayannopoulos, R. Wilson and K. D. Irvine, 1997, "Fringe Modulates Notch-Ligand Interactions", *Nature*, Vol. 387(6636), pp. 908-12.

Papayannopoulos, V., A. Tomlinson, V. M. Panin, C. Rauskolb and K. D. Irvine, 1998, "Dorsal-Ventral Signaling in the Drosophila Eye", *Science*, Vol. 281(5385), pp. 2031-4.

Peng, H. W., M. Slattery and R. S. Mann, 2009, "Transcription Factor Choice in the Hippo Signaling Pathway: Homothorax and Yorkie Regulation of the Microrna Bantam in the Progenitor Domain of the Drosophila Eye Imaginal Disc", *Genes & Development*, Vol. 23(19), pp. 2307-19.

Pielage, J., A. Kippert, M. Zhu and C. Klambt, 2004, "The Drosophila Transmembrane Protein Fear-of-Intimacy Controls Glial Cell Migration", *Developmental Biology*, Vol. 275(1), pp. 245-57.

Polesello, C., F. Roch, V. Gobert, M. Haenlin and L. Waltzer, 2011, "Modeling Cancers in Drosophila", *Progress in Molecular Biology and Translational Science*, Vol. 100 pp. 51-82.

Popov, S., K. Venetsanou, P. J. Chedrese, V. Pinto, H. Takemori, A. Franco-Cereceda, P. Eriksson, N. Mochizuki, P. Soares-da-Silva and A. M. Bertorello, 2012, "Increases in Intracellular Sodium Activate Transcription and Gene Expression Via the Salt-Inducible Kinase 1 Network in an Atrial Myocyte Cell Line", *American Journal of Physiology: Heart and Circulatory Physiology*, Vol.

Poretti, G., I. Kwee, B. Bernasconi, P. M. Rancoita, A. Rinaldi, C. Capella, E. Zucca, A. Neri, M. G. Tibiletti and F. Bertoni, 2011, "Chromosome 11q23.1 Is an Unstable Region in B-Cell Tumor Cell Lines", *Leukemia Research*, Vol. 35(6), pp. 808-13.

Punzo, C., S. Plaza, M. Seimiya, P. Schnupf, S. Kurata, J. Jaeger and W. J. Gehring, 2004, "Functional Divergence between Eyeless and Twin of Eyeless in Drosophila Melanogaster", *Development*, Vol. 131(16), pp. 3943-53.

Rangarajan, R., Q. Gong and U. Gaul, 1999, "Migration and Function of Glia in the Developing Drosophila Eye", *Development*, Vol. 126(15), pp. 3285-92.

Read, R. D., W. K. Cavenee, F. B. Furnari and J. B. Thomas, 2009, "A Drosophila Model for Egfr-Ras and Pi3k-Dependent Human Glioma", *PLoS Genetics*, Vol. 5(2), pp. e1000374.

Ready, D. F., T. E. Hanson and S. Benzer, 1976, "Development of the Drosophila Retina, a Neurocrystalline Lattice", *Developmental Biology*, Vol. 53(2), pp. 217-40.

Reinke, R. and S. L. Zipursky, 1988, "Cell-Cell Interaction in the Drosophila Retina: The Bride of Sevenless Gene Is Required in Photoreceptor Cell R8 for R7 Cell Development", *Cell*, Vol. 55(2), pp. 321-30.

Roignant, J. Y. and J. E. Treisman, 2009, "Pattern Formation in the Drosophila Eye Disc", *The International Journal of Developmental Biology*, Vol. 53(5-6), pp. 795-804.

Romito, A., E. Lonardo, G. Roma, G. Minchiotti, A. Ballabio and G. Cobellis, 2010, "Lack of Sik1 in Mouse Embryonic Stem Cells Impairs Cardiomyogenesis by Down-Regulating the Cyclin-Dependent Kinase Inhibitor P57kip2", *PLoS One*, Vol. 5(2), pp. e9029.

Ruiz, J. C., F. L. Conlon and E. J. Robertson, 1994, "Identification of Novel Protein Kinases Expressed in the Myocardium of the Developing Mouse Heart", *Mechanisms of Development*, Vol. 48(3), pp. 153-64.

Sasagawa, S., H. Takemori, T. Uebi, D. Ikegami, K. Hiramatsu, S. Ikegawa, H. Yoshikawa and N. Tsumaki, 2012, "Sik3 Is Essential for Chondrocyte Hypertrophy During Skeletal Development in Mice", *Development*, Vol. 139(6), pp. 1153-63.

Sasaki, T., H. Takemori, Y. Yagita, Y. Terasaki, T. Uebi, N. Horike, H. Takagi, T. Susumu, H. Teraoka, K. Kusano, O. Hatano, N. Oyama, *et al.*, 2011, "Sik2 Is a Key Regulator for Neuronal Survival after Ischemia Via Torc1-Creb", *Neuron*, Vol. 69(1), pp. 106-19.

Sato, A. and A. Tomlinson, 2007, "Dorsal-Ventral Midline Signaling in the Developing Drosophila Eye", *Development*, Vol. 134(4), pp. 659-67.

Screaton, R. A., M. D. Conkright, Y. Katoh, J. L. Best, G. Canettieri, S. Jeffries, E. Guzman, S. Niessen, J. R. Yates, 3rd, H. Takemori, M. Okamoto and M.

Montminy, 2004, "The Creb Coactivator Torc2 Functions as a Calcium- and Camp-Sensitive Coincidence Detector", *Cell*, Vol. 119(1), pp. 61-74.

Shaw, R. J., 2009, "Tumor Suppression by Lkb1: Sik-Ness Prevents Metastasis", *Science Signaling*, Vol. 2(86), pp. pe55.

Shyamsundar, R., Y. H. Kim, J. P. Higgins, K. Montgomery, M. Jorden, A. Sethuraman, M. van de Rijn, D. Botstein, P. O. Brown and J. R. Pollack, 2005, "A DNA Microarray Survey of Gene Expression in Normal Human Tissues", *Genome Biology*, Vol. 6(3), pp. R22.

Silies, M., Y. Yuva-Aydemir, S. R. Franzdottir and C. Klambt, 2010, "The Eye Imaginal Disc as a Model to Study the Coordination of Neuronal and Glial Development", *Fly*, Vol. 4(1), pp. 71-9.

Silies, M., Y. Yuva, D. Engelen, A. Aho, T. Stork and C. Klambt, 2007, "Glial Cell Migration in the Eye Disc", *The Journal of Neuroscience* Vol. 27(48), pp. 13130-9.

Sjostrom, M., K. Stenstrom, K. Eneling, J. Zwiller, A. I. Katz, H. Takemori and A. M. Bertorello, 2007, "Sik1 Is Part of a Cell Sodium-Sensing Network That Regulates Active Sodium Transport through a Calcium-Dependent Process", *Proceedings of the National Academy of Sciences of the United States of America*, Vol. 104(43), pp. 16922-7.

Spencer, S. A., P. A. Powell, D. T. Miller and R. L. Cagan, 1998, "Regulation of Egf Receptor Signaling Establishes Pattern across the Developing Drosophila Retina", *Development*, Vol. 125(23), pp. 4777-90.

Spletter, M. L., J. Liu, H. Su, E. Giniger, T. Komiyama, S. Quake and L. Luo, 2007, "Lola Regulates Drosophila Olfactory Projection Neuron Identity and Targeting Specificity", *Neural Development*, Vol. 2 pp. 14.

Spokony, R. F. and L. L. Restifo, 2007, "Anciently Duplicated Broad Complex Exons Have Distinct Temporal Functions During Tissue Morphogenesis", *Development Genes and Evolution*, Vol. 217(7), pp. 499-513.

Stanley, P. and T. Okajima, 2010, "Roles of Glycosylation in Notch Signaling", *Current Topics in Developmental Biology*, Vol. 92 pp. 131-64.

Struhl, G. and A. Adachi, 1998, "Nuclear Access and Action of Notch in Vivo", *Cell*, Vol. 93(4), pp. 649-60.

Strutt, D. I., V. Wiersdorff and M. Mlodzik, 1995, "Regulation of Furrow Progression in the Drosophila Eye by Camp-Dependent Protein Kinase A", *Nature*, Vol. 373(6516), pp. 705-9.

Szymczak-Workman, A. L., K. M. Vignali and D. A. Vignali, 2012, "Verification of 2a Peptide Cleavage", *Cold Spring Harbor Protocols*, Vol. 2012(2), pp. 255-7.

Szymczak, A. L. and D. A. Vignali, 2005, "Development of 2a Peptide-Based Strategies in the Design of Multicistronic Vectors", *Expert Opinion on Biological Therapy*, Vol. 5(5), pp. 627-38.

Takemori, H., J. Doi, N. Horike, Y. Katoh, L. Min, X. Z. Lin, Z. N. Wang, M. Muraoka and M. Okamoto, 2003, "Salt-Inducible Kinase-Mediated Regulation of Steroidogenesis at the Early Stage of Acth-Stimulation", *The Journal of Steroid Biochemistry and Molecular Biology*, Vol. 85(2-5), pp. 397-400.

Tamura, K. and M. Nei, 1993, "Estimation of the Number of Nucleotide Substitutions in the Control Region of Mitochondrial DNA in Humans and Chimpanzees", *Molecular Biology and Evolution*, Vol. 10(3), pp. 512-26.

Thiery, J. P., H. Acloque, R. Y. Huang and M. A. Nieto, 2009, "Epithelial-Mesenchymal Transitions in Development and Disease", *Cell*, Vol. 139(5), pp. 871-90.

Tomlinson, A., 1988, "Cellular Interactions in the Developing Drosophila Eye", *Development*, Vol. 104(2), pp. 183-93.

Tomlinson, A. and D. F. Ready, 1987, "Neuronal Differentiation in Drosophila Ommatidium", *Developmental Biology*, Vol. 120(2), pp. 366-76.

Treisman, J. E. and G. M. Rubin, 1995, "Wingless Inhibits Morphogenetic Furrow Movement in the Drosophila Eye Disc", *Development*, Vol. 121(11), pp. 3519-27.

Tsai, Y. C., J. G. Yao, P. H. Chen, J. W. Posakony, S. Barolo, J. Kim and Y. H. Sun, 2007, "Upd/Jak/Stat Signaling Represses Wg Transcription to Allow Initiation of Morphogenetic Furrow in Drosophila Eye Development", *Developmental Biology*, Vol. 306(2), pp. 760-71.

Uhlirova, M., H. Jasper and D. Bohmann, 2005, "Non-Cell-Autonomous Induction of Tissue Overgrowth by Jnk/Ras Cooperation in a Drosophila Tumor Model", *Proceedings of the National Academy of Sciences of the United States of America*, Vol. 102(37), pp. 13123-8.

van der Linden, A. M., K. M. Nolan and P. Sengupta, 2007, "Kin-29 Sik Regulates Chemoreceptor Gene Expression Via an Mef2 Transcription Factor and a Class Ii Hdac", *The EMBO Journal*, Vol. 26(2), pp. 358-70.

van der Linden, A. M., S. Wiener, Y. J. You, K. Kim, L. Avery and P. Sengupta, 2008, "The Egl-4 Pkg Acts with Kin-29 Salt-Inducible Kinase and Protein Kinase a to Regulate Chemoreceptor Gene Expression and Sensory Behaviors in Caenorhabditis Elegans", *Genetics*, Vol. 180(3), pp. 1475-91.

Van Vactor, D. L., Jr., R. L. Cagan, H. Kramer and S. L. Zipursky, 1991, "Induction in the Developing Compound Eye of Drosophila: Multiple Mechanisms Restrict R7 Induction to a Single Retinal Precursor Cell", *Cell*, Vol. 67(6), pp. 1145-55.

Venken, K. J., Y. He, R. A. Hoskins and H. J. Bellen, 2006, "P[Acman]: A Bac Transgenic Platform for Targeted Insertion of Large DNA Fragments in D. Melanogaster", *Science*, Vol. 314(5806), pp. 1747-51.

Vidal, M., D. E. Larson and R. L. Cagan, 2006, "Csk-Deficient Boundary Cells Are Eliminated from Normal Drosophila Epithelia by Exclusion, Migration, and Apoptosis", *Developmental Cell*, Vol. 10(1), pp. 33-44.

Vidal, M., L. Salavaggione, L. Ylagan, M. Wilkins, M. Watson, K. Weilbaecher and R. Cagan, 2010, "A Role for the Epithelial Microenvironment at Tumor Boundaries: Evidence from Drosophila and Human Squamous Cell Carcinomas", *The American Journal of Pathology*, Vol. 176(6), pp. 3007-14.

Vidal, M., S. Warner, R. Read and R. L. Cagan, 2007, "Differing Src Signaling Levels Have Distinct Outcomes in Drosophila", *Cancer Research*, Vol. 67(21), pp. 10278-85.

Voas, M. G. and I. Rebay, 2004, "Signal Integration During Development: Insights from the Drosophila Eye", *Developmental Dynamics*, Vol. 229(1), pp. 162-75.

Vural, M. E., 2008, *Expression of Sik1 and Sik3 in Postnatal Rat Retina*, M.Sc. Dissertation, Boğaziçi University..

Wang, B., J. Goode, J. Best, J. Meltzer, P. E. Schilman, J. Chen, D. Garza, J. B. Thomas and M. Montminy, 2008, "The Insulin-Regulated Creb Coactivator Torc Promotes Stress Resistance in Drosophila", *Cell Metabolism*, Vol. 7(5), pp. 434-44.

Wang, B., N. Moya, S. Niessen, H. Hoover, M. M. Mihaylova, R. J. Shaw, J. R. Yates, 3rd, W. H. Fischer, J. B. Thomas and M. Montminy, 2011, "A Hormone-Dependent Module Regulating Energy Balance", *Cell*, Vol. 145(4), pp. 596-606.

Wang, S. H., A. Simcox and G. Campbell, 2000, "Dual Role for Drosophila Epidermal Growth Factor Receptor Signaling in Early Wing Disc Development", *Genes & Development*, Vol. 14(18), pp. 2271-6.

Wang, Z., H. Takemori, S. K. Halder, Y. Nonaka and M. Okamoto, 1999, "Cloning of a Novel Kinase (Sik) of the Snf1/Ampk Family from High Salt Diet-Treated Rat Adrenal", *FEBS Letters*, Vol. 453(1-2), pp. 135-9.

Weber, U., V. Siegel and M. Mlodzik, 1995, "Pipsqueak Encodes a Novel Nuclear Protein Required Downstream of Seven-up for the Development of Photoreceptors R3 and R4", *The EMBO Journal*, Vol. 14(24), pp. 6247-57.

Wech, I. and A. C. Nagel, 2005, "Mutations in Rugose Promote Cell Type-Specific Apoptosis in the Drosophila Eye", *Cell Death and Differentiation*, Vol. 12(2), pp. 145-52.

Wharton, K. A., K. M. Johansen, T. Xu and S. Artavanis-Tsakonas, 1985, "Nucleotide Sequence from the Neurogenic Locus Notch Implies a Gene Product That Shares Homology with Proteins Containing Egf-Like Repeats", *Cell*, Vol. 43(3 Pt 2), pp. 567-81.

Witte, H. T., A. Jeibmann, C. Klambt and W. Paulus, 2009, "Modeling Glioma Growth and Invasion in Drosophila Melanogaster", *Neoplasia*, Vol. 11(9), pp. 882-8.

Wolff, T. and D. F. Ready, 1991, "The Beginning of Pattern Formation in the Drosophila Compound Eye: The Morphogenetic Furrow and the Second Mitotic Wave", *Development*, Vol. 113(3), pp. 841-50.

Wu, M., J. C. Pastor-Pareja and T. Xu, 2010, "Interaction between Ras(V12) and Scribbled Clones Induces Tumour Growth and Invasion", *Nature*, Vol. 463(7280), pp. 545-8.

Xie, X. and V. J. Auld, 2011, "Integrins Are Necessary for the Development and Maintenance of the Glial Layers in the Drosophila Peripheral Nerve", *Development*, Vol. 138(17), pp. 3813-22.

Yang, Z., 1997, "Paml: A Program Package for Phylogenetic Analysis by Maximum Likelihood", *Computer Applications in the Biosciences*, Vol. 13(5), pp. 555-6.

Yokohori, N., K. Aoshiba and A. Nagai, 2004, "Increased Levels of Cell Death and Proliferation in Alveolar Wall Cells in Patients with Pulmonary Emphysema", *Chest*, Vol. 125(2), pp. 626-32.

Yoon, Y. S., W. Y. Seo, M. W. Lee, S. T. Kim and S. H. Koo, 2009, "Salt-Inducible Kinase Regulates Hepatic Lipogenesis by Controlling Srebp-1c Phosphorylation", *The Journal of Biological Chemistry*, Vol. 284(16), pp. 10446-52.

Yoshida, H. and M. Goedert, 2012, "Phosphorylation of Microtubule-Associated Protein Tau by Ampk-Related Kinases", *J Neurochem*, Vol. 120(1), pp. 165-76.

Yoshida, H. and M. Goedert, 2012, "Phosphorylation of Microtubule-Associated Protein Tau by Ampk-Related Kinases", *Journal of Neurochemistry*, Vol. 120(1), pp. 165-76.

Zeng, Q., S. Li, D. B. Chepeha, T. J. Giordano, J. Li, H. Zhang, P. J. Polverini, J. Nor, J. Kitajewski and C. Y. Wang, 2005, "Crosstalk between Tumor and Endothelial Cells Promotes Tumor Angiogenesis by Mapk Activation of Notch Signaling", *Cancer Cell*, Vol. 8(1), pp. 13-23.

Zhai, Z., N. Ha, F. Papagiannouli, A. Hamacher-Brady, N. Brady, S. Sorge, D. Bezdan and I. Lohmann, 2012, "Antagonistic Regulation of Apoptosis and Differentiation by the Cut Transcription Factor Represents a Tumor-Suppressing Mechanism in Drosophila", *PLoS Genetics*, Vol. 8(3), pp. e1002582.

Zolkiewska, A., 2008, "Adam Proteases: Ligand Processing and Modulation of the Notch Pathway", *Cellular and Molecular Life Sciences*, Vol. 65(13), pp. 2056-68.